Faculty of Engineering of the University of Porto- Portugal

Department of Mechanical Engineering and Industrial Management

Universidade do Porto
Faculdade de Engenharia
FEUP

Ministério da Educação
prodep III
PROGRAMA DE DESENVOLVIMENTO EDUCATIVO PARA PORTUGAL

RENAULT C.A.C.I.A.

RENAULT

C.A.C.I.A.

5th year- Structural Mechanics

Final Project (PFC-4) 2003/2004

Study of distortion and hardness related with heat treatment parameters applied in automotive gear production

Project Supervisors:

Prof. Viriato Antunes (FEUP)
Eng. António Completo (Renault-CACIA)
Eng. Carla Costa (Renault-CACIA)
Eng. Quê Vu Do (Renault-CACIA)

Ricardo dos Santos Gouveia Afonso

621(047.3)
LEM 2003/AFOr

UNIÃO EUROPEIA
Fundo Social Europeu
prodep III
Mais Educação

Faculty of Engineering of the University of Porto- Portugal

Department of Mechanical Engineering and Industrial Management

Universidade do Porto
Faculdade de Engenharia
FEUP

Ministério da Educação
prodep III
PROGRAMA DE DESENVOLVIMENTO EDUCATIVO PARA PORTUGAL

RENAULT C.A.C.I.A.

RENAULT

C.A.C.I.A.

5th year- Structural Mechanics

Final Project (PFC-4) 2003/2004

Study of distortion and hardness related with heat treatment parameters applied in automotive gear production

Project Supervisors:

Prof. Viriato Antunes (FEUP)
Eng. António Completo (Renault-CACIA)
Eng. Carla Costa (Renault-CACIA)
Eng. Quê Vu Do (Renault-CACIA)

Ricardo dos Santos Gouveia Afonso

UNIÃO EUROPEIA
Fundo Social Europeu

prodep III
Mais Educação

621(047.3)/LEM 2003/AFOR
Universidade do Porto
Faculdade de Engenharia
Biblioteca
Nº 87327
CDU 620.1(047.3)
Data 20/4/2007

Projecto / Project	**Estudo da deformação e dureza relacionadas com os parâmetros dos tratamentos térmicos aplicados na concepção de engrenagens automóveis**	**Study of distortion and hardness related with heat treatment parameters applied in automotive gear production**
Instituições / Institutions:	DEMEGI-FEUP Departamento de Engenharia Mecânica e Gestão Industrial da Faculdade de Engenharia da Universidade do Porto. Renault- CACIA Companhia Aveirense de Componentes para a Indústria Automóvel.	
Supervisor at FEUP:	Professor Viriato Antunes	
Supervisors at CACIA:	Quê Vu-Do and António Completo	
Período / Period:	Set. 2003 – Jul. 2004	
Referência / Reference:	**RELATÓRIO TÉCNICO**	**TECHNICAL REPORT**
Autor / Author:	Ricardo dos Santos Gouveia Afonso	
Páginas / Pages:	136	
Lugar / Place:	Renault- CACIA	
Data / Date:	19/07/2004	

Index

Summary and Objectives 4
Introduction 5

1.Carbonitriding 7
2. Process Control 10
2.1 Furnace functioning 10
2.2 Schematic Furnace Description 11
3. Furnace atmosphere 13
3.1 Atmosphere constitution 13
3.2 Ammonia 13
3.3 Nitrogen 17
3.4 Carbon 17
3.5 Gas transfer and furnace atmosphere control 19
3.6 Temperature control 20
3.7 Cooling Techniques 21
4. Case Composition 22
5. Gear Quality-geometrical accuracy 24
5.1 High performance 24
5.2 Dimensional variation and its relation with the basic principles 25
6. Control of undesirable structures 27
6.1 Control and reduction of retained austenite 27
6.2 Porosity and voids prevention 28
7. The four case studies 29
7.1Aiming for higher hardness: G9T Z41 left and G9T Z41 right pinions 30
7.1.1 Results and discussion 30
7.1.2 Conclusions 37
7.2 Z41 left and right pinions: distortion study 38
7.2.1 Results and discussion 38
7.2.2 Conclusions 42
7.3 JC4 and G9T Z98D distortion study 43
7.3.1 G9T Z98D: Results and discussion 43
7.3.2 JC4: Results and discussion 48
7.3.3 Conclusions 51
7.4 Assembling PF5 and JR Shaft 52
7.4.1 Results and discussion 52
7.4.2 Residual Stress analysis and results relation 58
7.4.3 Heat treatment process, geometry and carbon effect on residual stress distribution 64
7.4.4 Retained austenite and residual stress relation 68
7.4.5 Retained austenite quantification results 70
7.4.6 Subzero cooling- microstructure identification results 73
7.4.7 Subzero treatment- hardness and geometry results 76

7.4.8 Conclusions 82
Final conclusions 84
Obtaining the desired final structure 84
Further Work 87
References 88
APPENDIX 1 90
Allotropic iron forms 91
Atomic representation 91
Calculating atomic occupation 92
APPENDIX 2 94
Equilibrium diagrams (Fe-C) 95
T.T.T. Diagrams (Transformation –Time – Temperature) 98
APPENDIX 3 101
Microstructure analysis 102
APPENDIX 4 106
X-ray diffraction 107
APPENDIX 5 110
External gear teeth 111
Internal gear teeth 115
APPENDIX 6 117
Shot Peening 118
APPENDIX 7 119
Preparing hardness measuring- methodology 120
APPENDIX 8 123
Gear teeth geometrical properties 124
APPENDIX 9 129
Deformation evolution for Z41 130
APPENDIX 10 132
Z41 left pinions heat treatment and subzero cooling hardness comparison results 133

Summary and Objectives

- ✓ The problems dependent from retained austenite, distortion and too low or too high hardness present in carbonitrited parts are well known to be restrictive of the mechanical performance of such parts.

- ✓ Carbonitriding, is known as the modification of a carburised gas that consists of introducing ammonia into the gas carburising atmosphere, in order to add nitrogen to the carburised case as it is being produced. It is obvious, that full comprehension of the problems inherent to this technique, can only be achieved when gas moisture and its reactions have been completely understood.

- ✓ The microstructure of ferrous alloys is very complicated to study it, requires good knowledge about steel microstructures. It is well known in metallurgy that composition and processing establishes the microstructure, and that microstructure influences most properties and service behaviour. The microstructure of steel alloys used in carbonitriding, can only be fully understood when chemical composition, material homogeneity and its processing and section size are known.

- ✓ To uphold control of the quality of steel products and to diagnose problems in processing, testing, or service, the microstructure should be identified and, quantified, however, normally, this is not possible and it can only be accomplished when the phases or constituents present are properly distinguished, which is extremely difficult.

- ✓ **The main objectives** of this work are the study of distortion, hardness and the parameters that enhance the presence of retained austenite in gearbox parts, its relation with residual stresses and how to decrease it, having in consideration that aiming for hardness, low distortion and toughness, and at the same time decreasing retained austenite presence, might be a complex compromise.

Introduction

To accurately study the distortion and hardness changes in gear box shafts and pinions and its relation with heat treatment parameters, one must be able to have full perception of all production and manufacture process. The study, and most important, the conclusions withdrawn from the obtained results, cannot be correctly interpreted if the relation between all manufacture stages has not been understood. Even if sometimes not all stages of the manufacture process are important for the study of a determined problem, not to know them or ignore them, leads to misjudgement.

Distortion analysis, at such production level, must be extremely accurate. Taking the complexity of gear teeth box geometry, and dealing with a few microns, to impart any changes in production that are able to provoke any desired corrections, might sometimes be impossible.

Analysing hardness is also a difficult process. When imparting hardness and gear teeth box geometrical improvements in certain parts, the induced changes are most of the times obtained through several experimentation phases where the variables are raised or lowered depending on the level of hardness or geometrical property to be altered.

In order to have full perception of the different mechanisms that take place in the diverse mechanical components treated in a carbonitrited atmosphere, it is vital to acquire accurate knowledge of the process mechanisms and the physical and chemical transformations involved in the carbonitriding process. To do so, full familiarity with the component's microstructure is important, so that the micro-structural transformations induced by the process are correctly interpreted (see **appendix 3**).

A phase is a homogeneous, physically distinct substance. Martensite is a phase when formed by quenching but becomes a constituent after tempering as in decomposes from body centered tetragonal (bct) martensite to body centered cubic (bcc) ferrite and cementite. Definitions are given in the process of describing and illustrating various phases and constituents in ferrous alloys (see **appendix 3**).

Later, for the experimental work, some microstructure pictures were taken to identify and distinguish different phase and constituents and difficulties to identify the differences are visible, especially if one have not yet acquire the required degree of experience.

To acquire complete understanding of phase and constituent changes in steel mechanical parts treated under carbonitrided atmospheres, some study of the allotropic iron forms and its transformations is required (see **appendix 1**). The main distinction between ferrite and austenite is the radical difference in the ability to dissolve carbon.

There is a need to obtain martensite instead of austenite, though it is the austenitic transformation that allows the appearance of martensite. This is part of the problem in obtaining resistant parts without retained austenite presence.

Though retained austenite is normally undesirable, its presence is still motive of non-consensus.

In **appendix 2,** the relevant theoretical background of metallurgy applied to gear box parts studied in this work is explained. Equilibrium diagrams and TTT diagrams are analysed as well as the influence of alloy elements in the part's behaviour regarding heat treatment process and a brief overview of nucleus and case temperability and its relation with volume changes throughout carbonitriding process, which is extremely important for the distortion.

1.Carbonitriding

Carbonitriding is by definition, a diffusion thermo-chemical treatment followed by a fast quench, where surface enrichment is accomplished with carbon and nitrogen simultaneously. Is used for parts requiring high superficial hardness, high resistance to chafing fatigue, and which are subject to moderate superficial loads and it is a modified form of gas cementation.

Nitriding is a case hardening process, which nitrogen atoms diffuse through the surface of the work piece, and causes nitride compounds at the surface, in the surface and in the distance which nitrogen diffuses. Work piece with nitride layer at the surface and nitride particles below surface will get better properties such as higher surface hardness, better wear resistance, higher fatigue strength, better corrosion resistance, least distortion and better hot hardness. Ionitriding is the latest technology of nitriding processes in which NH3 is ionized to N+ and bombarded into the work piece that causes the higher efficiency.

Carburizing might be considered as one of the most effective and therefore used techniques of superficial carbonisation and therefore, of superficial hardening.

Resembling cementation, in carbonitriding the carbonised surface is obtained by diffusion of carbon atoms from the cement to the steel piece surface under pre-determined chemical reactions, followed by carbon's diffusion from surface to the interior of the steel piece, diffusion resulting from an atomic migration.

The most visible advantage of the treatment is that the treatment cycle is relatively short. A hardening atmosphere combines in the same installation nitrogen and carbon enrichment for smaller residual surface constraints. A martensitic layer development by hardening under the carbonitrited one, increase mechanical properties.

In carbonitriding, the addition of nitrogen makes the process especially suited to plain, low carbon steel that would not otherwise respond to standard carburizing.

So, there are three very important facts associated to the carbonitring process:

- Dissociation of ammonia in the furnace atmosphere;
- Nascent nitrogen at the work surface;
- Nitrogen diffuses into steel simultaneously with carbon;

Therefore, along with a superficial carbonisation, there is also an introduction of ammonia inside the cementation atmosphere in order to provoke azoth enrichment on the superficial part of the steel tool pack in which is being applied the carbon enrichment. The azoth appears from the dissociation of ammonia in the furnace atmosphere and its diffusion on the treated steel tool happens simultaneously with the carbon.

Generally carbonitriding is executed under inferior treatment periods and temperatures from the ones used in cementation processes. The technique is more appropriate in particular to treat small dimension steel pieces with different and complex geometries, due to less volumetric deformation obtained.

The lower temperatures and less severe quenches of this process permit a better dimensional control and suppress the creation of geometrical distortions.

For the above stated reasons, the group of steel categories for which a superficial hardening might be obtained is higher in carbonitriding than in cementation. Especially when the nucleus properties are relatively unimportant, carbonitriding allows the use of low carbon steels, and therefore, less expensive steels that are easily manufactured and conformed. All steels used for the studied parts are considered to belong to the previous stated group of low carbon steels.

So, carbonitriding is used to obtain a hard shell of approximately 0.1mm depth, as generally imparts a hard, wear resistant case from 0.075 to 0.75mm deep.

The fatigue life of either a carburized or carbonitrided component will be determined by the case depth thickness. The thicker the case, the higher the fatigue strength will be. However this will reach a point where the fatigue strength will diminish due to the case being too thick, and therefore toughness will decrease.

In steels in which nitrites are formed, like aluminium or titanium, the hard shell depth acquired through the process is substandard.

The thickness of the hard outer layer is dependent on the application of the steel piece to be treated and also on the stiffness of the nucleus. Thicker layers are obtained in steel components that have to ensure high resistance to shear and compressive loads.

Increasing the case strength gradient and improving contact fatigue, are two direct consequences of increasing the case residual compressive stresses all due to the addition of the carbonitrided shell to the steel alloy structure.

A homogeneous layer is acquainted from a uniform atmosphere temperature, circulation and its renovation. This has to go together with a uniform load distribution in the furnace. Depending on the parts geometry and size, the number of parts for each load changes, mainly in order to maintain a certain consistency in the volume and mass being treated inside the treatment chamber.

A superior temperability than the one achieved from cementation methods is obtained. This raise of steel temperability obtained from carbonitriding is due to the azoth presence. It becomes an important advantage of carbonitriding in contrast with cementation as that the absorbed azoth during treatment slows the critical steel tempera velocity. However, azoth also stabilizes austenite, and so, employing high nitrogen levels might provoke the appearance of retained austenite, particularly in alloy steels.

Carbonitriding and quenching can produce a hardened case with less expense, as the process is carried out for a shorter time and at a lower temperature than is gas carburising, with the required case depth range, using either carbon or low-alloy steel.

Using oil quenching is an advantage, when the objective is less distortion with full hardness. Also higher penetration effectiveness is achieved.

The major problem in controlling carbonitriding processes in this kind of batch furnaces is that the rate of nitrogen absorption depends on the free ammonia content of the furnace atmosphere and not the percentage of ammonia in the inlet gas.

However, normally there is no reliable sensor to take full monitoring of the free ammonia content of the furnace atmosphere.

2. Process Control

2.1 Furnace functioning

The main goal of process controlling is to provide an atmosphere controlled furnace for carbonitriding neutral hardening, normalising, annealing, and stress relieving. The steel pieces heat-treated with the furnace must be very clean and there should be a good carbon control.

There are a number of variables implicated in carbonitriding control process.

The key variables in carbonitriding are time, temperature, and the process environment. Temperatures are typically maintained at 800°C to 900°C to insure control of the diffusion process. The higher process temperatures would be used for deeper case specifications. Lower temperatures may be used regardless of case depth requirements to reduce distortion. Time at the processing temperature is controlled to insure the proper development of the specified case. The process environment is provided by the introduction of methane (for carbon) and ammonia (for nitrogen) to the furnace, in the presence of a controlled carrier gas. By maintaining the proper ratios of the working gases, the processed parts are provided with a thin skin of carbon and nitrogen rich steel.

Accurate gas variation control must be taken, especially when varying the enriching gas; high quantities of hydrocarbonets should not be introduced to prevent steel clay formation. This clay formation will complicate the material cleaning and provoke material deterioration, as well as affecting carbonitriding process velocity.

So, the inlet gas control and the technique used to introduce the atmosphere constituents are of great importance to achieve accurate process control.

As the inlet gas should be introduced continuously, without pauses, a vaporising system is preferred instead of gas injection cylinders, because there is the obvious advantage of a constant, non-stop inlet gas basis with uniform quality. If cylinders are used, the gas flow in each cylinder must sufficiently slow to prevent valves from frozen.

For the valves and conduction gas pipes, stainless steel is recommended.

In the next chapters a description of the furnace atmosphere as well as the interaction of the different atmosphere constituents is analysed among with its repercussions in case composition, case depth, mechanical properties and retained austenite control.

2.2 Schematic Furnace Description

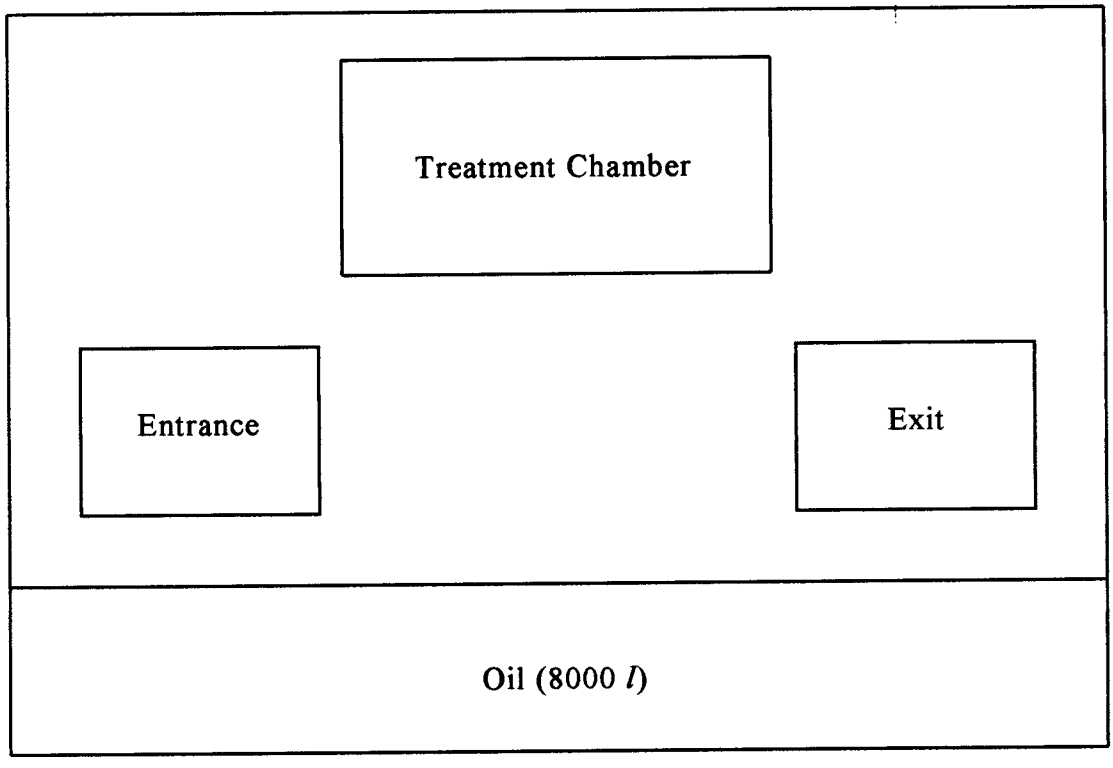


Figure 1- Furnace sketch.

Each time the doors open, only one load enters the furnace.

If the furnace is functioning with a load being treated, then entrance and exit doors are both closed. Whenever this happens, two loads are inside the furnace: one inside the treatment chamber and another one located near the entrance door at a stage temperature.

When carbonitriding treatment and diffusion time is over, the load is transferred from the treatment chamber by the treatment chamber elevator, which moves towards the middle area of the furnace, carrying the treated load and positioning it between the entrance and exit doors. Through all the described operations both doors remain closed.

At the time the treated load reaches this position, a transfer mechanism, located at this stage at the left of the entrance door, pushes the two loads to the right, positioning the treated load in front of the exit door, on the quenching elevator and the untreated load in the treatment chamber elevator.

With the transfer at its maximum right position, the two loads, side by side, each one on its elevator, are ready to be moved in opposite vertical directions. The untreated load is transferred to the treatment chamber while the load located in front of the exit door is moved into the oil chamber by the quenching elevator.

A few seconds after the positioning of both loads, one inside the oil quenching chamber and the other inside the treatment chamber, both doors open simultaneously.

After quenching time is over (15 min.), the quenching elevator carries the load up, positioning it once more, in front of the exit door, ready to be pulled out of the furnace.

Finally, another load is carried into the furnace through the entrance door, and doors will close once more with two loads inside.



Figure 2- Aspect of furnace load's entrance door (opened).

The photo shows an operator positioning a load through the entrance door.

On the left, inside the blue ellipse, the controller box indicates the location of each load and the position of the doors. In the red ellipse, the exhausts located over each door, aspire the gas flow that are inevitably expelled from inside the furnace. The visible flames are of vital importance to control the pressure and improve the exhausts' aspiration.

3. Furnace atmosphere

3.1 Atmosphere constitution

A mixture generally forms carbonitriding atmospheres. A carrier gas, an atmosphere enriching gas and ammonia forms this mixture. The atmosphere is then produced with a typical cementation gas and the addition of ammonia, in a quantity that varies between 2% and 12%. The ammonia used should be 99.9% pure, as it must prevent the existence of carbon dioxide as well as water and several oils in the furnace atmosphere.

The three different gases are controlled and mixed before the furnace's entry. Continuous, large dimension furnaces require several gas addition points so that high furnace atmosphere homogeny is achieved. The atmosphere control is usually obtained with the production of the carrier gas along with the combination of the enriching gas and ammonia and the carbon's potential control.

Also, if carbon potential is not accurately controlled, especially if there is a high superficial concentration of carbon (higher than 0.9%), the risks of retained austenite are increased.

By varying the amount of ammonia and enriching gas, that will take part of the carbonitriding atmosphere, it is possible to control the carbon and nitrogen desired atmosphere quantities.

It is especially important to study each atmosphere component separately and then study accurately the effects of all atmosphere constituents' interaction.

3.2 Ammonia

The atom adsorption depends on the concentration of free ammonia in the treatment atmosphere.

For higher temperatures the addition of ammonia to the atmosphere applied to add azoth to the process, becomes less effective. This is due to the increase of decomposition velocity of ammonia. Ammonia's spontaneous decomposition in molecular nitrogen and hydrogen fastens with the increase of temperature. As azoth is molecularly inert its diffusion to the interior of the steel is diminished.

For a given temperature, the fraction of ammonia added to the steel pieces in the furnace that will be spontaneously decomposed, is dependent on the settling time of the furnace's atmosphere. So, it is important to enforce a slow velocity process, with an accurate temperature control; for the higher the gas flow is, the lower the decomposed fraction of ammonia (in nitrogen and hydrogen) will be.

Also, the lower the temperature, the higher the nitrogen superficial concentration will be. On the other hand, the higher the carbonitriding temperature is, the less effective the addition of ammonia will be to the atmosphere, being ammonia the nitrogen's diffuser. This situation occurs because the level of spontaneous

decomposition of ammonia in hydrogen and molecular nitrogen increases with the rise of temperature.

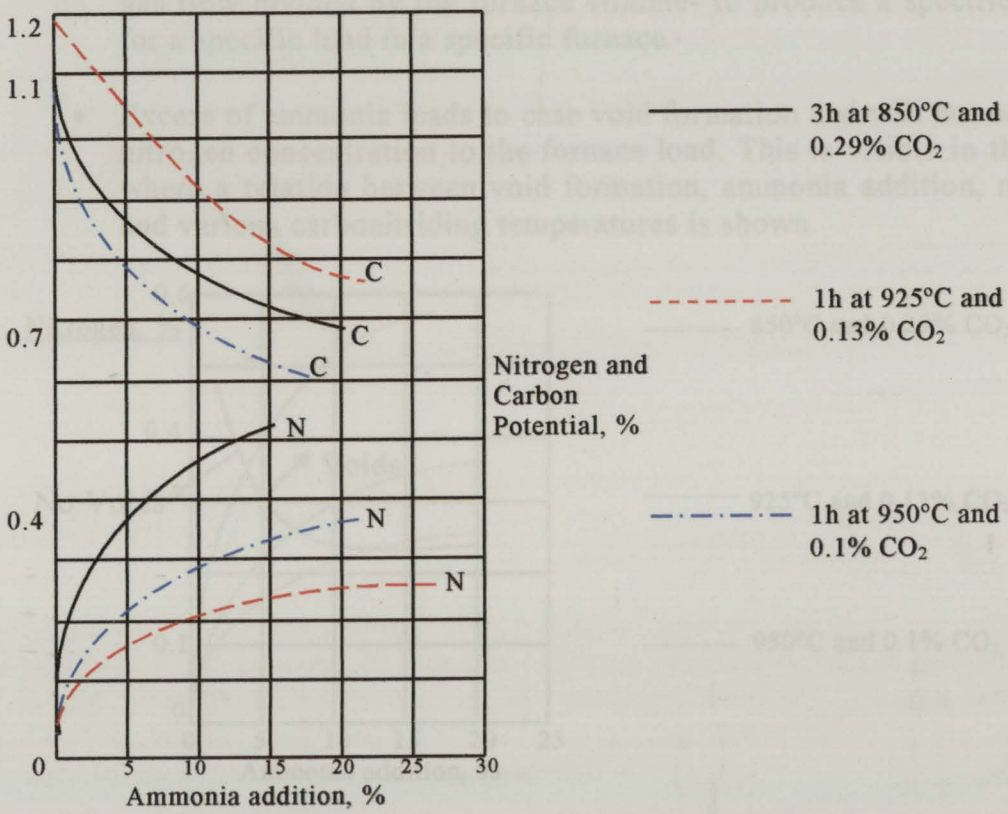
It is concluded that, the higher the current of gas in the treatment atmosphere the lower the ammonia's fraction that will be decomposed in azoth and hydrogen.

There are many stages in a process like the one being studied and so, the purpose of introduced different gas types and quantities is different from one stage to another. In a carbonitriding technique, the purpose of introducing ammonia during the last portion of the carburizing cycle is to suppress the austenite formation during the quench procedure. The side benefit of carbon nitriding is that there will be an improvement in the surface hardness. But its primary objective is to reduce the austenitizing temperature, which will in turn reduce the retained austenite.

The ammonia's dilution effect subjected to the ammonia's addition to a carburised atmosphere follows the chemical reaction:

$$2NH_3 \longrightarrow N_2+3H_2$$

The next graphic shows effect of the addition of ammonia in both carbon and nitrogen potentials:

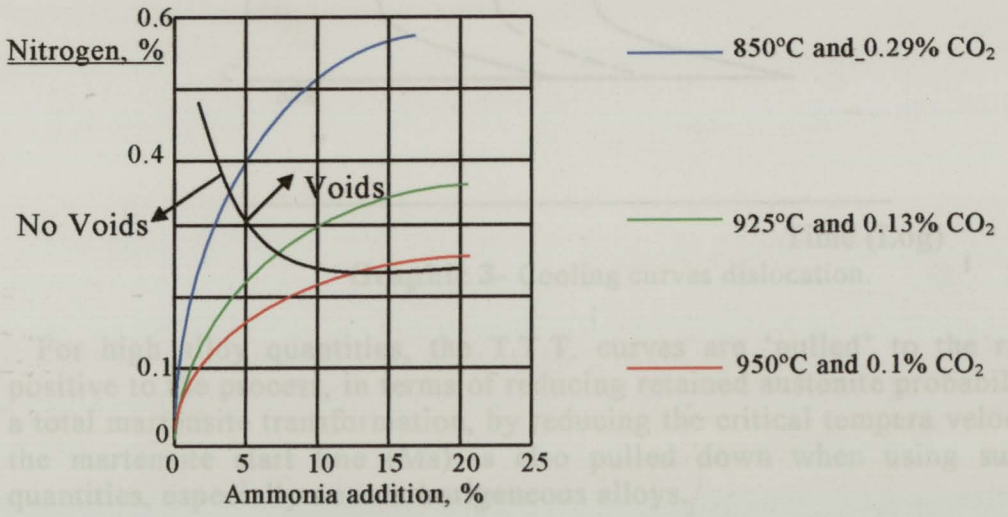


Graphic 1 - Nitrogen and Carbon Potential levels (%), depending on the introduced percentage of ammonia. Source: Ref. 2.

The previous graphic also shows that lower temperatures promote higher nitrogen concentrations at the surface.

The essential considerations regarding the ammonia control:

- Ammonia is introduced to add nitrogen to the parts being carbonitrided and to reduce austenitizing temperature, which is essential to reduce retained austenite.
- However, a minimum ammonia percentage (this depends from steel composition) must be introduced, to ensure reasonable levels of temperability. So, if ammonia concentration levels are too high, there will be an increase in retained austenite values (austenite retention increases with an increase in ammonia content).
- As load surface, dimensions and density rise, a higher quantity of ammonia is required to satisfy the higher need for nitrogen.
- Low ammonia percentages, must be used with high rates of gas change –total gas flow divided by the furnace volume- to produce a specific microstructure for a specific load in a specific furnace.
- Excess of ammonia leads to case void formation and will not contribute to rise nitrogen concentration to the furnace load. This is visible in the next graphic, where a relation between void formation, ammonia addition, nitrogen content and various carbonitriding temperatures is shown.



Graphic 2 – Effect of ammonia additions on nitrogen content and formation of subsurface voids. Source: Ref. 6.

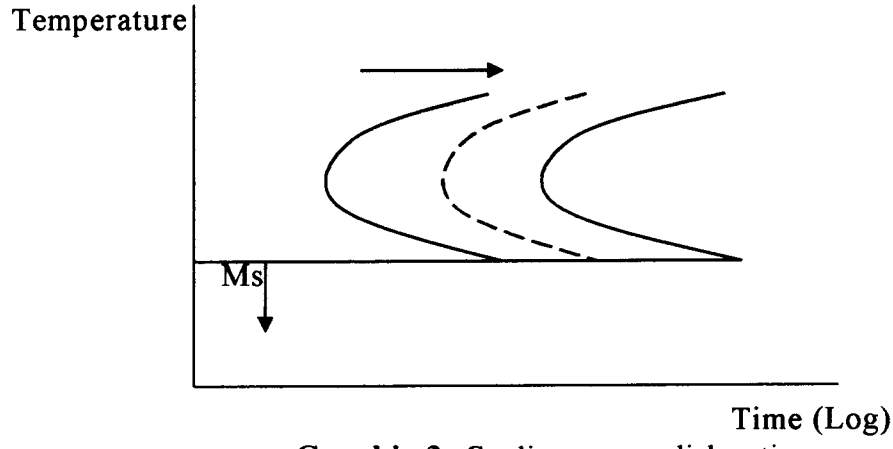
- Higher ammonia percentages should be use for higher furnace temperatures. But, for high temperatures, the addition of ammonia is not so effective, as ammonia decomposes in molecular nitrogen and hydrogen at very high velocities.

- A higher level of atmosphere recirculation, means higher atmosphere uniformity and allows the use of lower ammonia concentrations.

- In the austenitic dominium, which means at very high temperatures, the level of nitrogen absorption diminishes with time, so, shallower cases and small furnace cycles require high ammonia quantities. Which is understandable, because it is visible that nitrogen is absorbed mainly to austenite and also to ferrite (but at a lower rate), and austenite dominium prevails at higher temperatures.

- Lower ammonia percentages can be used with high carbon potentials. But for shallow case depths, especially if the load size or the load surface area increases, hydrocarbon additions may be necessary.

- In high percentage steel alloys, lower quantities of ammonia must be used (especially for steel alloys containing high percentages of Ni and Mn).



Graphic 3- Cooling curves dislocation.

For high alloy quantities, the T.T.T. curves are 'pulled' to the right, which is positive to the process, in terms of reducing retained austenite probability, promoting a total martensite transformation, by reducing the critical tempera velocity. However, the martensite start line (Ms) is also pulled down when using such high alloy quantities, especially non-carborigeneous alloys.

3.3 Nitrogen

The nitrogen presence during treatment process delays the critical steel tempera velocity, raising the steel alloy temperability. But nitrogen also actuates as an austenite stabilizer, and so, promoting the existence of retained austenite.

The rise of furnace treatment temperature raises the nitrogen concentration and its dilution capability, which brings TTT curves down and to the right, as nitrogen has a strong gamageneous action promoting austenite stability while lowering Ms-martensitic transformation line.

Nitrogen modifies carbon solubility limits in austenite diminishing the transformation points $\alpha \longrightarrow \gamma$, raising temperability and stiffness levels.

So, increasing nitrogen quantities and raising the concentration of alloys such as Ni will move TTT curves to the right.

It is concluded that lower temperatures ease the rise of nitrogen's concentration at the surface.

On the other hand, if the vapour blanket that occurs during the process is maintained for a long period, there is an increase in risk of retained austenite.

In carbonitriding, the nitrogen's dispersion in the furnace's atmosphere directly affects the carbon's potential level.

The capability of nitrogen's dilution and its direct effect on process atmosphere depends on the process temperature, quantity of ammonia and ratio between total atmosphere's current velocity and the furnace's volume.

The dilution with nitrogen and hydrogen affects the measure of oxygen potential in a simple manner: the level of achievable carbon potential for a given oxygen potential is higher for a carburised atmosphere than the one achieved for carbonitrided atmosphere.

3.4 Carbon

Carbon is used of course, to improve case hardness and wear resistance.

The main chemical reactions that sustain the carbon addition process, from the atmosphere to the steel surface and core are:

$$CO + H_2 \rightarrow (C) + H_2O$$
$$2CO \rightarrow (C) + CO_2$$
$$CH_4 \rightarrow (C) + 2H_2$$

The first reaction is the fastest one, which explains the considerable atmosphere concentrations of carbon monoxide and molecular hydrogen. When diluted in nitrogen these two gases go together with low amounts of carbon dioxide, water vapour and methane.

The carbon mass transferred per second at a surface distance of $1cm^2$, defines the speed of carbon transfer rate. However the speediness of such a process, composed by so many stages, is determined by the speed of the slowest stage or reaction. This slowest reaction acts as a process delay stage, and so, determining the process velocity.

In the carbon adsorption phenomenon, the slowest process stage is the one related to the chemical reaction in which CO and CH_4 molecules are adsorbed. These molecules, grant carbon to the treated part under the following chemical reactions:

- CO molecules dissociation (being 'ad' the adsorbed molecule):

$$CO_{ad} \rightarrow C_{ad} + O_{ad}$$

- The carbon atoms penetrate in steel's crystalline net, while oxygen separates itself from the surface and reacts with hydrogen and carbon monoxide molecules:

$$H_2 + O_{ad} \rightarrow H_2O$$
$$CO + O_{ad} \rightarrow CO_2$$

The first reaction is faster than the CO_{ad} dissociation, but the second is slower, consequently, in terms of carbon transfer process, it will be the one to determine the process speed.

However the above stated reactions are applied in carburising atmospheres, as in carbonitrided atmospheres the addition of ammonia has the dilution effect stated above (chapter 4.2):

$$2NH_3 \longrightarrow N_2 + 3H_2$$

This dilution with nitrogen affects oxygen potential capacity. The amount of carbon possible with a certain oxygen potential is higher in a carburising atmosphere than in a carbonitrided atmosphere.

The carbon amount introduced depends on alloy steel composition and on the case depth and hardness necessary to a given application.

For high carbon and alloy percentage steels, M_f (martensite finish) line is at a very low temperature and this means the existence of retained austenite, which definitely affects the properties and good performance of the treated steel.

When high carbon percentages are used, lower quantities of ammonia must be provided to ensure a sufficiently high martensite transformation, since high carbon concentrations may lead to an Ms line dislocation (Ms is pulled down), which might lead to austenite stabilization.

In carbonitriding processes, the primary observable facts are the carbon and nitrogen transfer from the global furnace atmosphere to the steel and the carbon and nitrogen diffusion absorbed to the inner case.

3.5 Gas transfer and furnace atmosphere control

Considering a gas flow, acting onto a part surface in which the part is heated and carbonitrided, there are three distinct areas to consider:

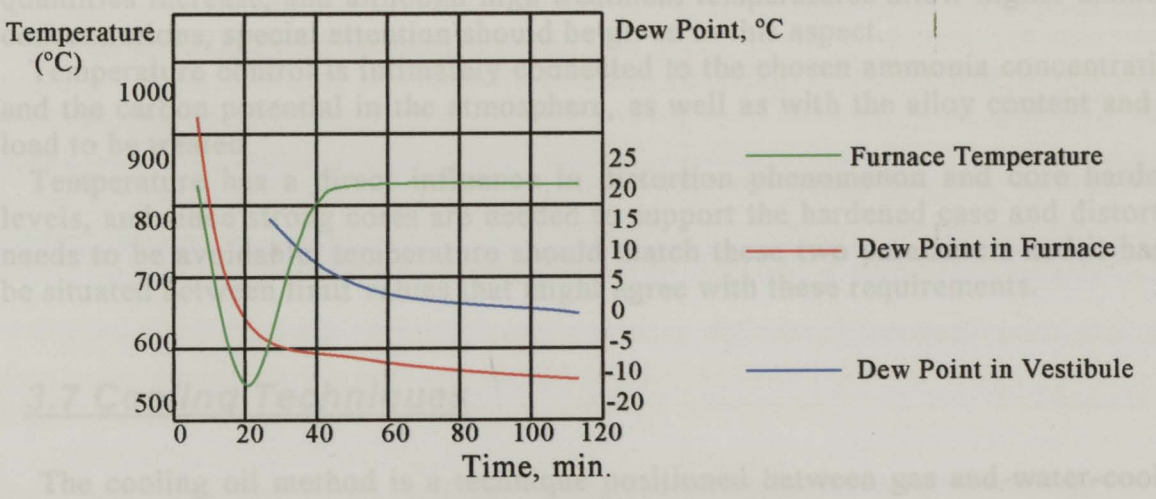
Area 1: Located at a considerable distance from the heated part, molecules move towards the part, with the gas flow, as if the load was not present;
Area 2: At a very short distance from the part surface, below a considered limit atmosphere case (of approximately 10μm thick), the gas density is much superior and the molecules mobility is much lower than in area 1 'outer gas';

Area 3: Molecules in direct contact with the surface are now adsorbed. A monomolecular case is formed, in which the carbonitrided reactions take place.

The carbonitriding atmosphere composition should be carefully controlled for consistent results. After the rate of ammonia flow and treatment temperature have been established, the ammonia flow must be held to limits of about ±10% of predetermined flow gage reading.
Because of the usually lower carbon content of the carbonitrided case, the lower operating temperature used in this process that makes possible the superior dew points and higher carbon dioxide quantities, and the higher hardenability of the obtained shell, greater latitude is possible for control parameters (water vapour, oxygen levels, carbon dioxide, and/or methane compounds) than for the same steel process by carburising methods. So, carbon dioxide levels will not be the same in carburising methods and in carbonitriding processes for the above stated reasons.

If ammonia concentrations are higher (e.g. 5%), the carbon potential remains fairly constant and of course, nitrogen concentrations will become higher as penetration capability gets higher, increasing distance below surface infiltration (higher case depth), as dew point effect on carbon and nitrogen concentrations remains the same as the one observed for the example represented on graphic 9.

Another interesting factor to be studied regarding atmosphere control and understanding is the one related with the different atmosphere constituents' values when both furnace and vestibule atmospheres are considered.
The variation of furnace temperature with time, and its relation with dew point levels in the furnace and in the vestibule at different times during the carbonitrided cycle is shown in the next graphic:



Graphic 4 – Effect on gears carbonitrided in a batch-type furnace. Dew points in the furnace and vestibule at various elapsed times. Ref. 2.

For high loads and high furnace dimensions, there are furnace areas where temperatures may be decreased for some particular reason, especially at the end of the cycle. This brings a problem regarding case homogeneity for all parts to be treated, and the three areas previously considered for gas flow furnace activity may not be exactly equal for all gear parts. Consequently, different case depths and compositions may be obtained, which brings dimensional and therefore, future functional problems to the treated gear parts.

That is why it is so important to introduce the mixture of carburising gas and ammonia at frequent intervals over the length of furnace, mostly in problematic furnace regions where temperature is decreased or the gas mixture is insufficient, although it is advantageous to introduce ammonia only to those areas where working temperature is equal to the operating temperature for carbonitriding.

3.6 Temperature control

The most important factors to take into account in carbonitriding temperature selection are:

- Steel composition and load level;
- Furnace dimensions and overall equipment;
- Dimensional control;
- Fatigue and wear resistance;
- Microstructural constituents;
- Cost (energy, time, man work, etc.).

To reduce retained austenite, ammonia content must be reduced as the alloy quantities increase, and although high treatment temperatures allow higher ammonia concentrations, special attention should be given to this aspect.

Temperature control is intimately connected to the chosen ammonia concentrations and the carbon potential in the atmosphere, as well as with the alloy content and the load to be treated.

Temperature has a direct influence in distortion phenomenon and core hardness levels, and since strong cores are needed to support the hardened case and distortion needs to be avoidable, temperature should match these two parameters and it has to be situated between limit values that might agree with these requirements.

3.7 Cooling Techniques

The cooling oil method is a technique positioned between gas and water-cooling techniques. Cooling oil is maintained in a range of temperatures between 50 and 80°C.

Its major inconvenience is the inevitable greasy surface material creation. The main advantages are the satisfactory cooling velocities obtained for a great number of steel alloys as well as a superior cooling uniformity for all pieces.

Gas quenching may be used for low mass parts, where the use of gas vapours reduces possible part distortion. There is a gas quenching capability that should be taken into account when loading the furnace; therefore, load must be correctly positioned and distributed so it does not exceed the gas quenching capability.

For parts admitting a certain level of distortion, steel parts of low carbon content may be water quenched. This cooling method is often restricted to furnaces that contain a vestibule where load may be transferred before the cooling technique takes place, so that the furnace atmosphere becomes protected from water vapour.

Ammonia is extremely soluble in water and extremely corrosive especially to cooper-base materials. In continuous furnaces where water becomes exposed to an atmosphere containing ammonia these type of materials must be avoided.

4. Case Composition

The composition of a carbonitrided shell depends on the type steel and also on the process variables of time and temperature, and atmosphere composition.

Carbonitrided is often used to impart a hard, wear resistant case generally from 0.075 to 0.75 mm deep.

As understandable through previous chapters, the addition of a carbonitrided surface raises the residual tension of compression level in the carbonitrided case, improving contact fatigue resistance and resistance gradient through the carbonitrided case.

Microscopic analysis reveal a certain visual difference between core and case depth. As visible in the next image, case depth is easily distinguished, though at a higher zoom level, colours will have a different appearance.

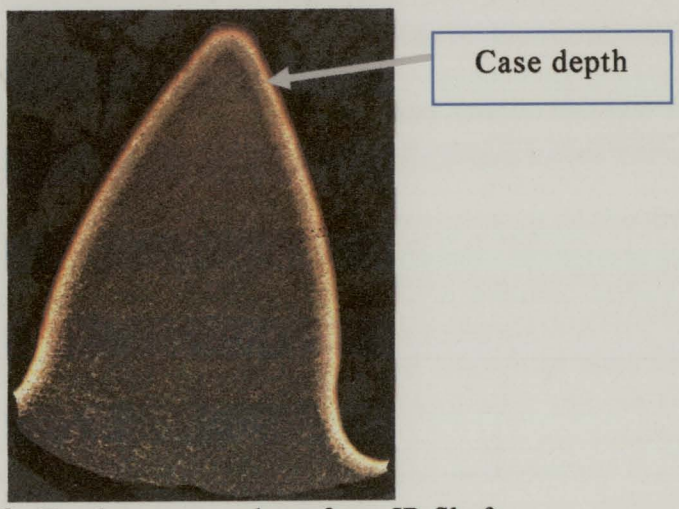


Figure 3- Tooth transversal cut from JR Shaft.

It is an important factor to be able to know the exact material microstructures after carbonitriding and, case and core microstructure are both easier to identify when the pieces are obtained by carbonitriding at low temperatures, particularly for relatively thinner shells.

It is harder to identify case and core microstructures for:

- Higher carbonitriding temperatures;
- Higher case depths;
- Higher-carbon quantities.

Whether or not the core as a martensitic structure is also a contributing factor in case-depth measurements.

Case depth uniformity obtained, depends on:

- Adequate atmosphere circulation and replacement;
- Temperature uniformity inside the furnace;
- Treatment time control;

- Uniformity of load furnace positioning so that all pieces (parts), are exposed uniformly to the furnace temperature;
- Part temperature before carbonitriding atmosphere exposure. All parts should be at a uniform temperature before being expose to the carbonitriding atmosphere.

A shallower depth of case and higher case depth homogeneity will be obtained for steels containing high quantities of powerful nitrite formers, such as Aluminium and Titanium.

There are other factors that have a direct influence in varying case depth, as superficial hardness and case stiffness gradient, as well as part dimensions and the cooling environment.

Depth of case also depends on the future service application of the steel being treated as well as on material's stiffness, especially core hardness.

5. Gear Quality-geometrical accuracy

5.1 High performance

The benefits of having higher gear tooth geometrical accuracy or quality can be increased gear life at a given load, increased load capacity at a constant life, or reduced noise generation. Higher quality numbers, correlate with more accurate gears. Gears are considered very accurate when tolerances, or acceptable variations from theoretically correct tooth forms, are very small. The theoretically correct tooth form is defined by the parameters tooth lead, tooth involute profile, tooth spacing, and run out.

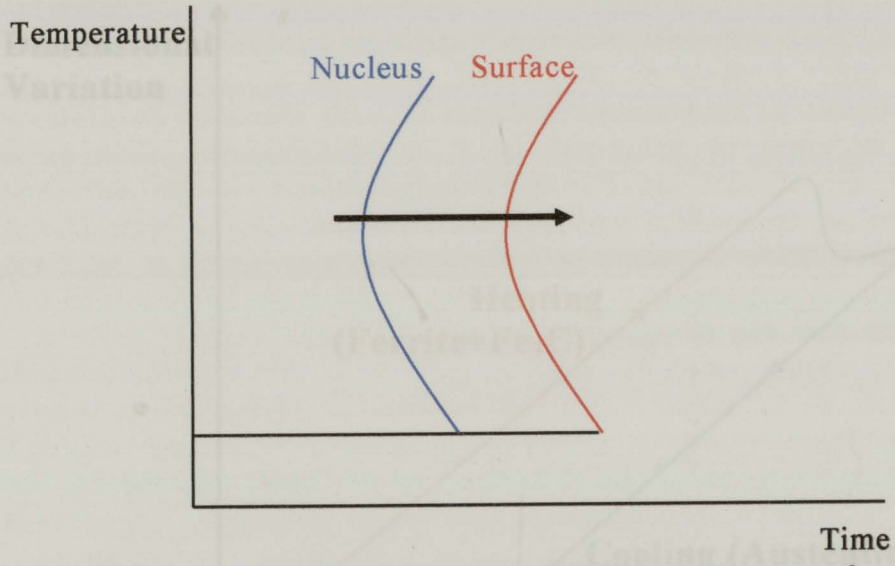
Transmission gears and shafts' high performance is associated with high mechanical quality levels. Such high gear quality can only be obtained from the combination of tough, through-hardened cores and hard, long wearing surfaces.

If, in during or post production periods, case hardened shells acquire important levels of retained austenite, the possibility of tough, long wearing surfaces is highly diminished.

Theoretically, perfect gears will exhibit constant angular velocity of the driven gear when the driving gear is rotated at a constant angular velocity. If there is no change in angular velocity as the output gear rotates, there is no angular acceleration or deceleration of the mass elastic system, and therefore no dynamic loading occurs on the gear teeth. Angular acceleration is basically the rate of change of angular velocity with respect to time. Theoretically perfect gears will also exhibit a smooth transfer of torque from tooth pair to tooth pair with no shock loads and no interference of engaging teeth. Gear tooth geometric quality is important in reducing loads due to rotating dynamic forces. The gear dynamics can cause impacts of the gear teeth, which are a source of noise generation as the gear pair rotates transferring torque from one tooth pair to the next. As a general rule, the higher the rotational speed of a gear set, the higher the gear set quality number should be.

5.2 Dimensional variation and its relation with the basic principles

Moving curves to right brings higher temperability, and as case composition holds higher amounts of nitrogen, case temperability should be higher than nucleus temperability and so cooling curves are also positioned differently.



Graphic – Temperability: nucleus e surface.

Consequently, when nucleus volume it is already decreasing, case volume it is still expanding. This phenomenon may possibly endorse distortion, which is comprehensible given the difference of expansion and contraction timings between surface and core part. This behaviour becomes more critical when dimensional tolerances are very low and geometrical accuracy and geometry are elements of high importance to the future part application.

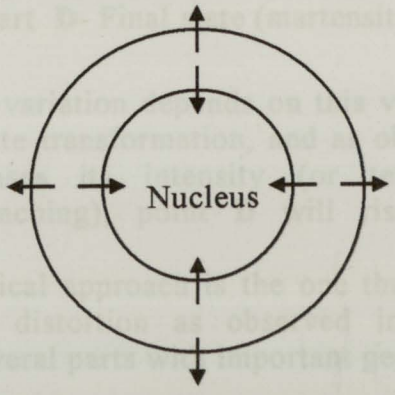
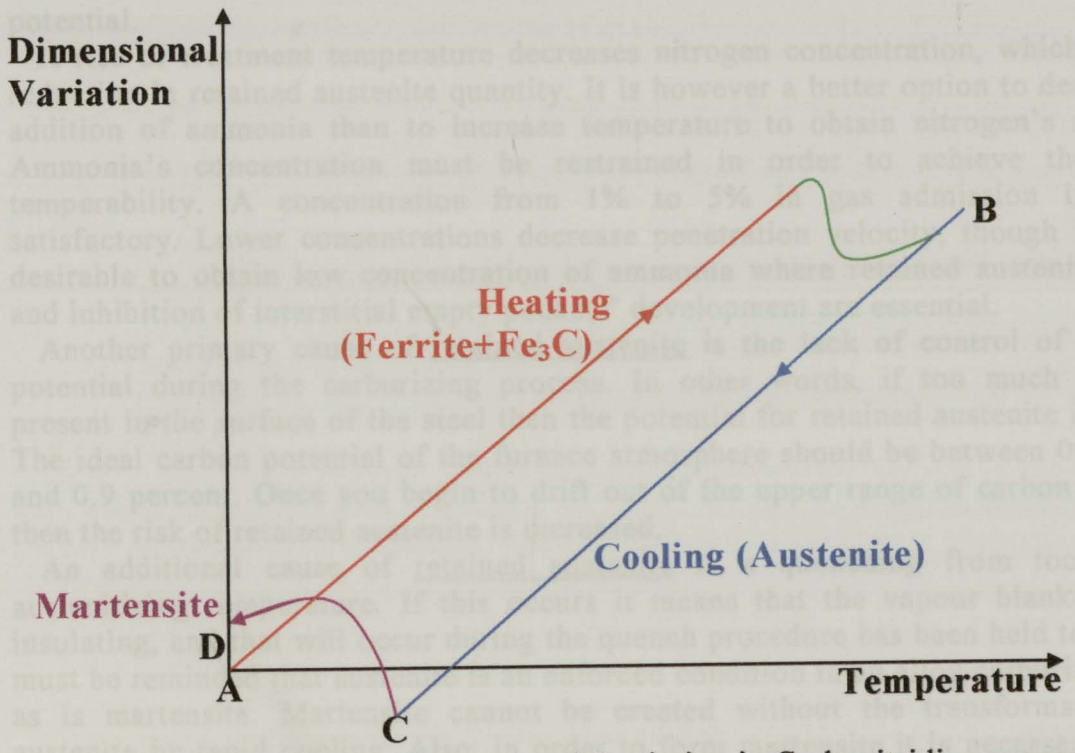


Figure 19 – Expansion timing between nucleus and surface.

The distortion phenomenon is therefore the most important geometrical problem to solve in a carbonitriding process, especially when treating gearbox parts where geometrical accuracy is extremely important.

Throughout heat treatment process, variations in the dimensional properties are produced, and depending on the part geometry and on the degree of such variations distinct dimensions are obtained.

In the next diagram, in green, is possible to observe the volumetric hysteresis that occurs in the transition between heating and cooling stages. This difference in the geometry is also due to the difference between the temperability of nucleus and surface.



Graphic 51 – Temperature-Dimensional Deviation in Carbonitriding processes.

Legend: **A**- Initial state **B**- Austenitizing temperature
C- Martensite start **D**- Final state (martensite finish)

The final dimensional variation depends on this volumetric difference established in the austenite-martensite transformation, and as observable in the diagram, as the cooling process increases its intensity (or temperature difference between carbonitriding and quenching), point **D** will rise, meaning higher volumetric expansion.

Another difficult physical approach is the one that indicates no relation between volume expansion and distortion as observed in the several subzero cooling treatments induced to several parts with important geometrical differences.

6. Control of undesirable structures

6.1 Control and reduction of retained austenite

The best way to reduce retained austenite is through a precise selection of the appropriate alloy steels and also through a correct process variables control such as the ammonia concentration, carbon potential, treatment temperature or carbon potential.

A rise of treatment temperature decreases nitrogen concentration, which means a reduction in retained austenite quantity. It is however a better option to decrease the addition of ammonia than to increase temperature to obtain nitrogen's reduction. Ammonia's concentration must be restrained in order to achieve the desired temperability. A concentration from 1% to 5% in gas admission is usually satisfactory. Lower concentrations decrease penetration velocity, though it may be desirable to obtain low concentration of ammonia where retained austenite control and inhibition of interstitial empty pockets' development are essential.

Another primary cause of retained austenite is the lack of control of the cabin potential during the carburizing process. In other words, if too much carbon is present in the surface of the steel then the potential for retained austenite is present. The ideal carbon potential of the furnace atmosphere should be between 0.7 percent and 0.9 percent. Once you begin to drift out of the upper range of carbon potential, then the risk of retained austenite is increased.

An additional cause of retained austenite is a quenching from too high an austenitizing temperature. If this occurs it means that the vapour blanket, that is insulating, and that will occur during the quench procedure has been held too long. It must be reminded that austenite is an enforced condition in an alloy carburizing steel, as is martensite. Martensite cannot be created without the transformation from austenite by rapid cooling. Also, in order to form martensite it is necessary to have carbon present in sufficient amounts when the steel is rapidly cooled. A further reason for the development of retained austenite is if the quench medium is too slow, then the critical cooling rate necessary to form martensite, will drift into the incubation area. So it is necessary that very careful control be incorporated to the whole process.

For instance, using nickel - an austenite stabiliser - is a problem if proper homogenisation does not occur during sintering. During low temperature exposure, retained austenite undergoes transformation and creates stresses within the structure, resulting in premature part failure.

Whenever there are compelling reasons for almost eliminating residual austenite phase in the microstructure, problems develop into a complex enigma.

Over time, retained austenite will decompose to untempered martensite. In carbonitriding, retained austenite will leave mixed phases in the formed case, which can lead to dimensional instability.

Retained austenite in a martensitic microstructure is especially undesirable in carbonitrided parts used in close-fitting assemblies. In these cases, the retained

austenite not only lowers hardness, but it also could bind or "seize up" during operation due to the volume increase throughout transformation.

Excessive retained austenite in tool steels usually is detrimental to die life, because it may transform into fresh martensite and cause cracking in the die, or reduce die wear resistance. In the case of a carburised gear tooth, retained austenite it is detrimental though gear teeth typically are not shock loaded. A good possibility is that the retained austenite would transform into martensite and the toughness of the austenite, when stabilized, could be beneficial.

As a brief conclusion on the factors that might increase or prevent retained austenite in a carbonitriding process, the risks involving retained austenite are minimized through proper ruling of several controlling aspects of the carbonitriding process:

- An increase in furnace temperature reduces the nitrogen content at the outer segments of the case, thus minimizing the amount of retained austenite. To do so, it is better to reduce the ammonia content, rather than increasing the temperature to reduce nitrogen content.
- Lowering carbon potential will reduce retained austenite.

The ammonia content should be restricted to a minimum required to obtain the desired level of hardenability. Levels of ammonia between 1 and 5% in the inlet gas are usually desirable; a lower quantity decreases the rate of penetration but it will prevent the appearance of retained austenite and might avoid case porosity.

6.2 Porosity and voids prevention

Under surface porosity in the recent created hard outer layer is associated with the excess of ammonia added to the furnace atmosphere.

The existence of such kind of porosity is also related with the rise of treatment temperatures, higher values of nitrogen and carbon as well as the addition of ammonia during the heating cycle.

However, the risk of this type of defect diminishes with the introduction of more elements to the steel.

Voids and sub-superficial porosity may appear in the carbonitrided case if the several process variables are not correctly adjusted. So, the possibility of void and porosity formation rises with:

- Temperature rise;
- Longer carbonitriding treatment cycles;
- Higher quantities of carbon and nitrogen in the carbonitrided case;
- Hard, cold work of the material before treatment;
- Higher additions of ammonia during the carbonitrided cycle;

Voids might be prevented whenever is possible, by the introduction of higher element's percentage to the steel.

7. The four case studies

1. **Aiming for higher hardness: Different hardness levels for two similar parts having the same heat treatment cycle (engine balancing machine: Z41 left and right pinions);**

2. **Comparing Z41 left and right pinions: distortion study**

3. **Comparing geometrical behaviour, concerning all production operations (mainly heat treatment), of two parts having very distinct inner diameters: JC4 and G9T distortion study;**

4. **Assembling PF5 (Pinion 5th Fix) and JR Shaft (Sec. Shaft). Assembling effort values, geometrical and hardness assessment and its relation with in service failure. Quantifying retained austenite and studying its relation with the previous investigated parameters: hardness, distortion and residual stresses;**

7.1Aiming for higher hardness: G9T Z41 left and G9T Z41 right pinions

7.1.1 Results and discussion

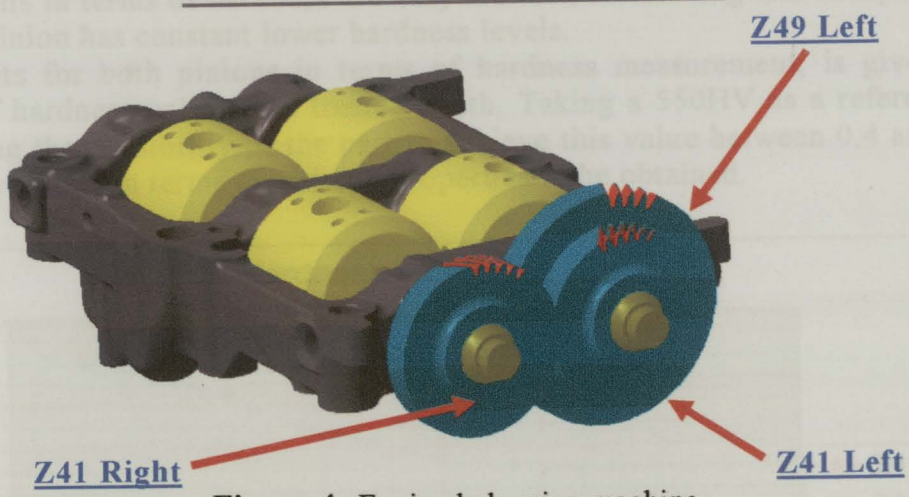


Figure 4- Engine balancing machine.

All engine balancing machine pinions are subjected to three different major machining/production operations: hobbing, heat treatment process (which includes carbonitriding, quenching, tempering and shot peening) and grinding. Operations being conducted by this exact order.

Regarding heat treatment, there is a carbonitriding and quenching cycle to follow and both parts are treated in the previous represented furnaces.

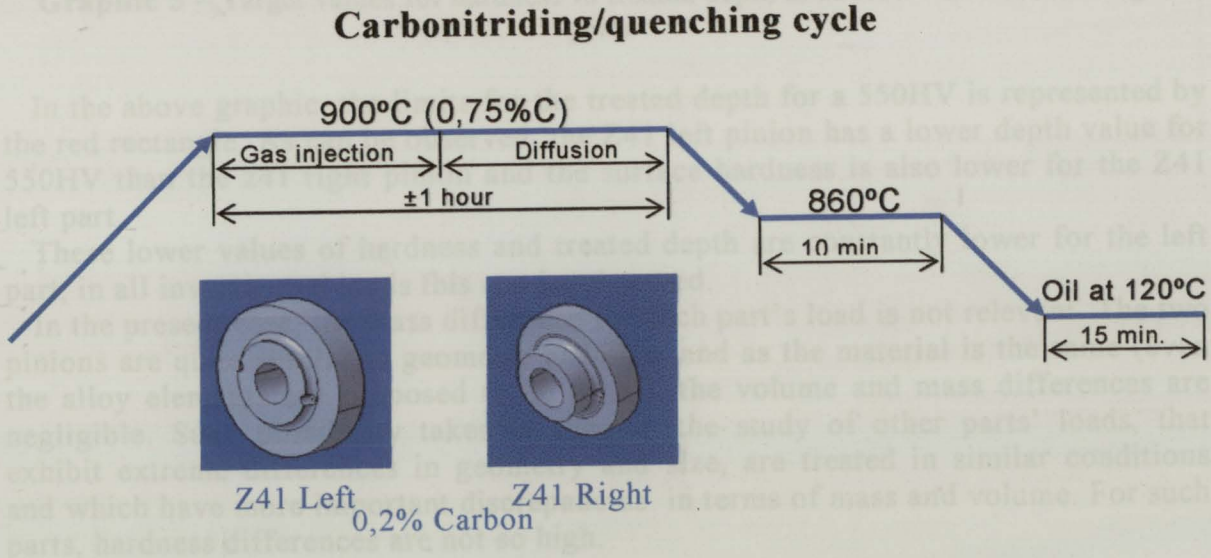


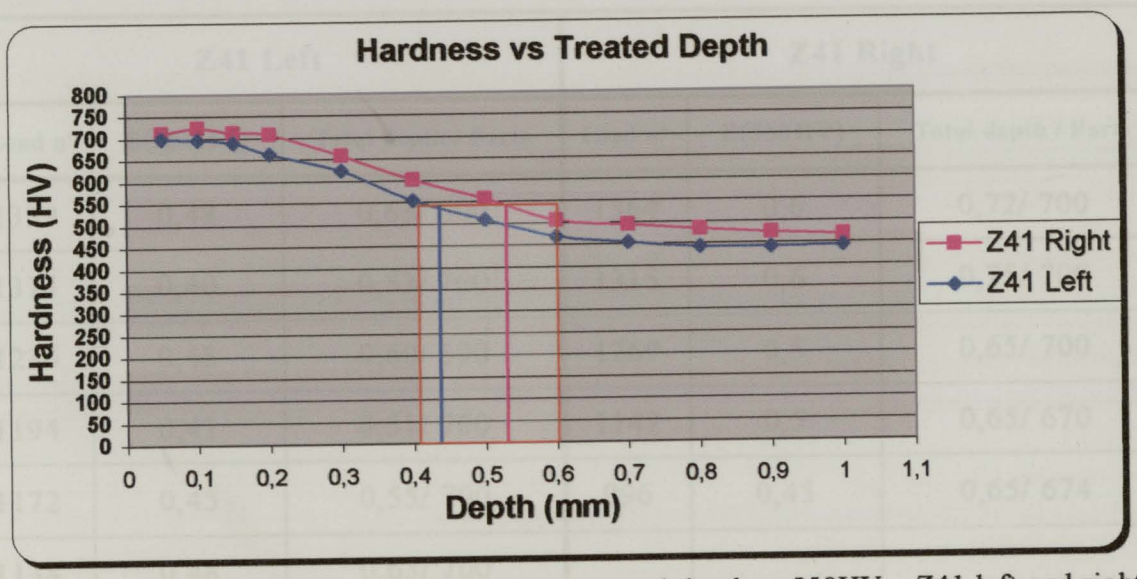
Figure 5 – Carbonitriding/ quenching cycle for Z41 left and right parts.

Carbon potential is set at 0,75%, and ammonia flow at 125 *l/h*. Accurate control of carbon potential is possible whilst control of nitrogen percentage in the treatment furnace atmosphere is impossible and so, several changes in the ammonia flow were made in order achieve better results.

It is then understandable that carbon is scientifically controlled whereas ammonia can only be controlled experimentally.

The results in terms of hardness are very distinct, concerning this two pinions. The Z41 Left pinion has constant lower hardness levels.

The limits for both pinions in terms of hardness measurement, is given for the relation of hardness values and treated depth. Taking a 550HV as a reference value and limiting the possibility of the part to achieve this value between 0,4 and 0,6 *mm* an objective is set in terms case depth properties to be obtained.



Graphic 5 – Target values for hardness *vs* treated depth at 550HV – Z41 left and right parts.

In the above graphic, the limits for the treated depth for a 550HV is represented by the red rectangle. As can be observed, the Z41 left pinion has a lower depth value for 550HV than the z41 right pinion and the surface hardness is also lower for the Z41 left part.

These lower values of hardness and treated depth are constantly lower for the left part, in all investigated loads this can be observed.

In the present case, the mass difference for each part's load is not relevant. The two pinions are quite similar in geometry and size, and as the material is the same (even the alloy elements are supposed to be equal), the volume and mass differences are negligible. Such possibility takes in account the study of other parts' loads, that exhibit extreme differences in geometry and size, are treated in similar conditions and which have more important discrepancies in terms of mass and volume. For such parts, hardness differences are not so high.

In the next board of results taken for several loads, the results for both parameters are related with the number of parts taken for each one of the studied loads. This analysis of the relevant parameters and its connection with mass and volume inside the furnace is sometimes vital to properly access the results and take relevant conclusions.

Theoretically, there is sometimes the idea that as mass and volume decreases, higher quantities of ammonia and/or carbon inside the treatment atmosphere are required for higher adsorption and diffusion, because more space is left in the furnace atmosphere. However, as observed in the next board, the loads with less parts (for the Z41 left part), are the ones exhibiting poorer results. Plus, the studied mixed load (n°1068), indicates once more, lower values for the left pinion, which shows that the carbon absorption is not equal for both parts.

Z41 Left			Z41 Right		
Load n°	E(550HV)	Total depth / Parts	Load n°	E(550HV)	Total depth / Parts
1339	0,48	0,63/ 600	1364	0,6	0,72/ 700
1314	0,40	0,53/ 700	1315	0,6	0,75/ 700
1236	0,48	0,60/ 690	1269	0,5	0,65/ 700
1194	0,41	0,51/ 700	1142	0,5	0,65/ 670
1172	0,45	0,55/ 700	996	0,45	0,65/ 674
1138	0,48	0,63/ 700			
944	0,5	0,65/ 600			
1068	0,45	0,58/ 380	1068	0,5	0,64/ 350

Board 1- Treated depth at 550HV and total treated depth analysis for several loads (G9T Z41 left and right).

Interpreting the results, it is easy to conclude that hardness and total depth values are lower for the Z41 pinion, which confirms the previous obtained results for the treated depth comparison between both parts.

Assumption: The left part needs higher hardness. To obtain so, more carbon or more nitrogen is needed in the case hardened. As ammonia control is extremely difficult and an ammonia's flow change result is highly uncertain, whilst carbon adjustment is a more viable possibility, in terms of variable control.

The lack of carbon absorption should be due to an unexpected difference of carbon quantity in large majority of the Z41 left parts. Assumption is that Z41 left part requires a higher carbon potential during heat treatment.

The consequences of such assumption should be accessed.

There is a higher probability of obtaining retained austenite with the rise of carbon potential and analysing the heat treatment cycle, taking in account that 900°C is the treatment temperature, this risk is revealed at this stage, as a logical possibility.

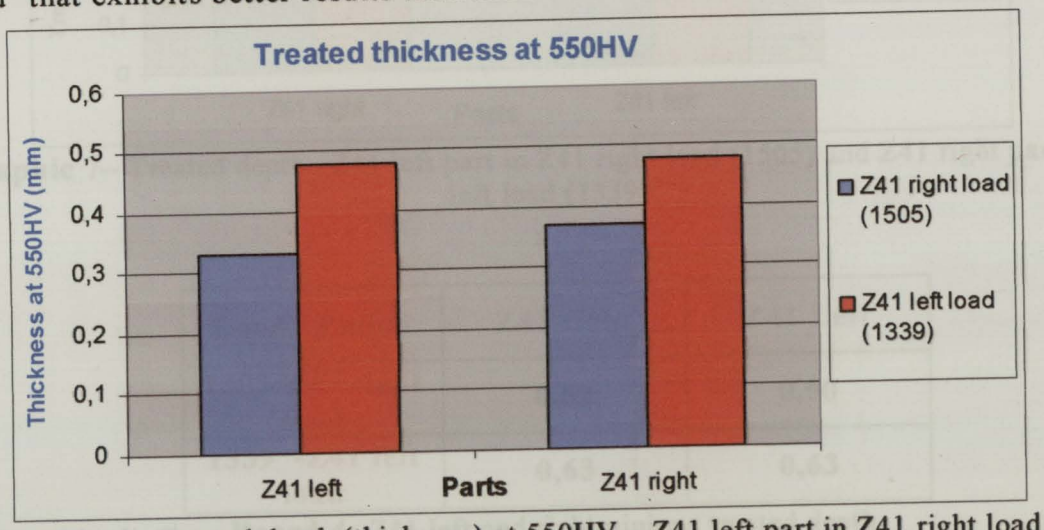
Analysing the average and variance of last board's results:

Z41 Left			Z41 Right		
mm	E(550HV)	Total depth	mm	E(550HV)	Total depth
Average	0,45	0,58	Average	0,53	0,68
Variance	0,00149	0,003	Variance	0,0045	0,0023

Board 2- Average and variance. Hardness and total treated depth analysis.

It is possible to observe the difference between hardness and depth levels between two parts. Though variance values are low, especially for the treated depth at 550HV for the Z41 left part, taken in account that the dispersion is considerable (maximum and minimum values), no major conclusions can be drawn from variance results but dispersion indicates not only a problem of hardness but also that enhances the variation of results, indicating that the problem is not solved.

To access the behaviour of 'left parts' in 'right loads' a Z41 left pinion was positioned in a Z41 right load. The next graphic represents an abnormal situation. A 'left part' is added to a non-conform 'right load' and a 'right part' is added to a 'left load' that exhibits better results than usual.



Graphic 6– Treated depth (thickness) at 550HV – Z41 left part in Z41 right load (1505) and Z41 right part in Z41 left load (1339).

Simplifying the above graphic the results for treated depth at 550 HV are:

Load / Pinion	Z41 right	Z41 Left
1505-Z41 right load	0,37	0,33
1339 -Z41 left load	0,48	0,48

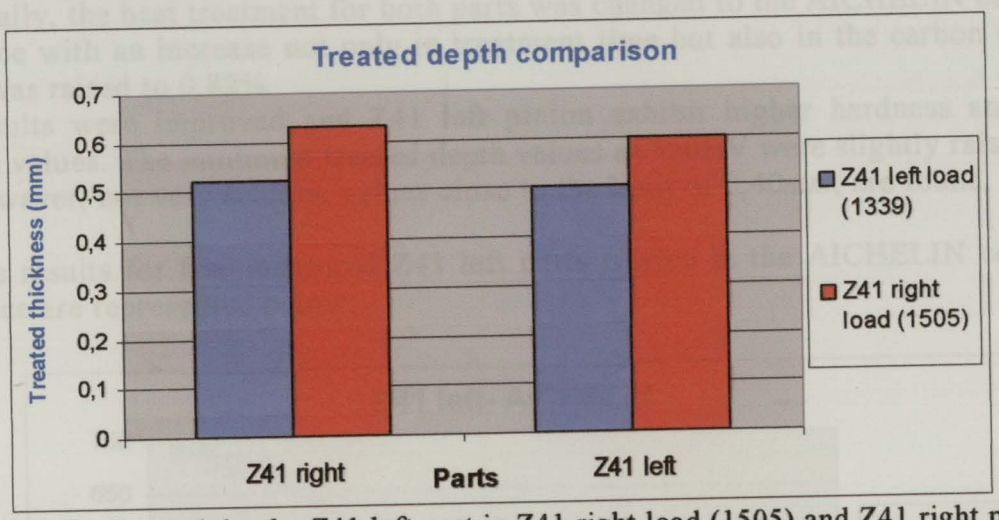
Board 3- Z41 left and right pinions depth at 550HV.

Even for a non-conform 'right load', the values for the Z41 left part are lower, and for the Z41 left load (1339), which has unusually high treated thickness values (at 550HV), the right part also exhibits good results.

This might point to a lower carbon absorption for the left part (load 1505), whereas right part is able to reach the good hardness result obtained for all 1339 'left load'.

These results, sustain the possibility of the existence of carbon percentage in a great number of Z41 left parts.

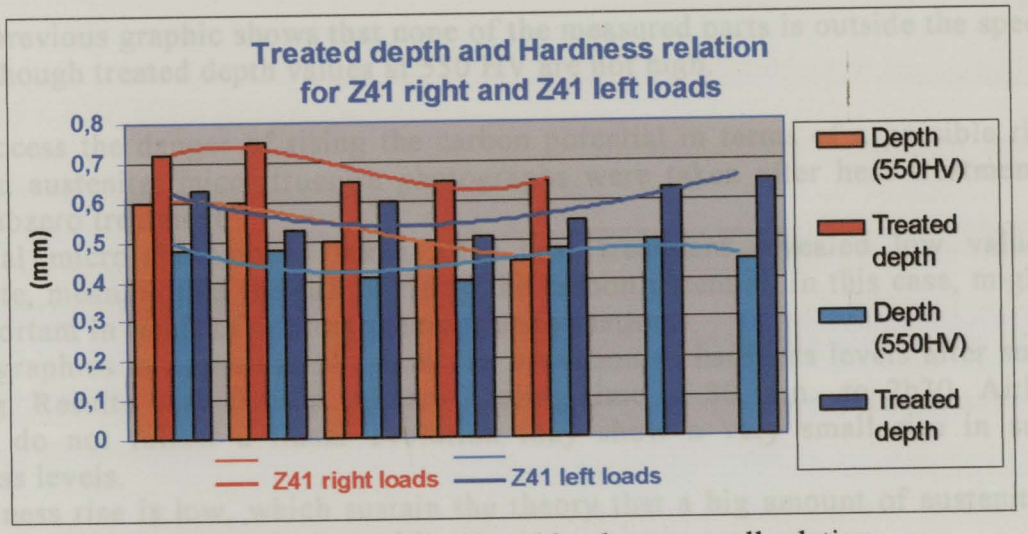
The following graphic completes the information given by the previous one. This time and for the same loads the treated depth is represented in the same manner.



Graphic 7– Treated depth– Z41 left part in Z41 right load (1505) and Z41 right part in Z41 left load (1339).

Load / Pinion	Z41 right	Z41 Left
1505-Z41 right load	0,52	0,50
1339 -Z41 left load	0,63	0,63

Board 4- Z41 left and right pinions treated depth.



Graphic 8– Treated depth and hardness overall relation.

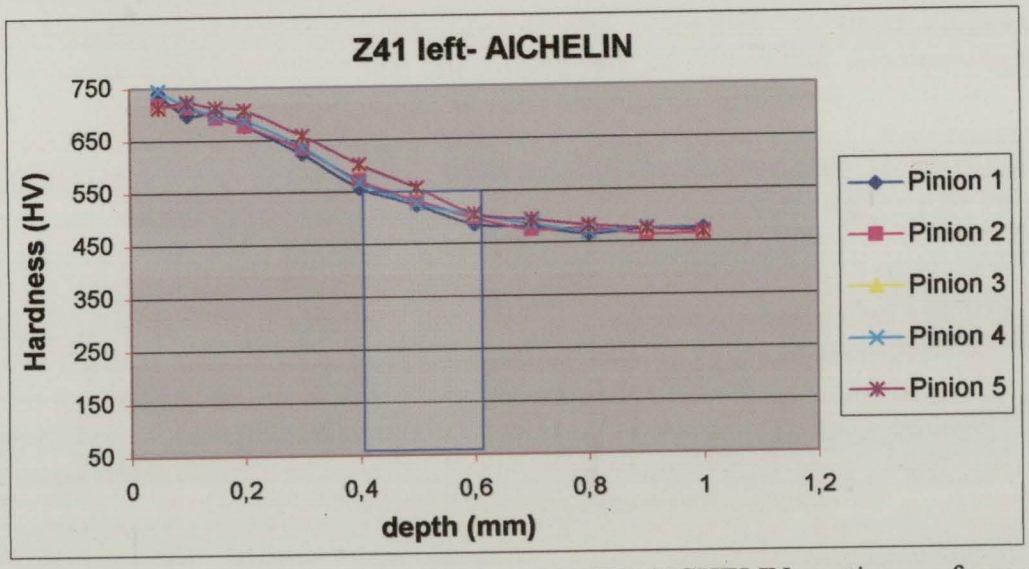
The results for the overall treated depth also sustain the same theories explained before.

Finally, the heat treatment for both parts was changed to the AICHELIN continuous furnace with an increase not only in treatment time but also in the carbon potential, that was raised to 0,82%.

Results were improved and Z41 left pinion exhibit higher hardness and treated depth values. The minimum treated depth values at 550HV were slightly raised.

However, not very seldom, values close to the limit of 0,40*mm*, are found.

The results for five measured Z41 left parts treated in the AICHELIN continuous furnace are represented below:



Graphic 9– Z41 left part treated depth at 550HV. AICHELIN continuous furnace.

The previous graphic shows that none of the measured parts is outside the specified limits though treated depth values at 550 HV are not high.

To access the danger of rising the carbon potential in terms of a possible risk of retained austenite, microstructure photographs were taken after heat treatment and after subzero treatment.

Digital micro-photographs taken after heat treatment revealed low values of austenite, meaning that the risk of rising the carbon potential, in this case, might not be important in terms of microstructure transformation.

The graphics in **appendix 10**, show the evolution of hardness levels after subzero cooling. Results vary from a subzero cooling time of 30 min., to 2h30. Although results do not follow a linear evolution they show a very small rise in surface hardness levels.

Hardness rise is low, which sustain the theory that a big amount of austenite was already transformed into a martensitic structure.

7.1.2 Conclusions

The difference of treated depth and hardness levels cannot be related with the difference of mass or volume between both parts.

The part geometry, it might be considered to be more complex for the Z41 right pinion, however, no relation can be drawn in terms of hardness variation.

Given the two previous statements and since both parts have the same heat treatment cycles, and hardness results are different, the difference must reside in the chemical composition.

Results from chemical composition assessment reveal that carbon percentage is slightly lower for the Z41 left pinion, confirming the first assumption.

The chemical composition tests may also reveal that more has to be done in terms of ammonia control, since instead of a carbon rise that might impart other micro-structural problems, a rise in ammonia levels is not so detrimental in terms of retained austenite rising.

Digital micro-photographs show that after heat treatment the retained austenite level is not important.

After subzero treatment there is no major change in hardness levels, possibly indicating that no important micro-structural changes happened during subzero cooling (no major austenite-martensite transformation). This sustains the assumption that rising carbon potential is a possibility to be taken in account.

Even though, in AICHELIN furnace, carbon potential is higher (0,82), heat treatment cycle and conditions are quite different, so, no major conclusions can be drawn from the hardness results taken in the continuous furnace.

A relevant chemical composition study should be undertaken, since there is no relevant knowledge in this subject for the majority of gear box and engine balancing machine parts.

Contrary to steels exhibiting 0,27% Carbon, Z41 Left pinion, that exhibits values near 20% Carbon, has in theory less carbon to transform (austenite- martensite), and so, in theory, lower values of austenite (giving also the lower carbon potential in heat treatment) are expected. This might explain the lower retained austenite levels encountered when compared to with JR Sec. Shaft and PF5 parts.

7.2 Z41 left and right pinions: distortion study

7.2.1 Results and discussion

Through all production process the different manufacturing stages impart distinct levels of distortion. Hobbing operations, induce important distortion levels at the gear teeth geometry.

Considering that heat treatment will provoke a rise of volume and some additional distortion in some of the most important geometrical characteristics, sometimes there is a need to adjust the process in order to take this additional geometrical deviation in account.

In terms of heat treatment is very complicated and most of the times impossible to correct the treatment parameters and variables to provoke a pre-desired change in the gear teeth geometry. Adapting the hobbing parameters to meet required future post-heat treatment geometry it is the most adequate solution to solve distortion problems.

Knowing the gear teeth geometrical differences induced by the heat treatment process, certain measures suffer a slight deviation that will be 'correct' during heat treatment. Two of the most important geometrical measurements are the run-out (Fr) and the pitch deviation (f_p), in this case the cumulative pitch deviation (Fp) is studied in detail.

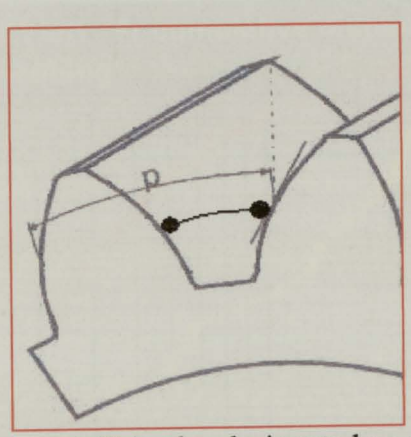


Figure 6- Run-out (Fr), also designated as concentricity.

The run-out is measured along the gear teeth, given a deviation of the distance between two tooth opposite flanks, preferentially in the theoretical contact point (primitive radius). Each obtained deviation is measured, giving a final value that is representative of the actual gear teeth concentricity.

On the other hand the cumulative pitch deviation represents the difference from the desired measure for the distance between two adjacent opposite flanks. The algebraic sum of all measures gives the total cumulative pitch deviation.

These two parameters are of vital importance to obtain an accurate characterisation of the gear teeth geometrical properties, being these measurements the most related with the part's global properties.

Other measurements exist, and though all measurements are dependent on each other, these are more related with profile, helix and superficial roughness properties rather than with the gear teeth division properties.

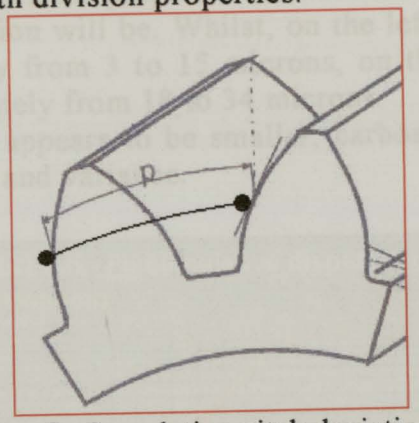
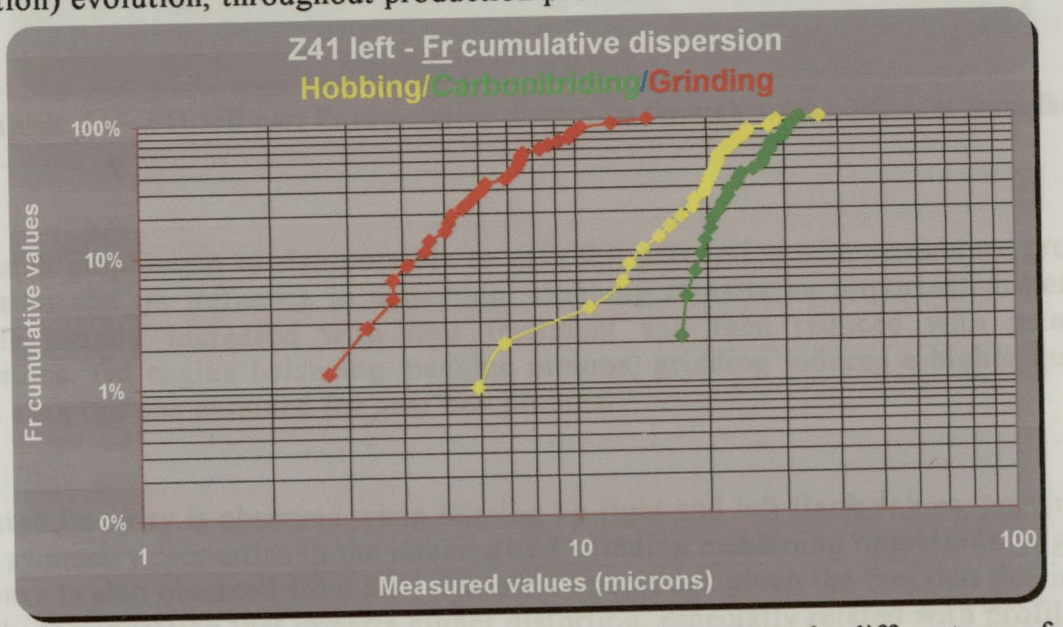


Figure 7- Cumulative pitch deviation Fp.

In terms of engine balancing machine there is a high quality hobbing when compared to the one obtained for the gear box teeth.

There is no shaving operations for the Z41 left and right pinions.

The next graphics are representative of Fr (run-out) and Fp (cumulative pitch deviation) evolution, throughout production process.

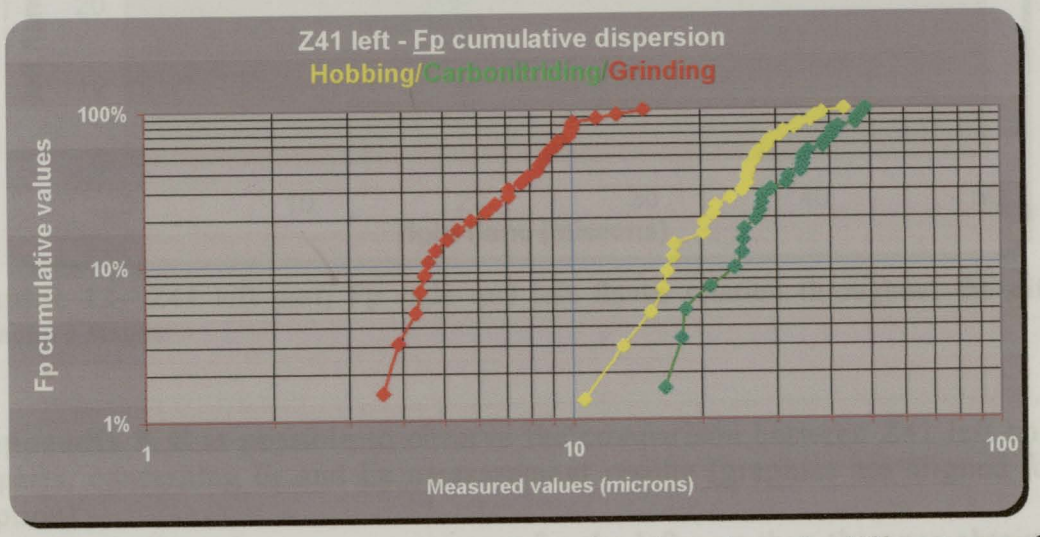


Graphic 10– Z41 left part Fr cumulative dispersion throughout the different manufacture stages.

The applied scale, a logarithmic scale, reveals a very important instrument allowing to interpret the obtained population averages and dispersion.

Two populations exhibiting the same width (distance between the lower and higher values), may have very distinct dispersions and variances, whereas the population is positioned to the left or right in the graphic. The more the population is located to the right, the higher the dispersion will be. Whilst, on the left, the dispersion values for grinding vary approximately from 3 to 15 microns, on the right, the carbonitriding population varies approximately from 18 to 34 microns.

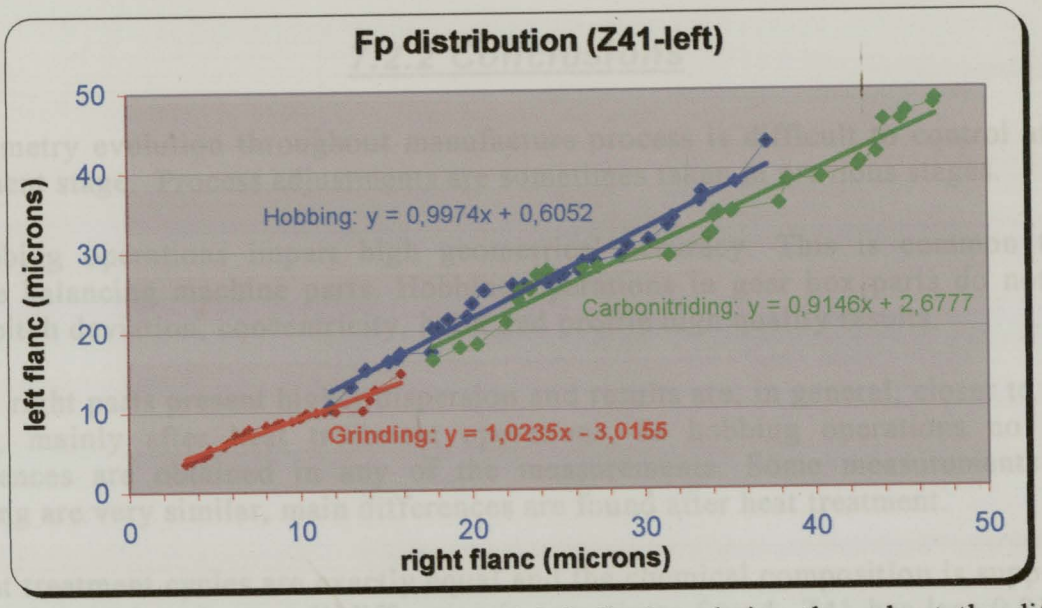
Though population width appears to be smaller, carbonitriding possesses, without any doubt higher dispersion and variance.



Graphic 11– Z41 left part Fr cumulative dispersion throughout the different manufacture stages.

In such graphics, it is also possible to gain full perception of manufacture process evolution and its influence in distortion. Hobbing imparts an important dispersion that is usually increased with heat treatment and then reduced with grinding operations. On engine balancing machine pinions, grinding induces a higher quality result than the one obtained for gear box pinions.

A high linearity is observed when relating Fp right and left flank values, proving good symmetry properties in the hobbing and grinding machining operations. A good response is also obtained from heat treatment operations given the fact that this is usually the operation that imparts higher distortion, especially related with profile and helix directional deviations and increased pitch deviations. This might be observed in the next graphic.



Graphic 12– Z41 left part, Fp right and left flanks relation throughout the different manufacture stages.

In **appendix 9**, it is possible to observe the comparison between Z41 left and Z41 right parts, concerning Fr and Fp measurement results (graphics are aligned for full perception).

The results indicate better measurements for the left part than the ones obtained for the right part. Being the heat treatment cycle exactly equal, there is a slight difference in both measures since hobbing operations, which might lead to the assumption that the small geometrical difference between the two parts is responsible for the difference. Z41 right parts are closer to upper limits than the 'left' ones.

The results encountered revealed to be inside the allowed limits and no non-conform parts were found.

7.2.2 Conclusions

Geometry evolution throughout manufacture process is difficult to control at heat treatment stage. Process adjustments are sometimes taken in previous stages.

Hobbing operations impart high geometrical accuracy. This is common to all engine balancing machine parts. Hobbing operations in gear box parts do not give such pitch deviation, concentricity, helix and profile high quality results.

Z41 right parts present higher dispersion and results are, in general, closer to upper limits, mainly after heat treatment operations. In hobbing operations no major differences are obtained in any of the measurements. Some measurements after hobbing are very similar, main differences are found after heat treatment.

Heat treatment cycles are exactly equal and the chemical composition is suppose to be equal too (though a small difference is sometimes found- Z41 has less 0,01-0,03 carbon percentage). The small deviations found in the Fp and Fr results, should happened due to the differences between both pinions.

The final tooth geometry result present not only profile and helix deviations but also an actual flank position change after hobbing and grinding operations. The space in black between green and red curves represent the final tooth profile after hobbing and grinding for G9T Z41.

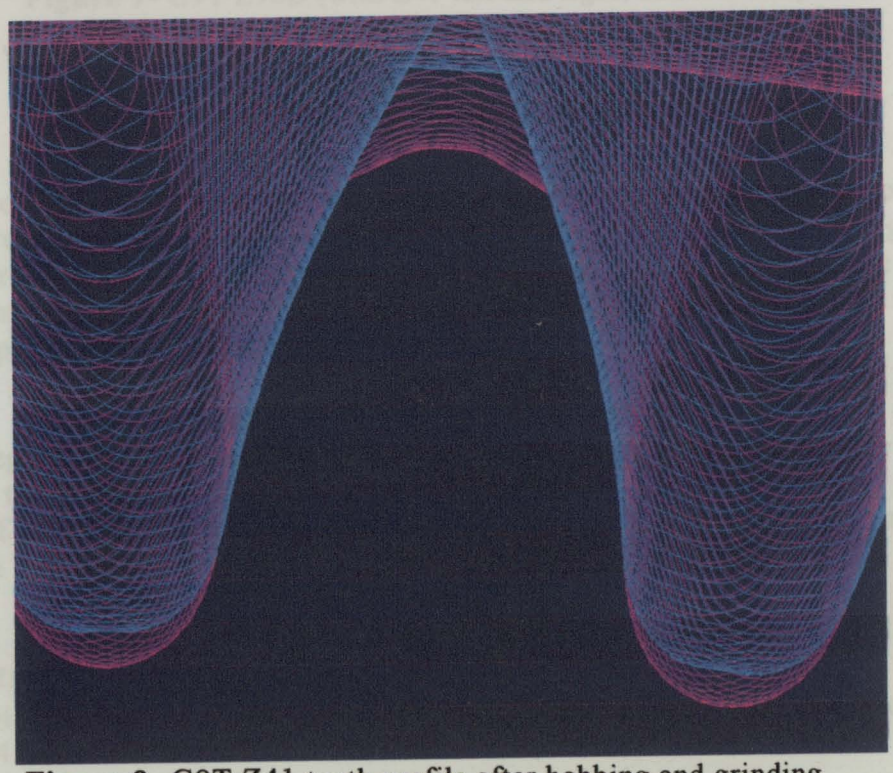


Figure 8- G9T Z41 tooth profile after hobbing and grinding.

7.3 JC4 and G9T Z98D distortion study

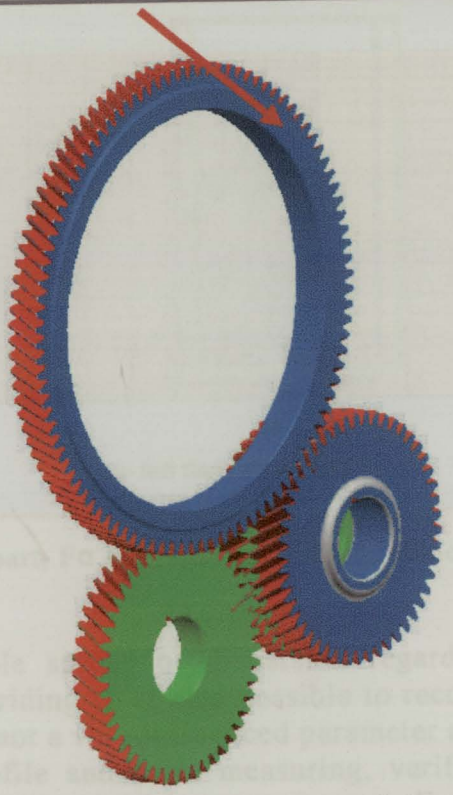


Figure 9- G9T Z98D (with Z41 left and right, and Z49 left).

7.3.1 G9T Z98D: Results and discussion

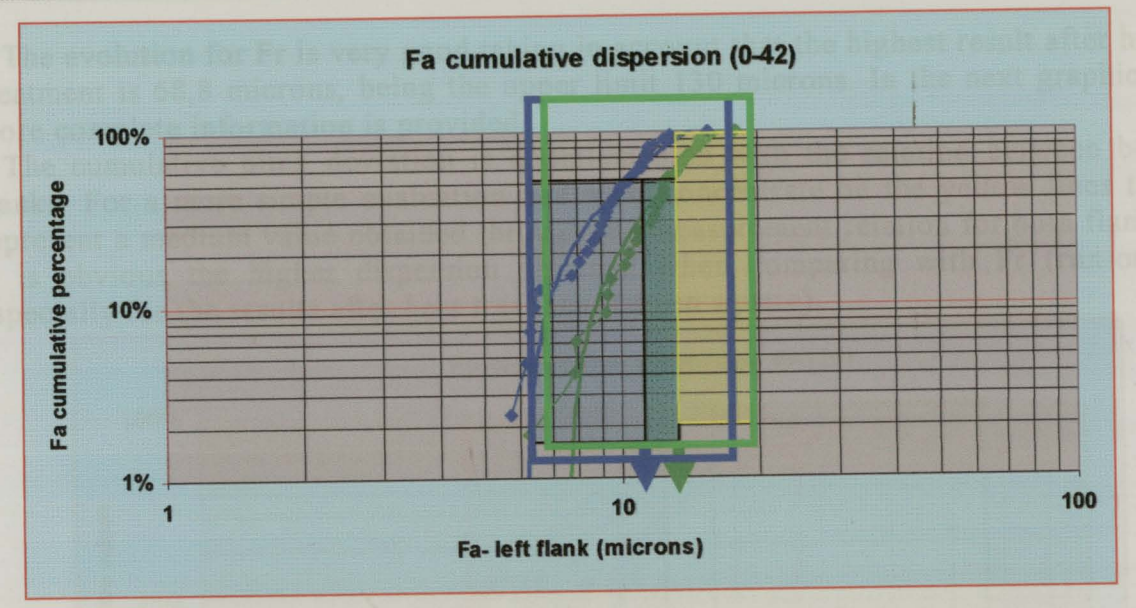
The main objective in the distortion study of such parts is obtaining a comparison of the different measurements that describe the evolution of the part's geometric behaviour through the production process, mainly after heat treatment. The analysis, allows to interpret this behaviour and conclude which are the most important geometrical parameters to be controlled for each part.

Given the different geometry observed for each part, especially the important difference regarding inner radius, some parameters may reveal more relevant than others at the time of geometry assessment.

Samples of 31 pieces were taken and studied in terms of all geometric parameters, helix, profile and division errors.

For helix parameters, non-conform parts were found extremely seldom and measurements revealed good results.

An example is the result for Fα-G9T Z98D. The upper limit for the allowed tolerance is 42 microns after heat treatment:



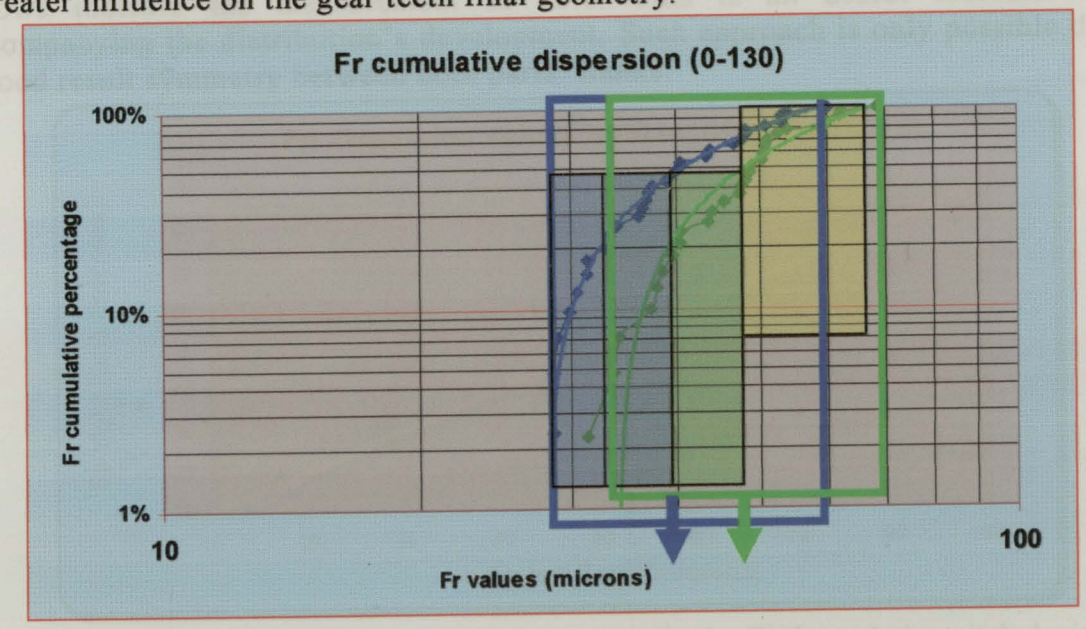
Graphic 13– Z98D left part, Fα left flank for hobbing (blue), and heat treatment (green) (0-42 microns).

There is no considerable spread or dispersion regarding Fα values both after Hobbing or after Carbonitriding. It is also possible to recognise the high linearity of the taken measures. Fα is not a very influenced parameter regarding heat treatment.

After analysing the profile and helix measuring, verifying that results are very similar both for JC4 and Z98D, division errors were studied.

The next graphic demonstrates the results for run-out and cumulative pitch deviation, where major differences were found.

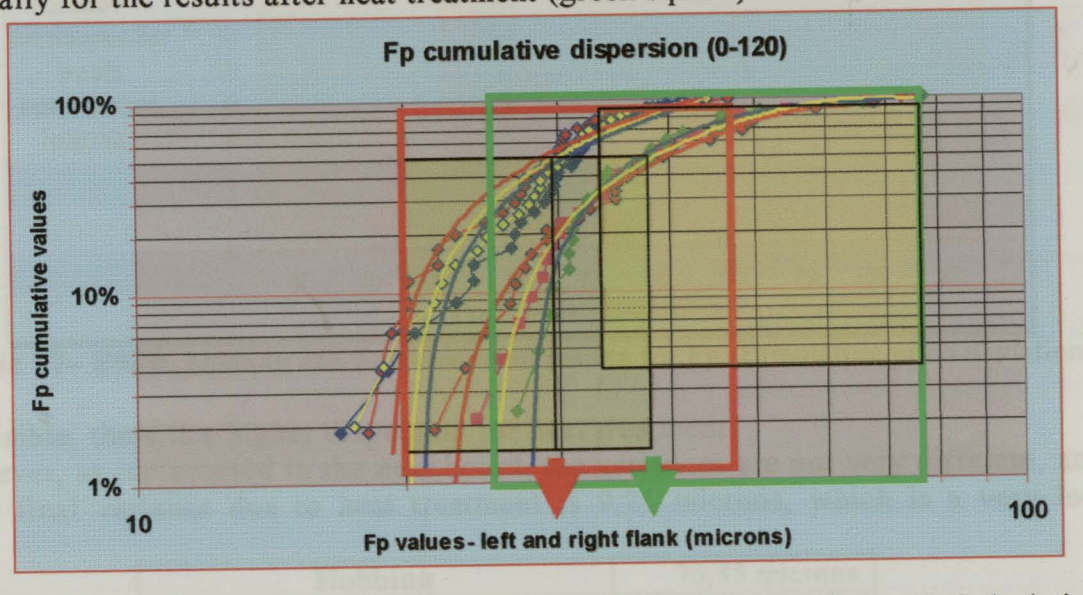
By analysing variance and dispersion is possible to determine which parameter has a greater influence on the gear teeth final geometry.



Graphic 14– Z98D, hobbing and heat treatment results for Fr (run-out).

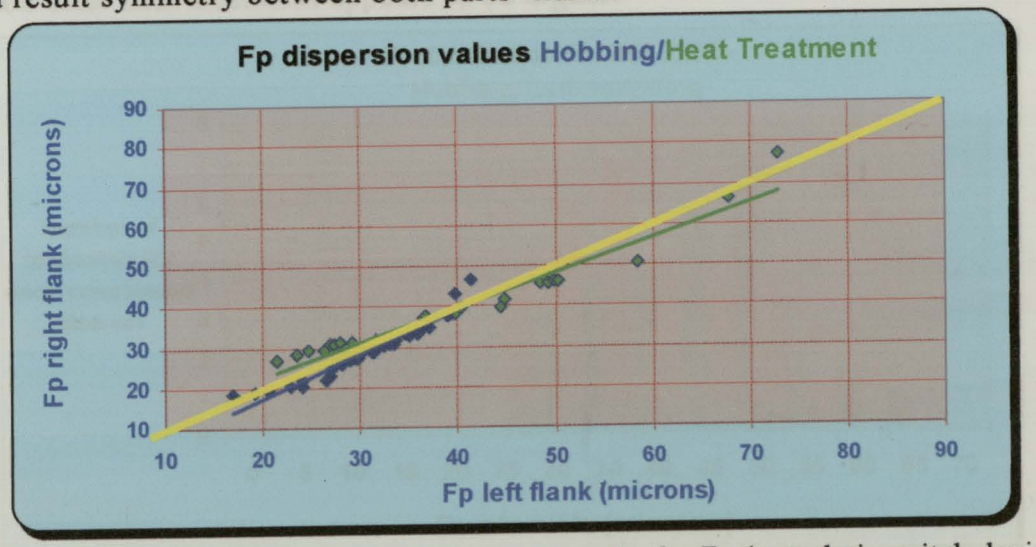
The evolution for Fr is very good taking in account that the highest result after heat treatment is 68,8 microns, being the upper limit 130 microns. In the next graphic, a more complete information is provided.

The cumulative pitch deviation is complemented with the relation between both flanks. For a more simple evaluation one must concentrate on the yellow lines that represent a medium value obtained through the measurement relation for both flanks. It is obvious the higher dispersion obtained when comparing with Fr (run-out), especially for the results after heat treatment (green square).



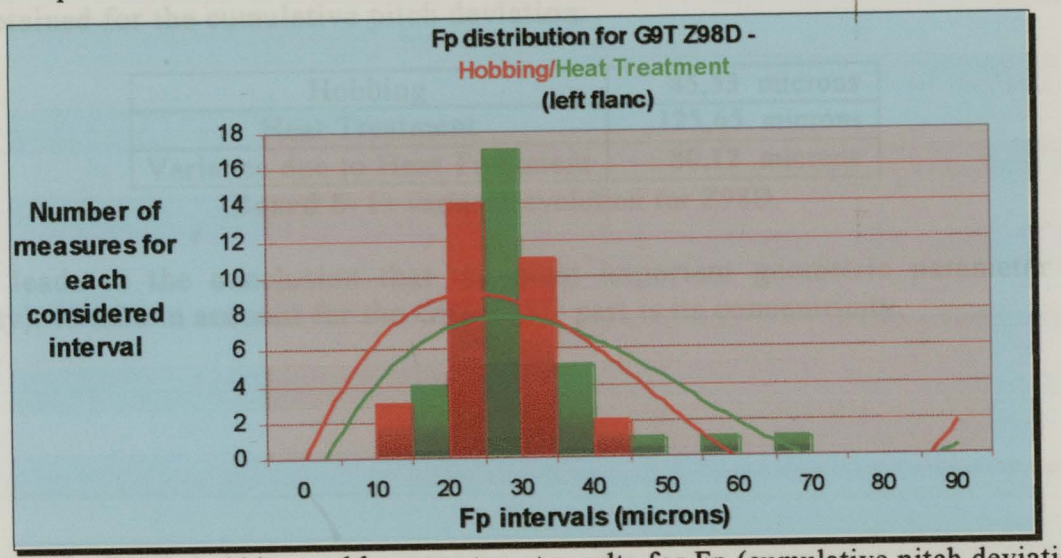
Graphic 15– Z98D, hobbing and heat treatment results for Fp (cumulative pitch deviation).

The squares allow an easier visualisation of the dispersion dimensions and the arrows indicate the measurement at 50%. This is an useful indicator when accompanying the distribution's development. Such approach is only possible due to a good result symmetry between both parts' flanks:



Graphic 16– Z98D, hobbing and heat treatment results for Fp (cumulative pitch deviation), relation between left and right flanks.

For full interpretation of the previous logarithmic graphics is now applied a more common representation for the distortion evolution, both for Fr and Fp:



Graphic 17– Z98D, hobbing and heat treatment results for Fp (cumulative pitch deviation).

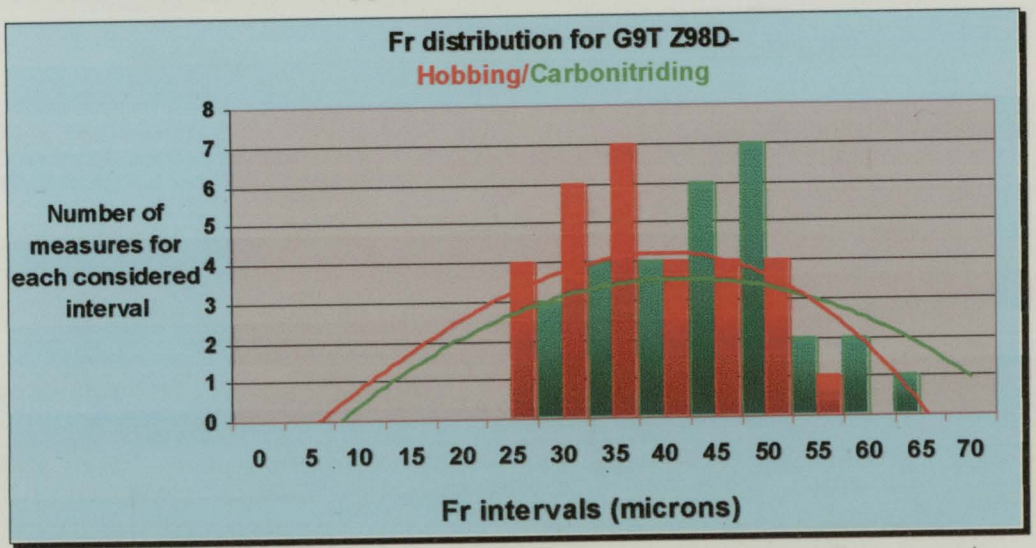
As visible, there is a higher dispersion for heat treatment.

However, as represented in the next board, the variances are not very different, and so, the final variance due to heat treatment is 9,21 microns, which is a very low value.

Hobbing	76,85 microns
Heat Treatment	86,06 microns
Variance due to Heat Treatment	**9,21** microns

Board 4- Fp variance evolution for Z98D.

For the run-out (as previously stated and observed in the logarithmic graphics), the dispersion after heat treatment appears to be higher.



Graphic 18– Z98D, hobbing and heat treatment results for Fr (run-out).

The results for the variance due to heat treatment (Fr), are very different than the ones obtained for the cumulative pitch deviation:

Hobbing	45,53 microns
Heat Treatment	125,65 microns
Variance due to Heat Treatment	**80,12** microns

Board 5- Fr variance evolution for Z98D.

This leads to the conclusion that the most important geometric parameter (or property), to take in account for the G9T Z98D part is its concentricity.

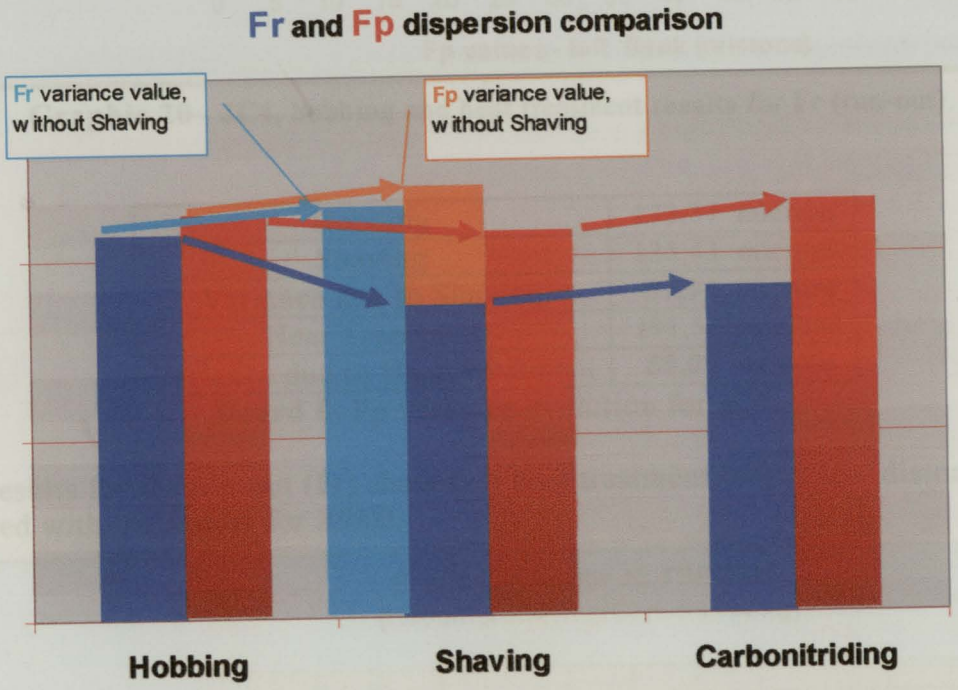
7.3.2 JC4: Results and discussion

The major difference between JC4 and Z98D is the inner diameter. Plus the outside diameter and thickness are also very different.

Due to the higher thickness and much lower inner and outside diameter from JC4, it is interesting to observe what would be the response (geometrical behaviour), to heat treatment operations in terms of distortion.

In terms of production process, the main distinction between the two parts is that while Z98D is not submitted to shaving operations, JC4 has a shaving improvement after hobbing and before heat treatment.

Major benefits are acquainted from shaving operations.

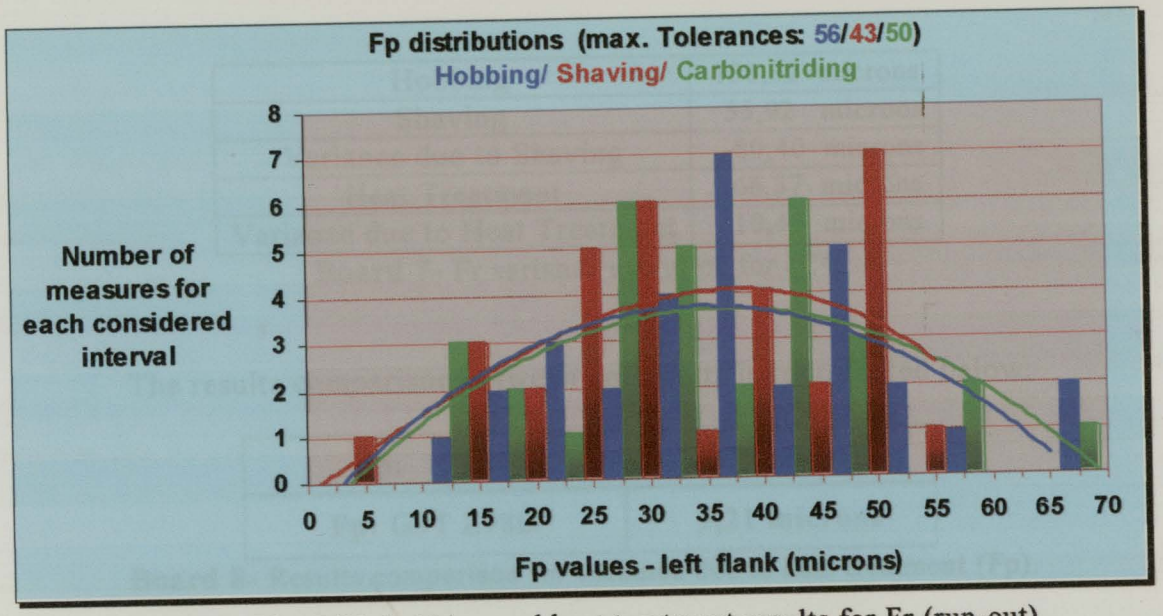


Graph 19- Variance evolution, with and without shaving throughout the production process.

If shaving would not be used, the variance at the end of heat treatment process would be positioned where the orange (Fp) and soft blue (Fr) rectangles are. The obtained improvement is visible.

The total cumulative pitch deviation and run-out results for JC4 are represented in the next two graphics the same way has represented before for the Z98D.

Hobbing variance is quite large and is then diminished by shaving, rising again after carbonitriding. Global variances for JC4 and G9T Z98D parts are quite different, plus, G9T parts are not subjected to shaving. As Fp results confirm, hobbing for G9T parts is much more accurate than for JC4.

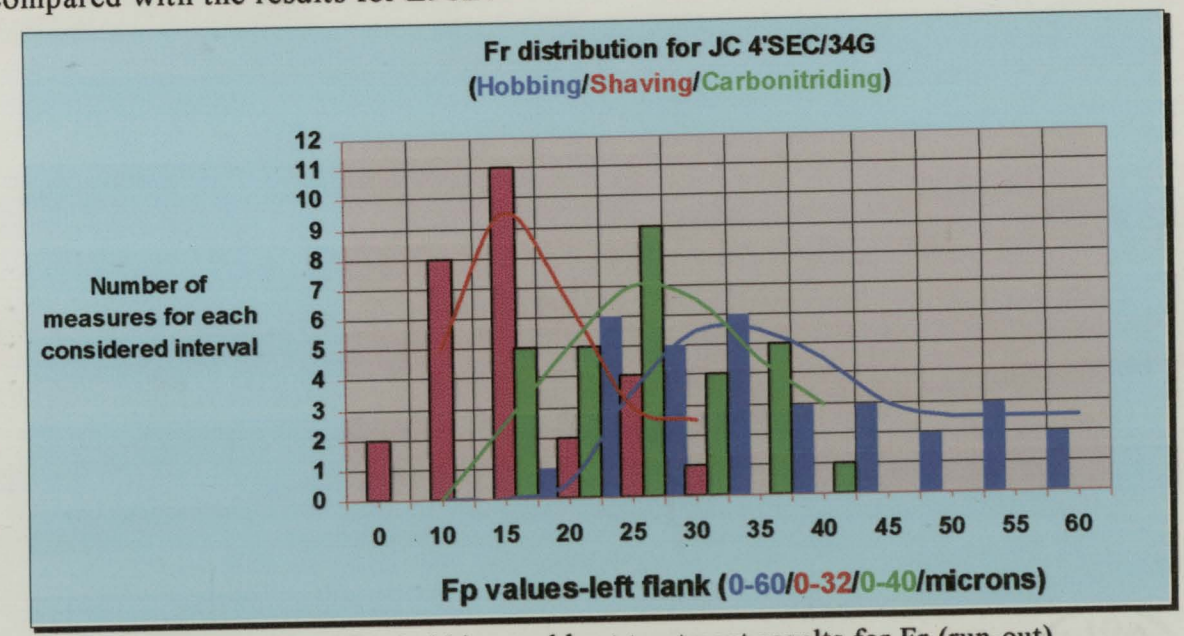


Graphic 20– JC4, hobbing and heat treatment results for Fr (run-out).

Hobbing	173,37 microns
Shaving	135,43 microns
Variance due to Shaving	-37,94 microns
Heat Treatment	191,51 microns
Variance due to Heat Treatment	**56,08** microns

Board 6- Fp variance evolution for JC4.

The results for the run-out (Fr) show that heat treatment impart low distortion when compared with the results for Z98D.



Graphic 21– JC4, hobbing and heat treatment results for Fr (run-out).

Hobbing	136,32 microns
Shaving	55,92 microns
Variance due to Shaving	-80,40 microns
Heat Treatment	66,37 microns
Variance due to Heat Treatment	**10,45** microns

Board 7- Fr variance evolution for JC4.

The results comparison between both parts is represented below:

Fp: JC4	**56,08 microns**
Fp: G9T Z98D	**9,21 microns**

Board 8- Results comparison for variance due to heat treatment (Fp).

Fr: JC4	**10,45 microns**
Fr: G9T Z98D	**81,12 microns**

Board 9- Results comparison for variance due to heat treatment (Fr).

These last results indicate the residual variance due to heat treatment, taking in account that for JC4 there is the improvement induced by shaving operations.

7.3.3 Conclusions

The main conclusion drawn from the distortion study is that, heat treatment affects parts with high inner diameters and thin sections in a negative manner concerning its concentricity.

G9T Z98D is the part with the highest relation inner diameter/cross section (thickness).

Taking in account that a mould that fits its inner diameter (Z98D) is used to suppress the effects of distortion in terms of concentricity values, and that the variance for Fr remains the highest, it is concluded that the results would be even higher if such measure would not be applied.



Figure 10- Mould used for G9T Z98D during carbonitriding.

A part like JC4 induces less geometrical problems in terms of run-out due to its compact geometry. However, it must be understood that shaving imparts significant corrections that will minimise the effects of heat treatment distortion, and still Fp results present an important dispersion.

7.4 Assembling PF5 and JR Shaft

7.4.1 Results and discussion

Two parts from the JR gear box were studied in detail, both having significant geometrical problems concerning their junction (assembling) areas. In addition, the two parts are extremely different therefore exhibiting diverse geometrical (especially volumetrically) behaviours concerning heat treatment process.

JR Shaft (27CD4) **PF5 (27CD4R)**

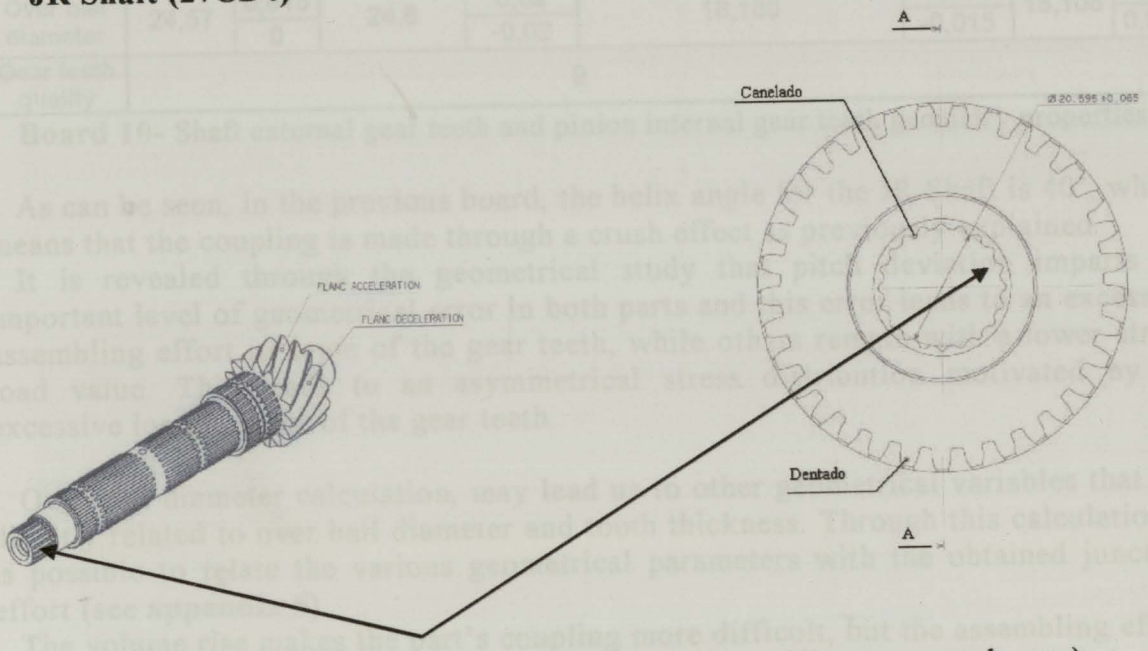


Figure 11- PF5 and JR Shaft studied zones (assembling area- crush zone).

The JR Shaft (male) will assemble the PF5 pinion (female) from its inside, after heat treatment the gear teeth measured values for both parts are constantly out of limits and the respective assembling effort rises.

This rise of assembling effort imparts high contact stress values at the interface, leading to crack initiation which induces premature failure.

Dimensional accuracy is therefore as important as in gear . Being PF5 internal gear a spur gear and JR Shaft internal gear a helical gear, the junction is made by a crushing effect that provokes a slight deformation and introduces contact stresses that cannot go over a certain value. If such value is passed, the risk of premature failure by cracking is very high.

	Shaft				Pinion			
	Before HT		After HT		Before HT		After HT	
Teeth nº	20							
Module	1,0583							
Pressure angle	45							
Helix angle	40,000				0			
Width	16							
Tip diameter	22,225		20,6405	0,0105 -0,0105	20,594		0,065 -0,065	
Root diameter	20,1		22,649		0,225 0			
Ball control	2,032							
Over ball diameter	24,57	0,015 0	24,6	0,02 -0,02	18,180	0,015 -0,015	18,108	0,068 0,034
Gear teeth quality	9							

Board 10- Shaft external gear teeth and pinion internal gear teeth geometry properties.

As can be seen, in the previous board, the helix angle for the JR Shaft is 40', which means that the coupling is made through a crush effect as previously explained.

It is revealed through the geometrical study that pitch deviation imparts an important level of geometrical error in both parts and this error leads to an excess of assembling effort in some of the gear teeth, while others remain with a lower stress load value. This leads to an asymmetrical stress distribution motivated by an excessive load in some of the gear teeth.

Over ball diameter calculation, may lead us to other geometrical variables that are directly related to over ball diameter and tooth thickness. Through this calculation it is possible to relate the various geometrical parameters with the obtained junction effort (see **appendix 5**).

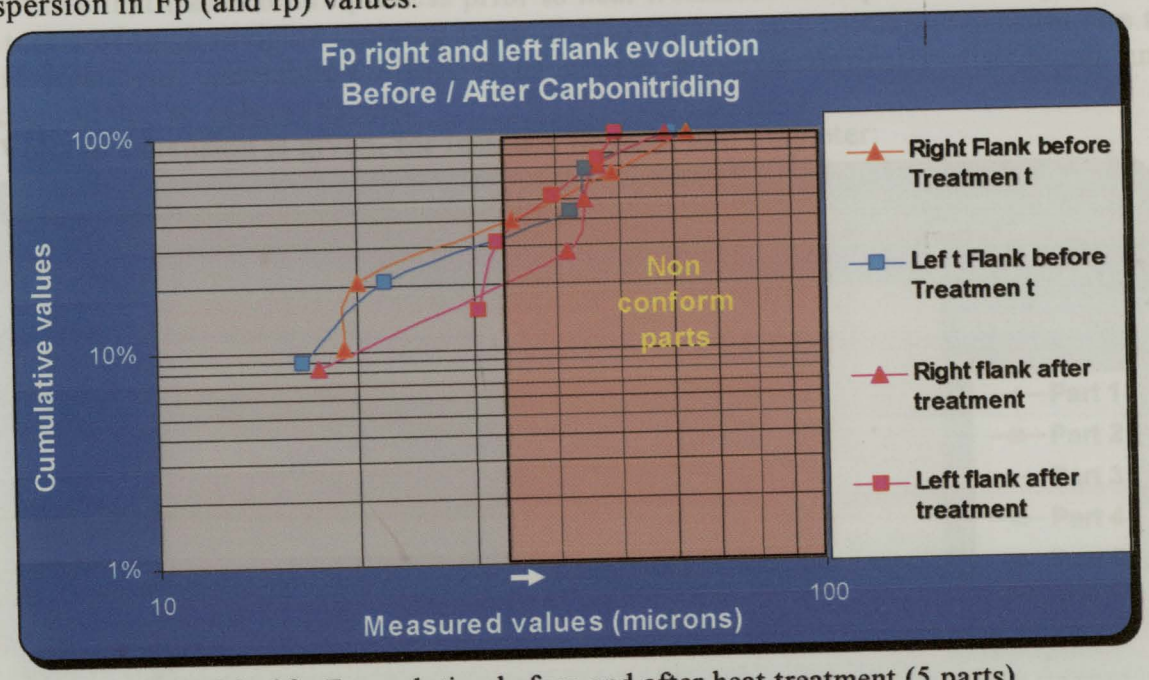
The volume rise makes the part's coupling more difficult, but the assembling effort is not only influenced by over ball diameter, root diameter and tip diameter, it is also influenced by the teeth division errors, concentricity and the other profile and helix errors.

Being a helical external gear teeth, some of the geometrical measures are easily recalculated:

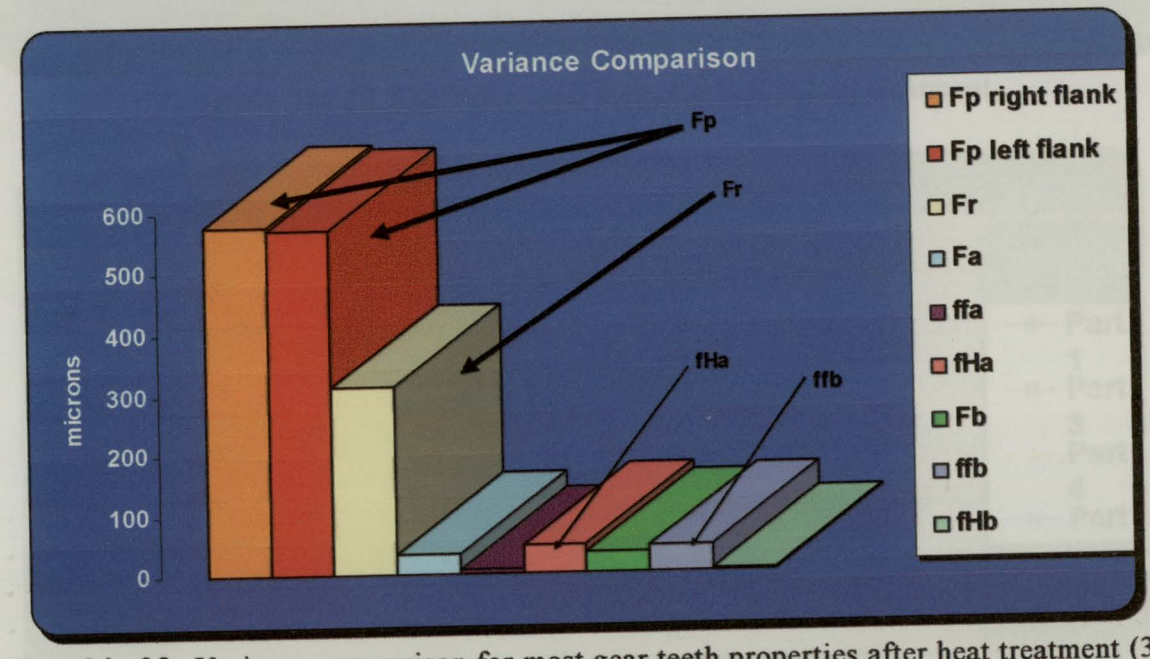
Primitive diameter	21,167	21,166
Base diameter	14,968	14,967
Module apparent	1,0584	-
Apparent pressure angle	45,0019	-
Base Helix diameter	28,2840	-
"Apparent" ball control	2,0321	-

Board 11- Gear teeth recalculated relevant measures for the assembling study.

A rise in the probability of premature failure is observed, possibly due to high dispersion in Fp (and fp) values.



Graphic 22- Fp evolution before and after heat treatment (5 parts).

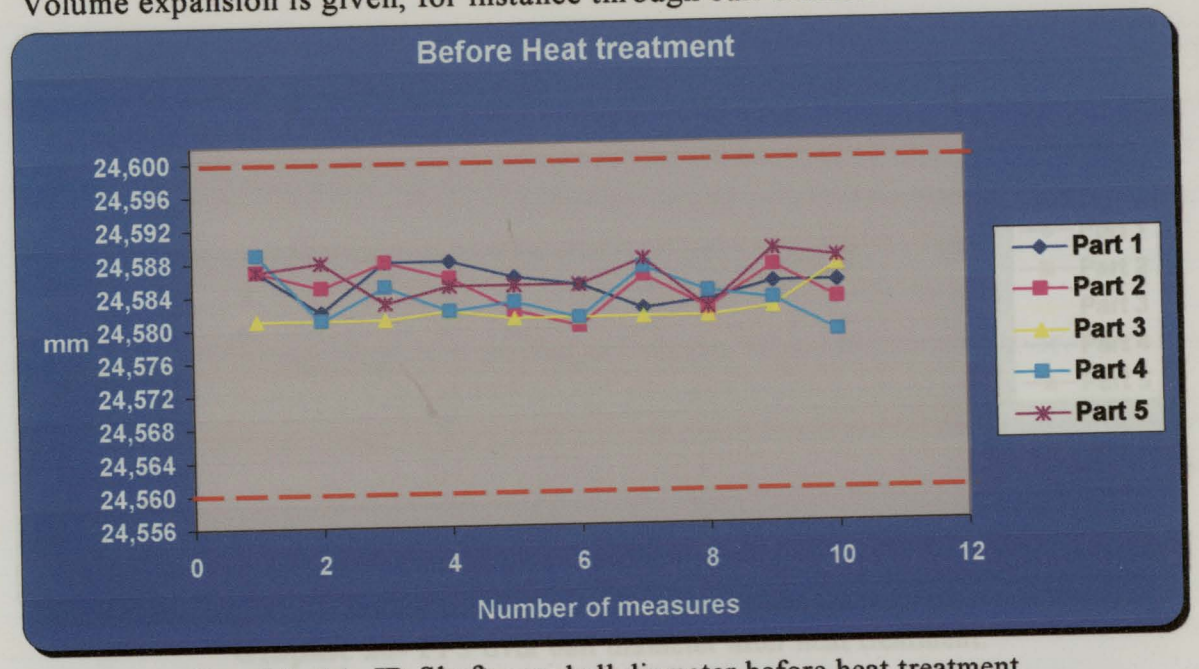


Graphic 23- Variance comparison for most gear teeth properties after heat treatment (30 parts population).

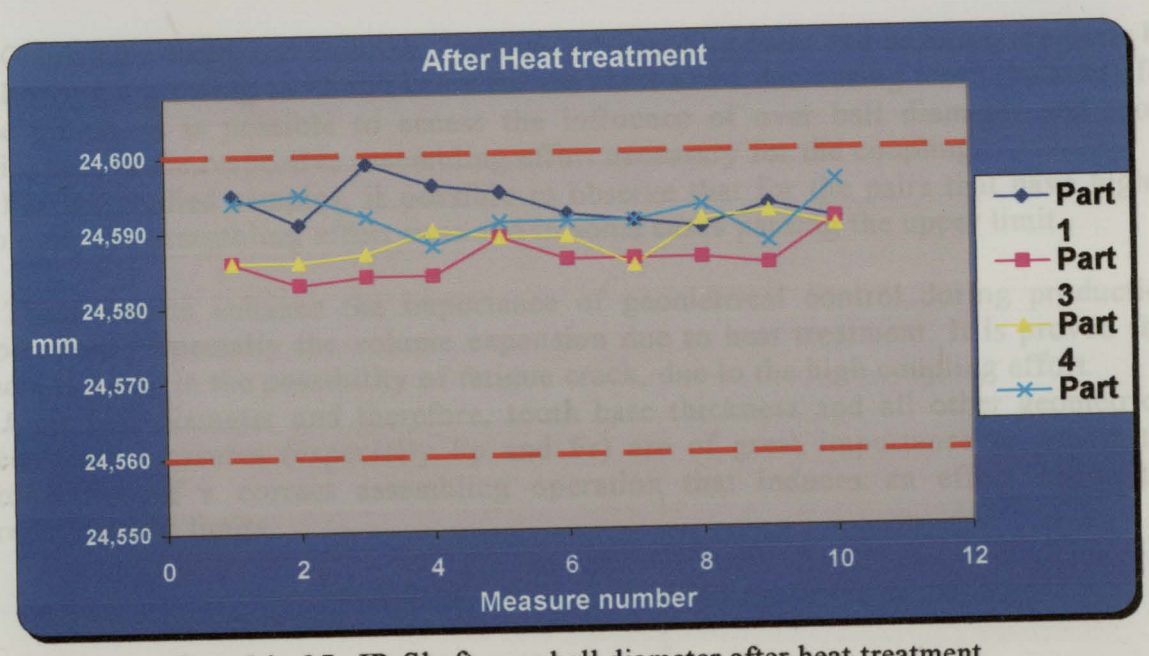
Fp variance is extremely high and a very high percentage is inside non-conform values.

There is already a high number of non-conform parts before heat treatment. This indicates that manufacture process prior to heat treatment is responsible for problems in terms of teeth division. Joining teeth division errors and volume expansion due to heat treatment, assembling effort is of course non-symmetrically distributed and increased due to volume exceed.

Volume expansion is given, for instance through ball diameter:



Graphic 24- JR Shaft over ball diameter before heat treatment.

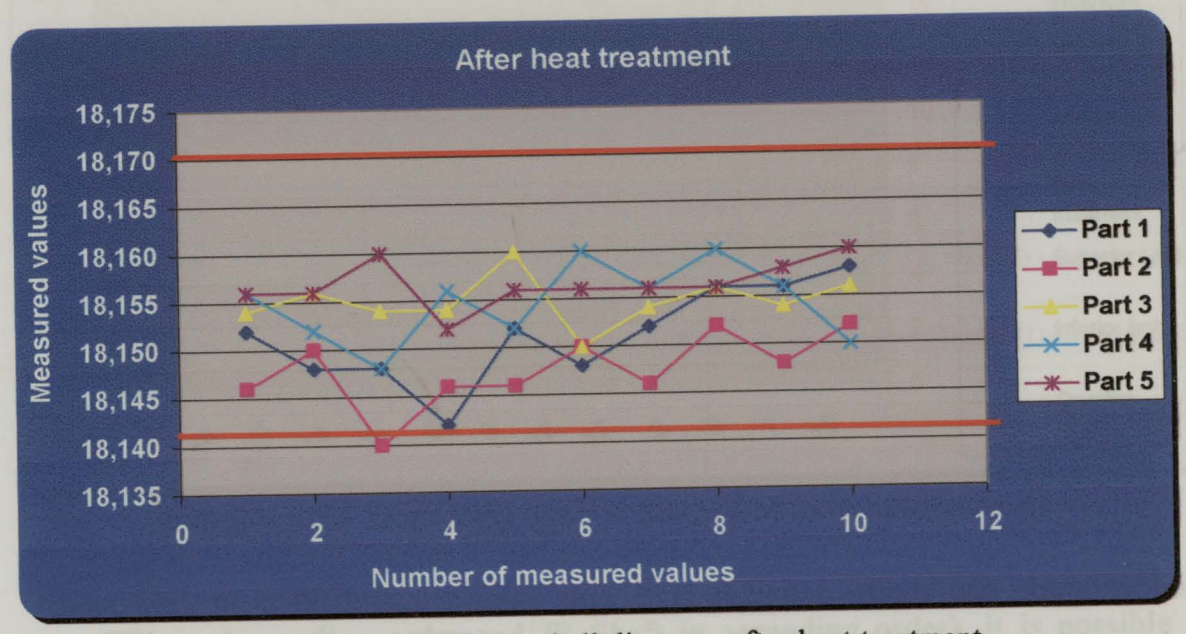


Graphic 25- JR Shaft over ball diameter after heat treatment.

It is visible the rise of over ball diameter (10 measures-20 teeth), representing volume expansion.

The values after heat treatment are very close to upper limits (red dash line).

For PF5 over ball diameter, before heat treatment the values are fairly inside limits. As in PF5 part, one deals with an internal diameter, over ball diameter decreases, which also indicates volume expansion. Some part's results are very close to low limits:



Graphic 26- PF5 over ball diameter after heat treatment.

Choosing a Shaft and a pinion, 'producing' coupling pairs and ordering the parts by following a growing tooth thickness for the shaft and a decreasing tooth thickness for the pinion, it is possible to access the influence of over ball diameter and tooth thickness in the respective assembling effort necessary for the coupling.

For the studied samples, is possible to observe that for the pairs that have higher volume, the assembling effort rises and in some cases passing the upper limit.

These results enhance the importance of geometrical control during production operations, especially the volume expansion due to heat treatment. It is proved that there is a rise in the possibility of fatigue crack, due to the high coupling effort.

Over ball diameter and therefore, tooth base thickness and all other geometrical gear teeth measures (especially Fp and Fr) are of great importance to access the probability of a correct assembling operation that induces an effort inside the predetermined limits.



Graphic 27 – Assembling effort in function of tooth base thickness.

Calculating base thickness through over ball diameter values and coupling both parts (PF5 in descending order and JR Shaft in ascending order), it is possible to observe over which value assembling (coupling) effort passes the upper limit.

Results indicate that gear teeth's volume is too high, for both parts.

7.4.2 Residual Stress analysis and results relation

JR Shaft and PF5 assembling effort depends on: volume expansion, surface hardness and case hardened residual stress distribution. Volume expansion results are studied and surface hardness is analysed in the next chapter. This chapter treats the stress analysis and includes the study of the cooling process and all the temporal and local phase transformations that this process induces, as well as the stresses provoked by each one of the transformation mechanisms.

Austenite-martensite transformation obviously enhances hardness and residual stress values, shifting residual stress values to more negative magnitudes. This means that transformations occurring in tensile stressed areas reduce stress values whereas transformations occurring in compressive stressed areas enhance stress magnitudes. The quenching technique used is therefore a fundamental variable to quantify and qualify the transformation and respective residual stress evolution. Martensitic transformations are always coupled with volume increase and either the surface initiates the transformation after or before the core, the final residual stress evolution throughout the part reveals opposite graphical results.

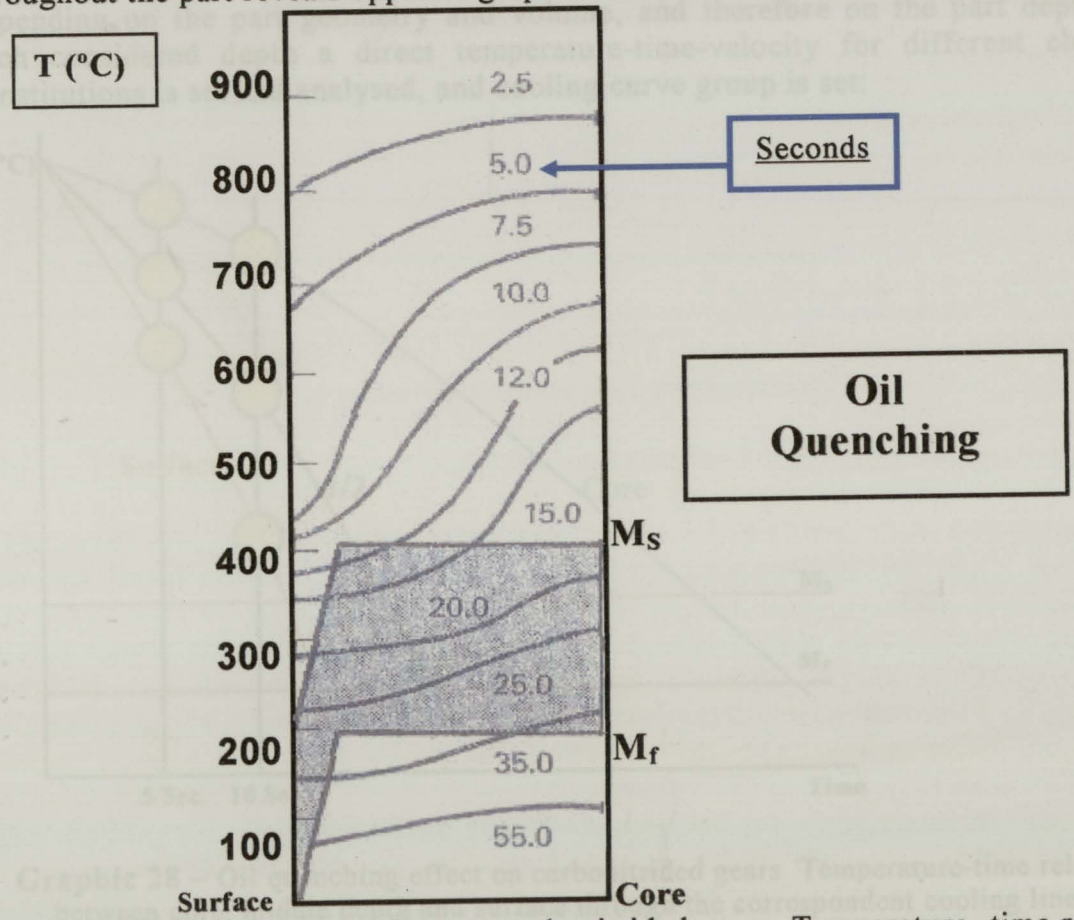


Figure 12 – Oil quenching effect on carbonitrided gears. Temperature- time relation between core and surface throughout cooling process. Source: Ref. 9.

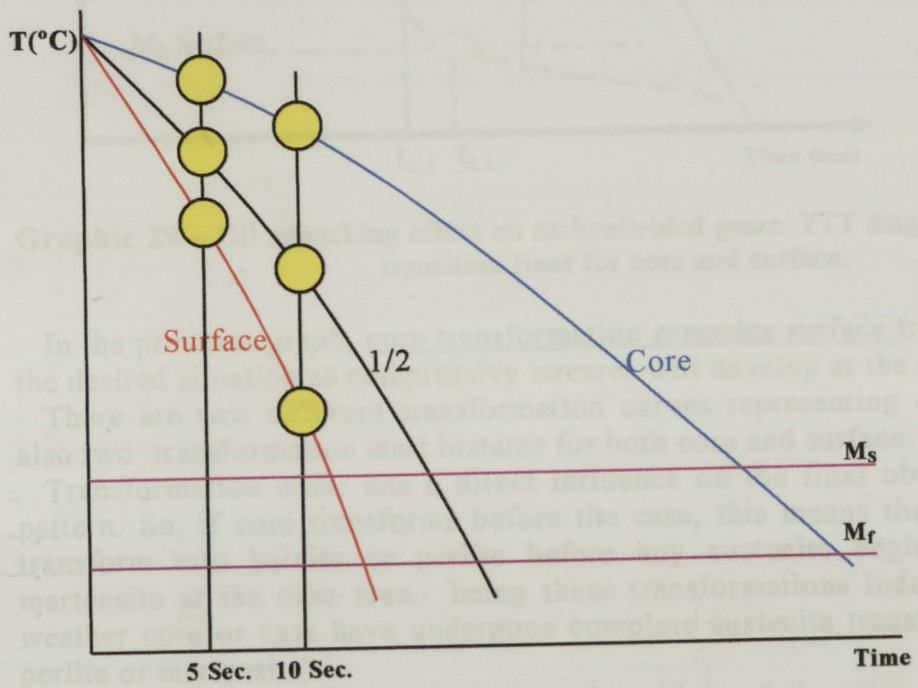
As observed in the previous graph, there are different martensite transformation timings when travelling from the core to the part surface. The difference in temperature-time relation curve is higher for the intermediate temperatures, which means that the part volume is to be taken in account.

The case is the last material to transform, and as martensite expansion induces compressive stresses (as the core is already transformed restraining the tendency of the core expand), the final residual stress pattern must show a higher value of compressive stresses in the surrounding case areas.

This difference of linearity in the transformation lines (represented in seconds), is as higher as the part volume increases so, thinner parts have a more horizontal transformation line.

The M_S and M_f lines, dependent on carbon (and alloy elements) content, have a descendent behaviour when approaching the surface. Knowing that carbon concentration near the surface is much higher than that existing in the core, the descendent M_S and M_f lines behaviour is therefore understandable.

Each transformation line is represented by different cooling lines in the corresponding CCT diagram. For a determined carbon quantity and alloy elements concentration, a CCT diagram is drawn and related to each represented cooling curve, depending on the part geometry and volume, and therefore on the part depth. For each considered depth a direct temperature-time-velocity for different chemical constitutions is set and analysed, and cooling curve group is set:

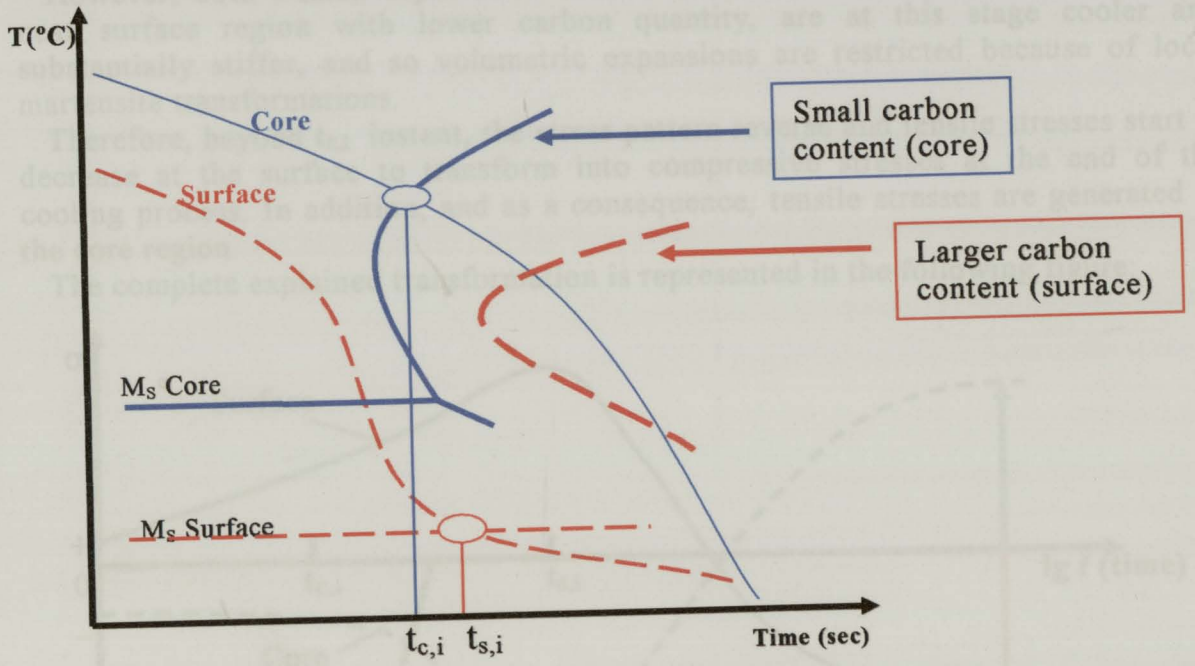


Graphic 28 – Oil quenching effect on carbonitrided gears. Temperature-time relation between core, middle depth and surface through the correspondent cooling lines.

Depending on the actual original value of steel carbon concentration and on the carbon concentration measured in the carbonitrided case, different corresponding

TTT diagrams will apply. During the continuous cooling, an assessment of the locally-occurring austenite decomposition processes can be performed on the basis of the measured or calculated cooling curves. For each chosen depth there is a corresponding CCT diagram that is related with each corresponding cooling line allowing a complete analysis of the part's cooling path and its corresponding final phase microstructure and residual stress pattern.

There are two main possibilities for the phase transformations occurring during quenching process. The first possibility is represented in the next diagram:



Graphic 29 – Oil quenching effect on carbonitrided gears. TTT diagram and corresponding transition lines for core and surface.

In the previous graph, core transformation precedes surface transformation. This is the desired situation as compressive stresses will develop at the surface.

There are two different transformation curves representing core and surface and also two transformation start instants for both core and surface: $t_{c,i}$, $t_{s,i}$.

Transformation order has a direct influence on the final obtained residual stress pattern. So, if core transforms before the case, this means that austenite begins to transform into bainite or perlite before any austenite begins to transform into martensite at the case area. being these transformations independent of the point weather core or case have undergone complete austenite transformation (in bainite, perlite or martensite).

As visible, the ferritic-perlitic transformation of the core starts at instant $t_{c,i}$, instant in which compressive stresses begin to act at the core, balanced by the correspondent tensile stresses developed at the surface.

This stress pattern distribution, with compressive stresses at the core and surface tensile stresses remains until instant $t_{s,i}$.

BIBLIOTECA FE PORTO

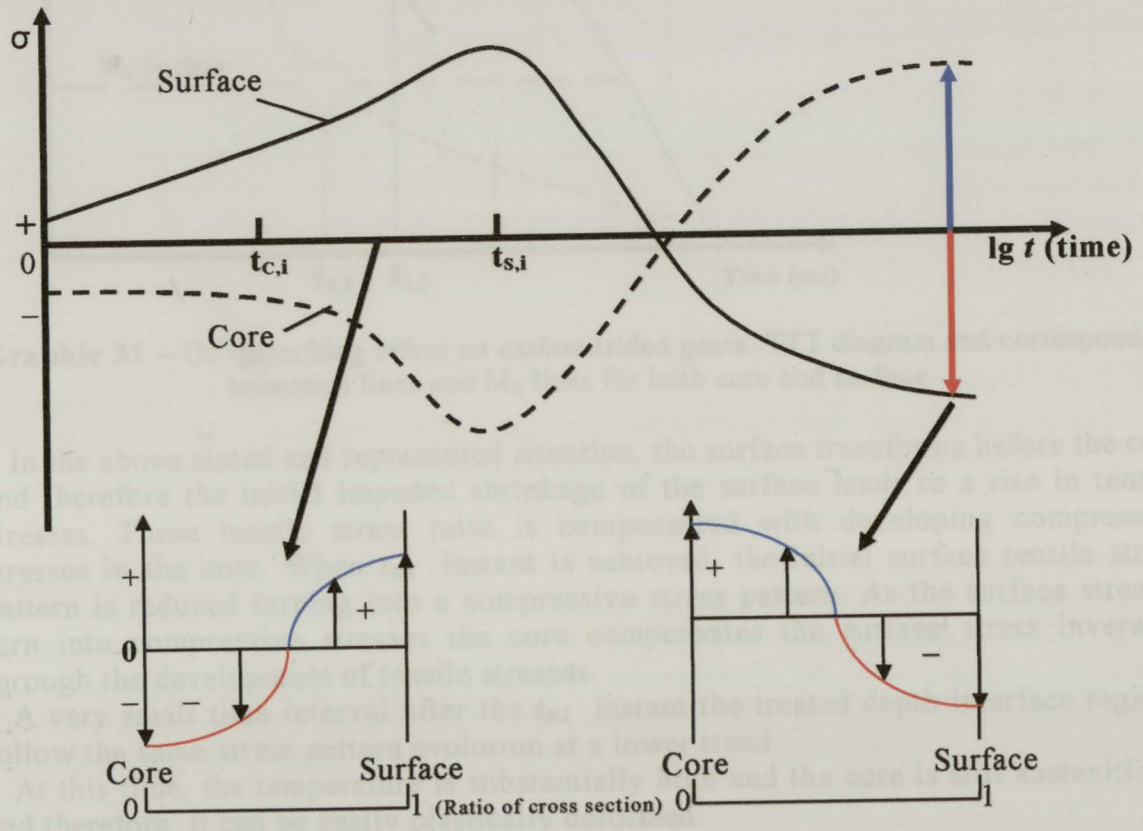
At this stage the temperature is still relatively high, and both core and surface areas may be subjected to plastic deformation. So, at this instant, quenching induces a global plastic deformation in both core and surface because the surface temperature is high enough so that case hardened shell may follow this momentary core volume change.

After this period, and in the sequence of the cooling process, the near surface part regions with lower carbon contents start to transform followed by the surface itself at instant $t_{s,i}$.

However, both treated depth and the interface between this treated area and the near surface region with lower carbon quantity, are at this stage cooler and substantially stiffer, and so volumetric expansions are restricted because of local martensite transformations.

Therefore, beyond $t_{s,i}$ instant, the stress pattern reverse and tensile stresses start to decrease at the surface to transform into compressive stresses at the end of the cooling process. In addition, and as a consequence, tensile stresses are generated in the core region.

The complete explained transformation is represented in the following figure:

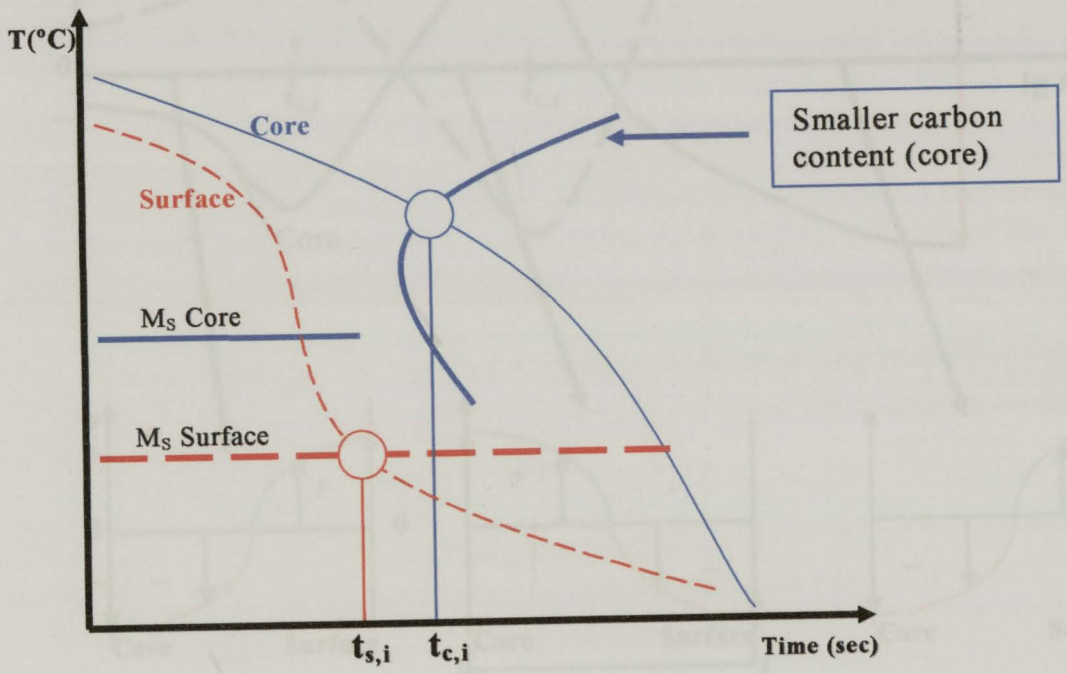


Graphic 30 – Longitudinal residual stress evolution pattern throughout cooling process (quenching or a carbonitrided stell). Source Ref. 5.

For the introduction effort considered for both JR Shaft and PF5 Pinion, the previous possibility is the more adequate, because compressive stresses at the surface

means the reduction of tensile stresses at the junction interface, therefore diminishing the possibility of bending stress fatigue raise during 'in life' service operations. Bending stresses are mainly induced by the rotational movement through the longitudinal pinion and shaft common axis.

However, there is a second possibility concerning the residual stress pattern evolution and final stress results both in core and case regions. This possibility is represented below:



Graphic 31 – Oil quenching effect on carbonitrided gears. TTT diagram and corresponding transition lines and M_S lines for both core and surface.

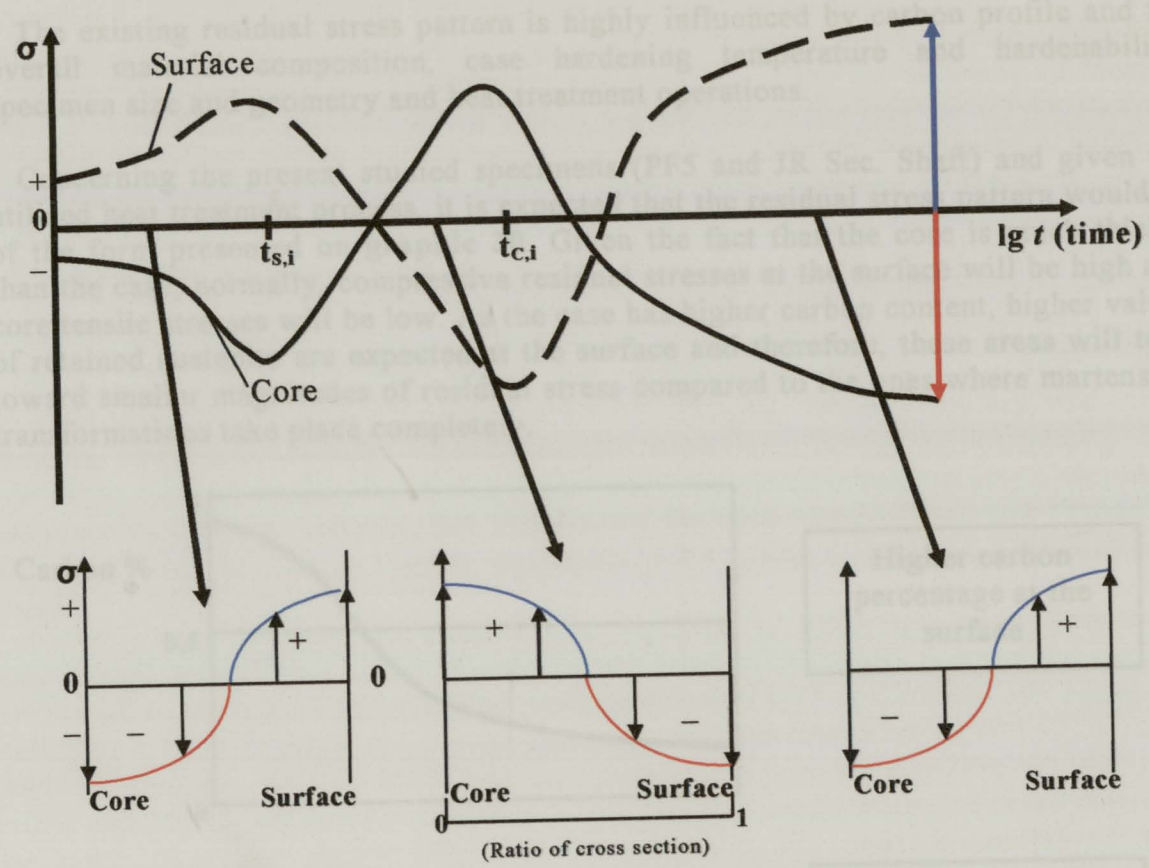
In the above stated and represented situation, the surface transforms before the core and therefore the initial impeded shrinkage of the surface leads to a rise in tensile stresses. These tensile stress raise is compensated with developing compressive stresses in the core. When $t_{s,i}$ instant is achieved, the initial surface tensile stress pattern is reduced turning into a compressive stress pattern. As the surface stresses turn into compressive stresses the core compensates the surface stress inversion through the development of tensile stresses.

A very small time interval after the $t_{s,i}$ instant the treated depth interface regions follow the same stress pattern evolution at a lower trend.

At this time, the temperature is substantially high and the core is still austenitised, and therefore, it can be easily plastically deformed.

Finally, when $t_{c,i}$ instant is reached, the core begins to transform following at last, the outer core areas previous transformation. The transformation consequently imparts expansion, but the core expansion is restrained by the surface transformed regions and therefore compressive stresses are developed in the core regions while tensile stresses are formed in the surface area (or case hardened area).

This transformation sequence and the correspondent stress pattern are represented in the following diagrams.



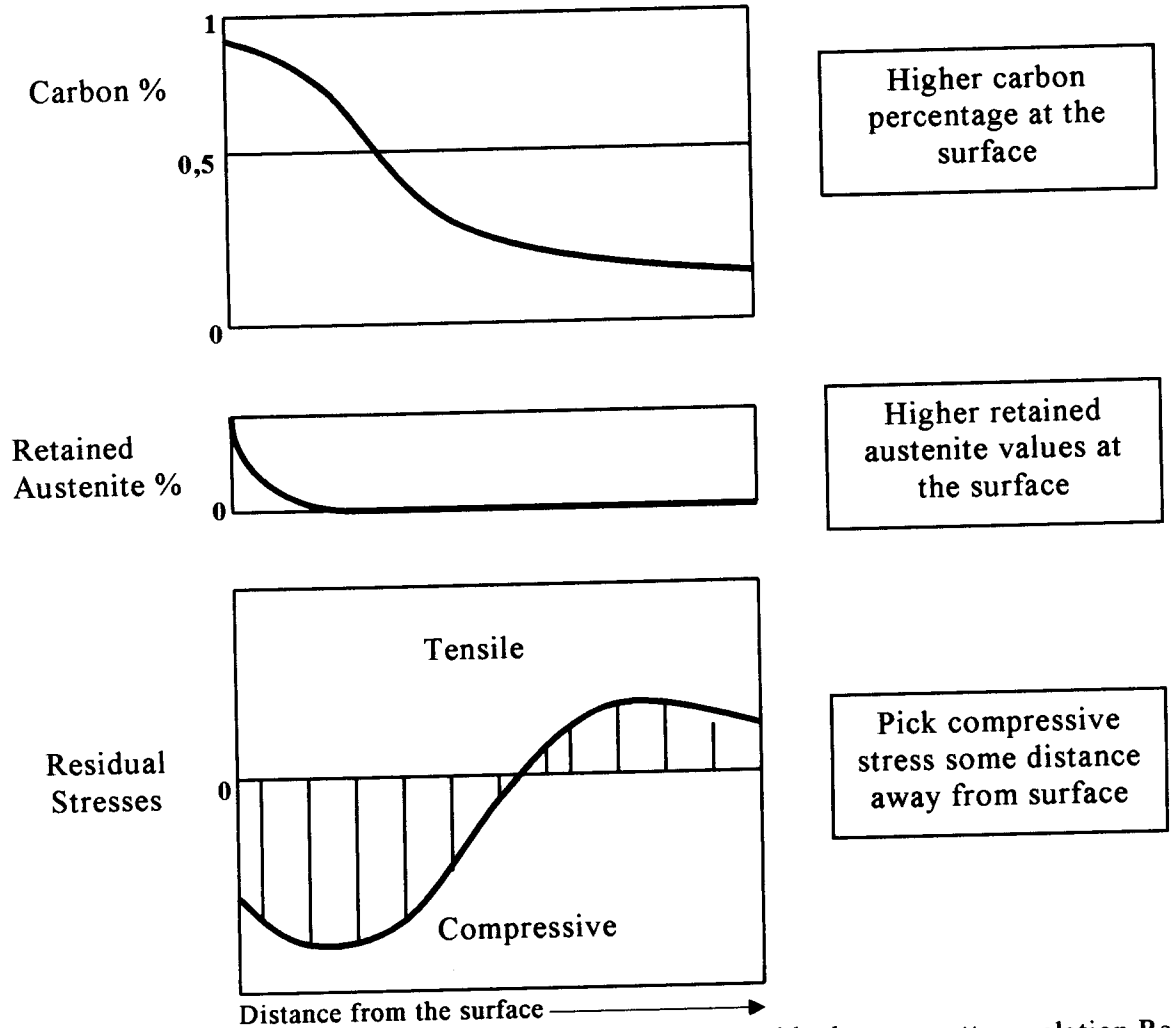
Graphic 32 – Longitudinal residual stress evolution pattern throughout cooling process (quenching or a carbonitrided stell) when martensitic transformations start at the surface, followed by ferritic-perlitic transformations in the core. Source Ref. 5.

There is a possibility of simultaneous transformations both within core areas and case depth regions. This may occur for very thin specimens or for specific alloy compositions. For such cases, the temporal curves represented in **figure 12**, are horizontal and, for abnormal or special alloy compositions with near surface areas and core regions having different carbon percentages, M_S temperatures happened simultaneously producing extremely high transformation stresses which may lead to internal cracking. Therefore, this is an undesired situation.

7.4.3 Heat treatment process, geometry and carbon effect on residual stress distribution

The existing residual stress pattern is highly influenced by carbon profile and the overall material composition, case hardening temperature and hardenability, specimen size and geometry and heat treatment operations.

Concerning the present studied specimens (PF5 and JR Sec. Shaft) and given the utilised heat treatment process, it is expected that the residual stress pattern would be of the form presented on **graphic 30**. Given the fact that the core is much thicker than the case, normally, compressive residual stresses at the surface will be high and core tensile stresses will be low. As the case has higher carbon content, higher values of retained austenite are expected at the surface and therefore, these areas will tend toward smaller magnitudes of residual stress compared to the ones where martensitic transformations take place completely.



Graphic 33 – Carbon content, retained austenite and residual stress pattern relation.Ref. 9.

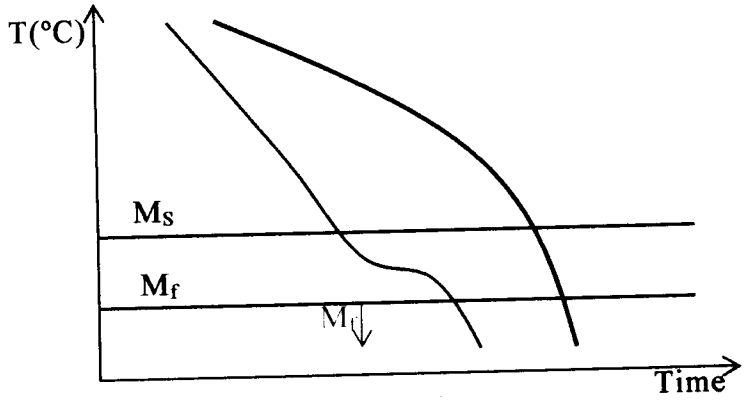
When the core is much thicker than the case, higher compressive stresses will develop at the surface.

As case hardening depth increases, higher residual stress values are expected in case depth, though, including retained austenite, the compressive stress values will have a slight decrease at the surface due to higher carbon content that will lead to a minor austenite-martensite transformation. Therefore, with the increase of treated depth, the maximum residual stress values are shifted to the interior of the part (in the core direction), and as can be seen in the previous diagram the maximum residual stress values are expected near the surface (and in these cases near to the surface than to the core depth)[9].

The stress values sign change is normally detectable in the interface between the treated depth and core, where a high change in carbon content occurs.

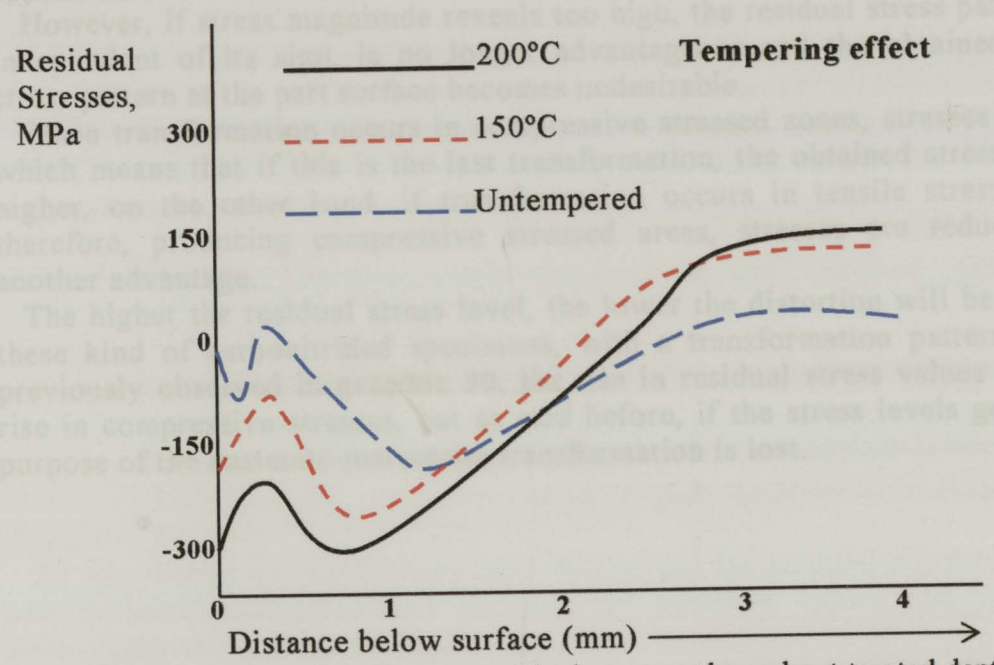
Specimen's work-size and shape are directly connected to cooling and carbonitriding process, surface heat transfer changes, when geometry and mass changes, therefore, cooling conditions are modified during carbonitriding and quenching operations. For instance, smaller diameter specimens show lower values of compressive residual stresses but differences between longitudinal and tangential stresses are higher than in thicker specimens, where such differences are much less visible.

Normally, an increase in compressive stresses is observed when quenching temperature is increased, whereas post-quench tempering usually reduces the surface compressive stresses. Carbonitrided (and post-quenched) specimens are tempered mainly to transform some of the brittle and unstable martensite into a tempered, more stable martensite. As the most common tempering temperatures are set between 160°C and 200°C, so that no hardness is lost and martensite becomes more stable at the same time. For higher tempering temperatures, M_S and M_f are raised and, therefore, martensite is stabilised. Contrarily, if a stage is done between M_S and M_f temperatures, then these two temperatures have the tendency to dislocate toward lower values, which means that austenite becomes more stable in opposition to what is experienced with stages at higher temperatures.



Graphic 34 – Stage between M_S and M_f temperatures producing austenite stabilisation (blue curve). Stage over M_S and M_f temperatures aiming for martensite stabilisation.

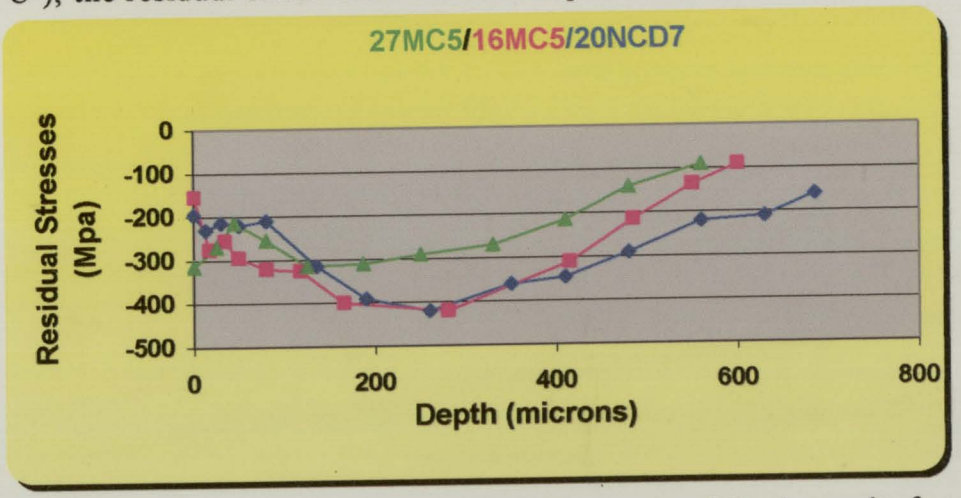
An important conclusion to take from tempering experiences is that the higher the tempering temperature, the lower the residual stresses, on the other hand, at 300°C almost all austenite has been transformed in martensite and the obtained martensitic structure's volume has decreased due to a relief in its tetragonality through carbide formation.



Graphic 35 – Tempering effect on residual stresses throughout treated depth. Ref. 5.

Experimentally, x-ray diffraction allows to visualise the residual stress pattern in carbonitrided parts such as the ones studied.

For three pinions subjected to carbonitriding treatment, oil quenched, containing 0,27%, 0,20% and 0,16% carbon (in this case with a composition named 27MC5 with M- and C-), the residual stress distribution is represented below:



Graphic 36 – Residual stress distribution throughout treated depth; results for alloys with different carbon contents.

It is visible that carbon plays a decisive role in the final stress distribution, especially at the specimen's surface.

The existence of such stress distribution is an advantage for an application such as the one existing for both PF5 and JR Shaft parts, where, maximum tensile stresses appear at the surface motivated by high bending and torsional loading.

However, if stress magnitude reveals too high, the residual stress pattern obtained, independent of its sign, is no longer advantageous and the obtained compressive stress pattern at the part surface becomes undesirable.

When transformation occurs in compressive stressed zones, stresses are enhanced, which means that if this is the last transformation, the obtained stress level will be higher, on the other hand, if transformation occurs in tensile stressed zones and therefore, producing compressive stressed areas, stresses are reduced, which is another advantage.

The higher the residual stress level, the lower the distortion will be. Evidently, in these kind of carbonitrided specimens, with a transformation pattern like the one previously observed in **graphic 30**, the rise in residual stress values has to mean a rise in compressive stresses, but as said before, if the stress levels get too high the purpose of the austenite-martensite transformation is lost.

7.4.4 Retained austenite and residual stress relation

The relation between the desire to obtain higher hardness values, a low distortion level and a residual stress distribution of high, but not too high; compressive stress values and a lower austenite quantity, is always a difficult compromise.

Austenite-martensite transformation induces volume expansion, however, the reduction of retained austenite also imparts better geometrical accuracy.

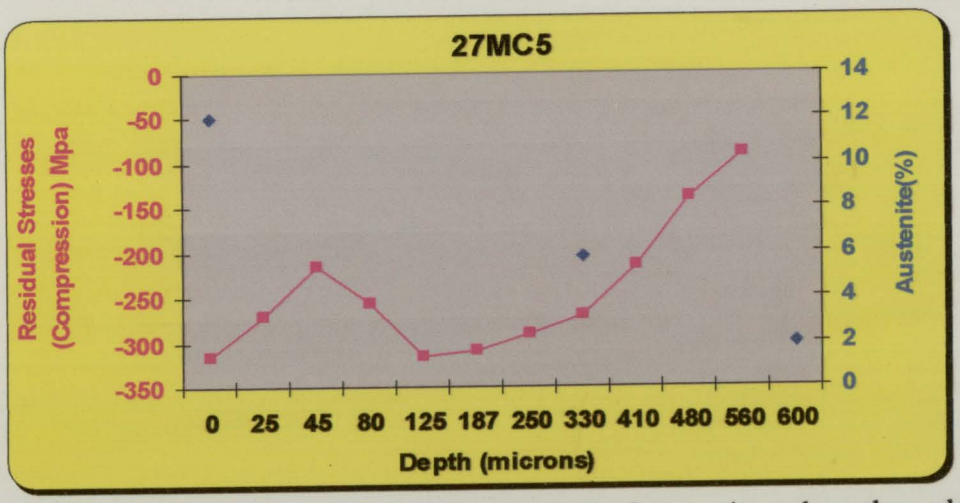
If the relation between all the parameters involved is difficult to obtain, sometimes even the variation of one of these parameters may bring distinct results, depending on the material and heat treatment cycle used. And, although several carbonitrided specimens may possess equal hardness profiles, they may have distinct microstructures and residual stress distributions, and therefore, performing fairly distinctly.

Certain is, that the higher the carbon content the higher the content of non-transformed austenite, and so it is expected that the higher percentage of austenite is to be found at the part's surface.

With the increase of treated depth, higher values of residual stresses will appear, however, the higher the carbon content the higher the level of retained austenite and therefore, the lower the residual stress values.

As one travels deeper through case hardening, the amount of carbon and nitrogen concentration gets lower and so does the austenite values and the compressive stresses, for the above stated reasons.

Through x-ray diffraction was possible to access the austenite evolution along the treated depth. Polishing and taking three different depths from a JR Shaft tooth sample, the percentage of retained austenite was obtained, and even if the quantification of retained austenite is hard and the results are sometimes not 100% reliable, the evolution is considered to be certain and the results are represented below:



Graphic 37 – Residual stress distribution *vs.* retained austenite values throughout treated depth; results for an alloy with 0,27% of carbon content.

The obtained percentage and evolution of the retained austenite pattern is considered to be acceptable and its relation with the residual stress distribution matches the theoretical predictions.

The compressive stresses tend to decrease along with the reduction of carbon content. Due to the respective transformation pattern followed during quenching process, compressive stresses are higher at the surface, where carbon percentage is also higher. Retained austenite decreases along treated depth due to a decrease in carbon percentage, as more carbon means more austenite to be transformed.

It is proved that even if the stress levels or austenite percentage are not exactly equal for all parts, the obtained patterns – residual stress pattern and retained austenite pattern- are common to all carbonitrided gear box parts.

7.4.5 Retained austenite quantification results

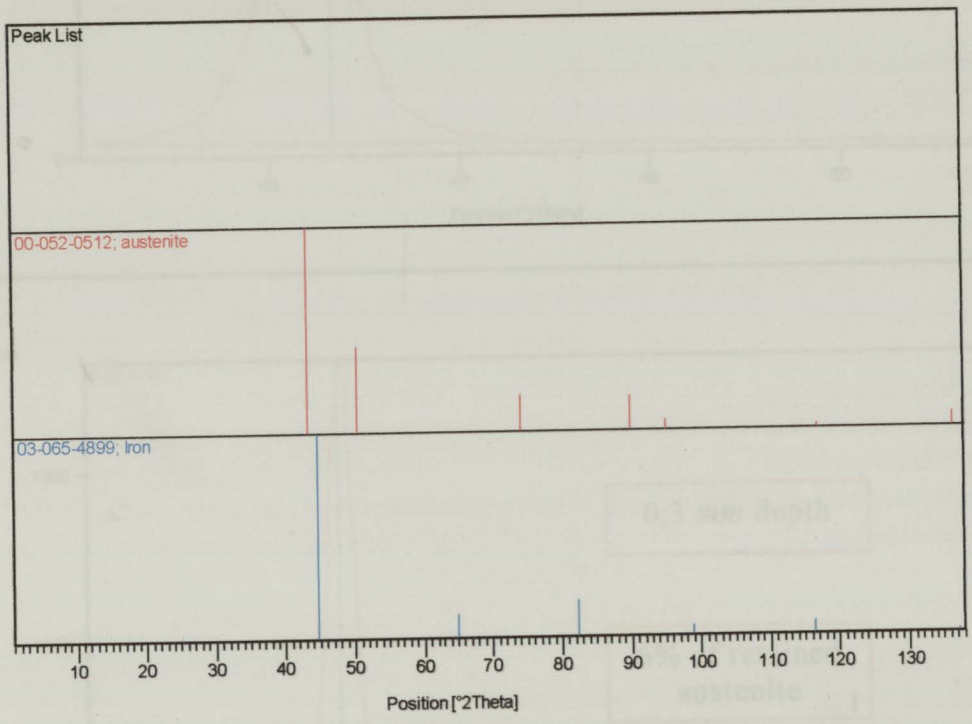
The first technique used for retained austenite quantification was x-ray diffraction.

The problems inherent to this technique led to non reliable results in most of the measured parts. The reliability of such technique is dependent on the incident angle and mainly on the dimensions of the inspected (diffracted) surface.

For the parts having small diffraction surfaces, the results were totally inconclusive. On the other hand, parts with higher diffracted surfaces shown the reduction of retained austenite values as one travels deeper in the carbonitrided hardened shell (as represented in the previous graphic), though, the quantification cannot be considered as 100% correct.

The results presented in the next pages were taken from the gear box JR Shaft at three different depths: surface, 0,3mm and 0,6mm.

Angles at which each constituent is detectable:



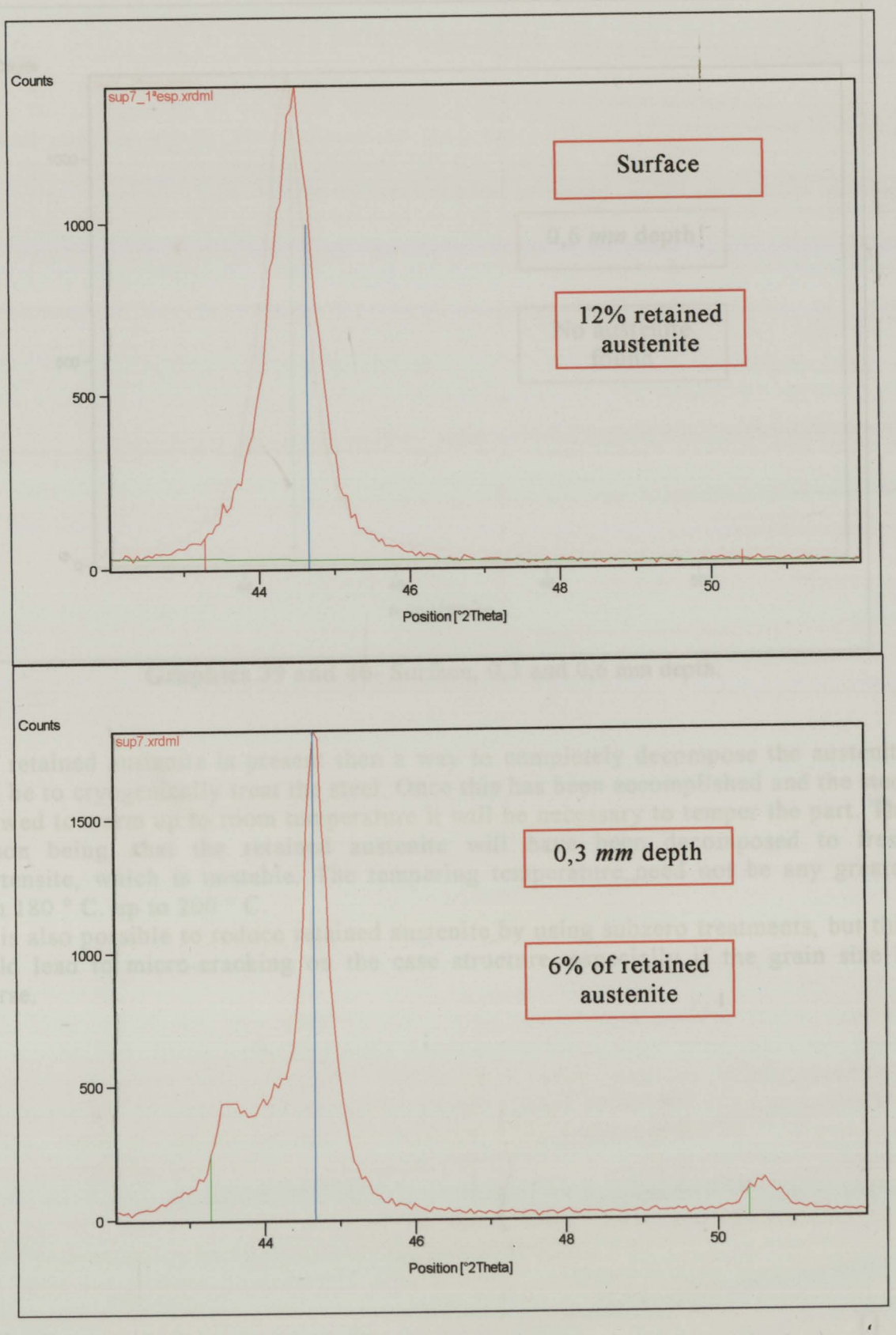
Graphic 38- Pick list: 2*Theta position for different micro-structures.

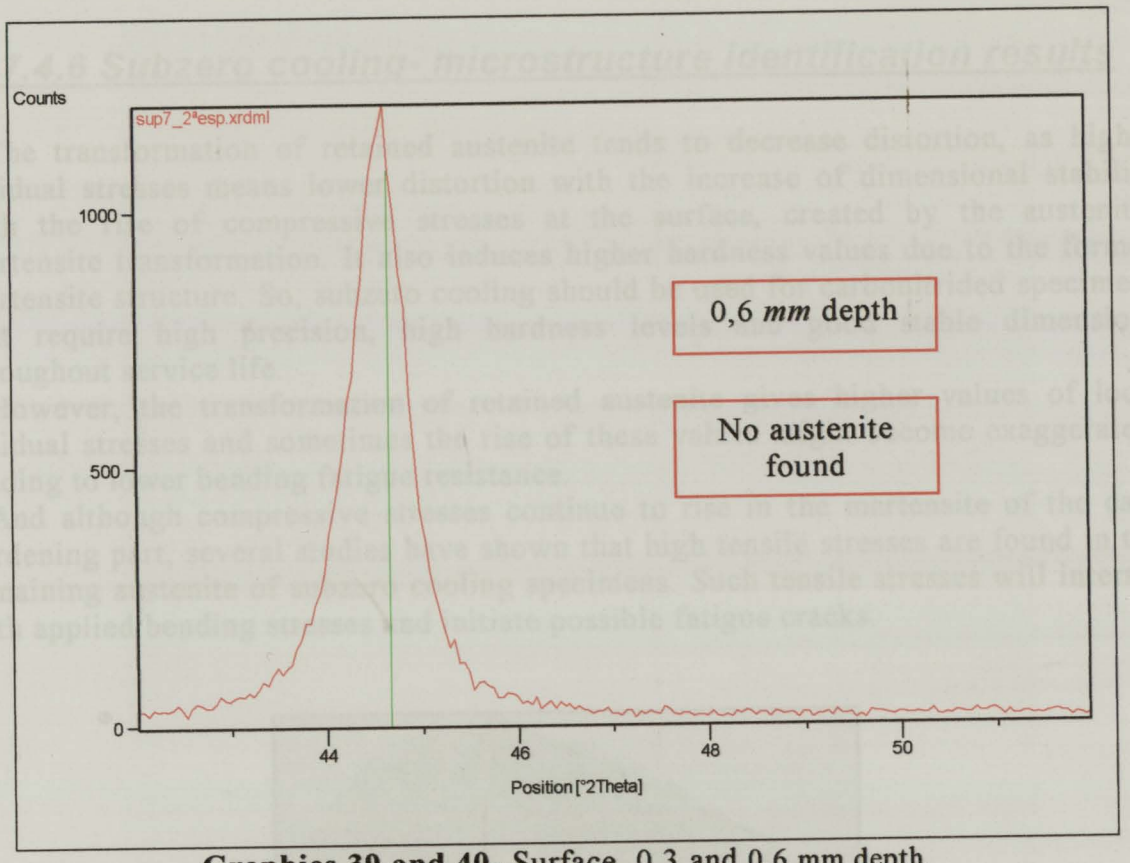
X-ray technique depends on analysis time as well as the sample dimensions (dimensions of the inspected area). This results are from the sample inspected for a longer time period and with an analysis area which dimensions are considered to be indicated to obtain satisfactory results.

However, the results show a lower level of retained austenite, than the quantity that seems to exist on the digital micro-photographs analysed in the following section.

Results from JR Sec. Shaft:

BIBLIOTECA F.E. PORTO


Counts
sup7_1ªesp.xrdml
Surface
12% retained austenite
1000
500
0
44
46
48
50
Position [°2Theta]
Counts
sup7.xrdml
0,3 mm depth
6% of retained austenite
1500
1000
500
0
44
46
48
50
Position [°2Theta]



Graphics 39 and 40- Surface, 0,3 and 0,6 mm depth.

If retained austenite is present then a way to completely decompose the austenite will be to cryogenically treat the steel. Once this has been accomplished and the steel allowed to warm up to room temperature it will be necessary to temper the part. The reason being, that the retained austenite will have been decomposed to fresh martensite, which is unstable. The tempering temperature need not be any greater than 180 ° C. up to 200 ° C.

It is also possible to reduce retained austenite by using subzero treatments, but this could lead to micro-cracking on the case structure, especially if the grain size is coarse.

7.4.6 Subzero cooling- microstructure identification results

The transformation of retained austenite tends to decrease distortion, as higher residual stresses means lower distortion with the increase of dimensional stability with the rise of compressive stresses at the surface, created by the austenite-martensite transformation. It also induces higher hardness values due to the formed martensite structure. So, subzero cooling should be used for carbonitrided specimens that require high precision, high hardness levels and good stable dimensions throughout service life.

However, the transformation of retained austenite gives higher values of local residual stresses and sometimes the rise of these values might become exaggerated, leading to lower bending fatigue resistance.

And although compressive stresses continue to rise in the martensite of the case hardening part, several studies have shown that high tensile stresses are found in the remaining austenite of subzero cooling specimens. Such tensile stresses will interact with applied bending stresses and initiate possible fatigue cracks.

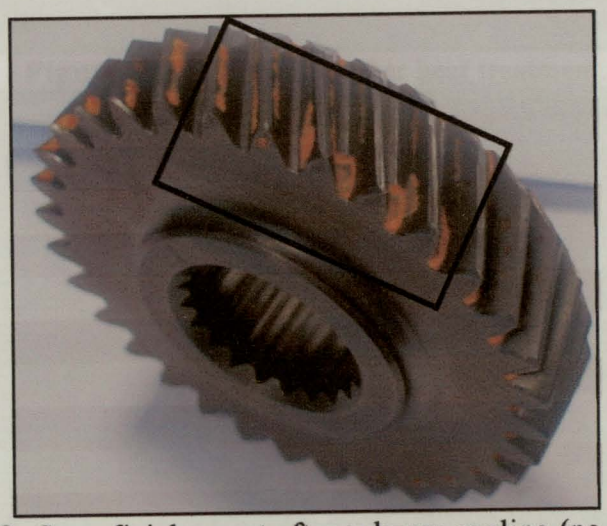


Figure 13- Superficial aspect after subzero cooling (no cleaning).

The first experience was made with one specimen of both parts in study: the PF5 and the JR Sec. Shaft, and the results for the distortion were good since no major volume expansion was obtained, which is a very positive result since the transformation of austenite in martensite should always impart volume rise.

Also, most of the geometrical parameters measured revealed an improvement, which matches the theoretical predictions.

The parts were cooled at -6°C during 48 hours. An exaggerated treatment period was set to impart visible changes in the treated parts and access the real modifications that subzero treatments are able to produce.

If parts are cleaned immediately after subzero treatment occurs, then no 'brown shallow case' is present (see previous picture). Parts are however, easily cleaned even many hours after subzero cooling.

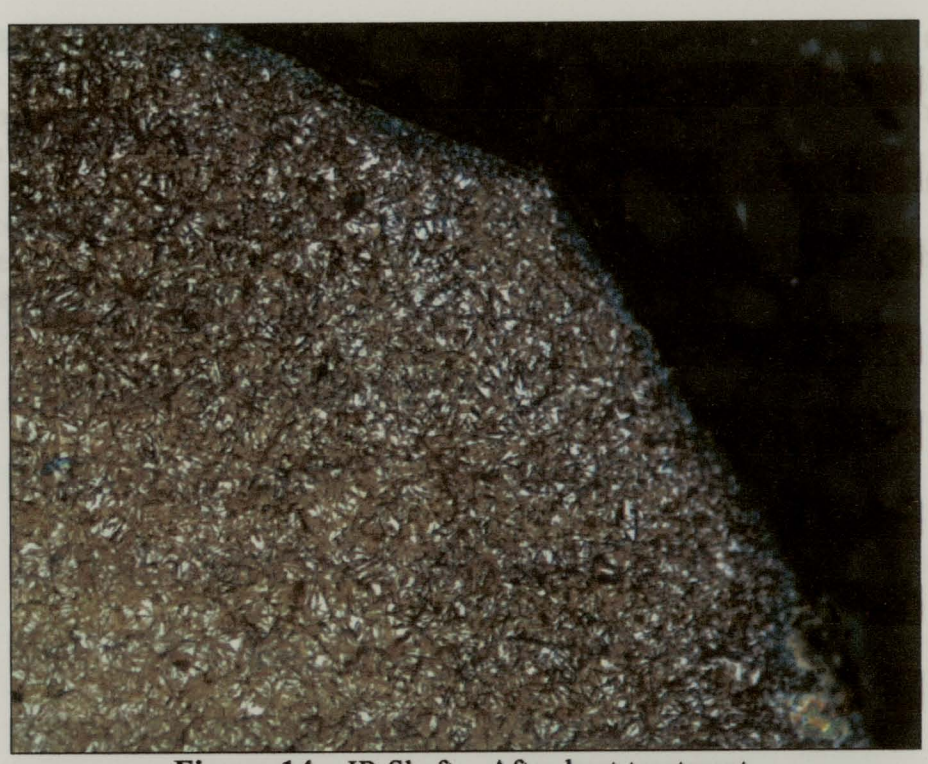


Figure 14- JR Shaft – After heat treatment.



Figure 15- JR Shaft – After subzero cooling.

Note: For further results (including PF5 results), refer to **appendix 3**.

It is visible that after heat treatment there is a considerable amount of retained austenite. The white 'points' are representative of austenite grains and its quantity is quite high.

After subzero treatment, the 'white area' has diminished, confirming the austenite-martensite transformation by lowering the temperature until Mf (martensite finish)- see **appendix 2**. Treated depth seems to be higher due to higher martensite transformation.

As seen before, the hardness levels were raised, also confirming the transformation of austenite in martensite.

The blue zones located near the edges are provoked by a surface over heating at cutting operations.

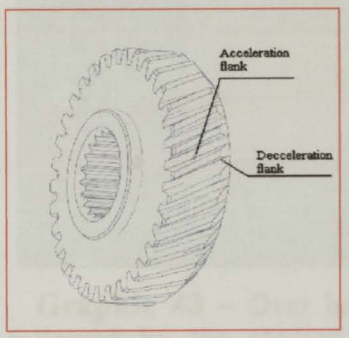
7.4.7 Subzero treatment- hardness and geometry results

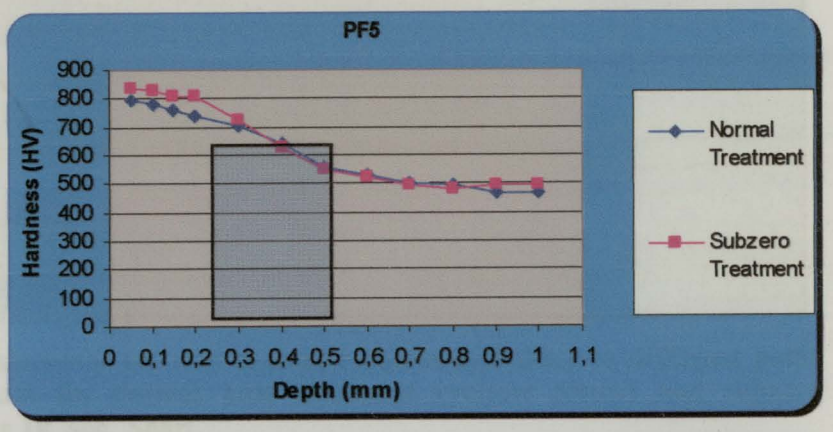
Hardness analysis

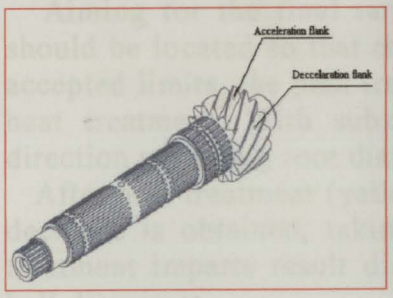
Regarding hardness measuring, the results were very satisfactory, since the parts shown an improvement (rise) in 30*HV*.

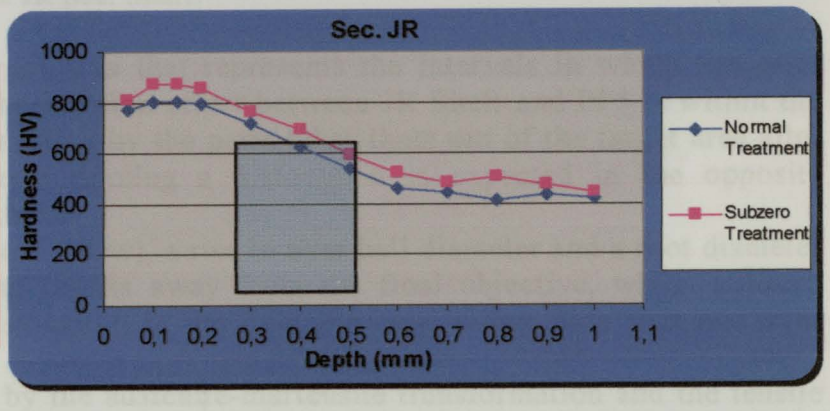
The comparison of hardness values, was made taking in account the possible rise of hardness values a few weeks after heat treatment due to micro-structural final rearrangements and stabilisation at room temperature. So, the hypotheses of hardness rise due to this phenomenon reveals to be not important.

The hardness results for both parts are represented below:









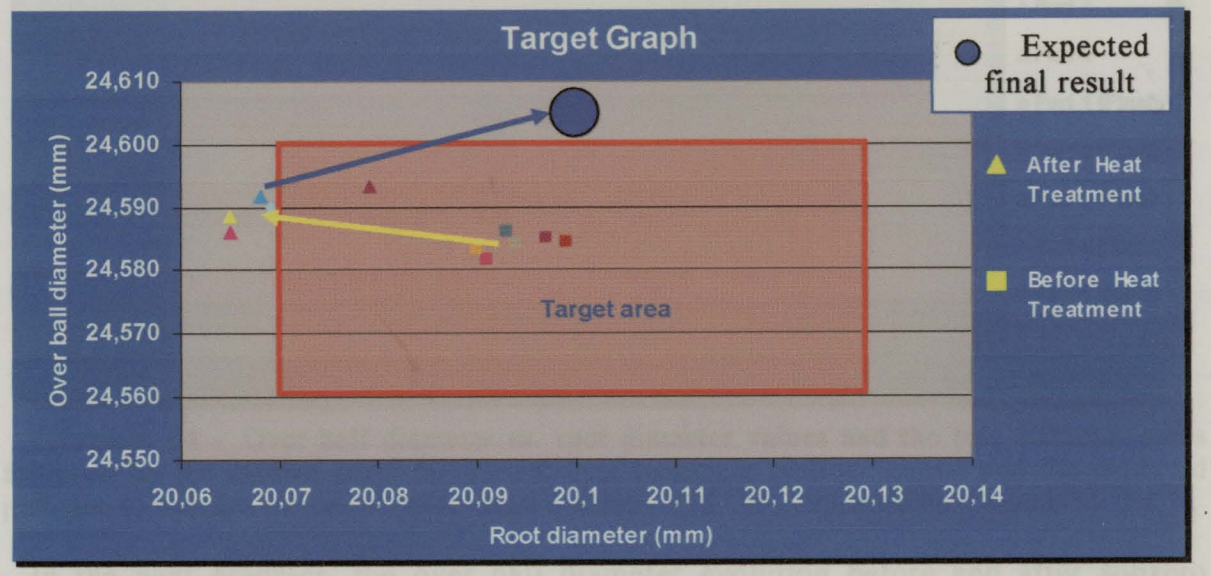
Graphics 41 and 42 – Hardness distribution ***vs.*** treated depth values for normal heat treatment and heat treatment followed by subzero treatment; results for both PF5 and JR Sec. Shaft.

It is possible to observe the raise of hardness for both parts and a growth of treated depth especially for the JR Shaft. The treated depth's limits for both parts are limited by the blue squares (between nearly 0,25 and 0,5 mm).

This rise in hardness values proves the rise in martensite percentage and the drop of austenite levels within the considered parts.

Distortion analysis

In terms of distortion measurement, the expected results are represented in the following graphic, where a relation between over ball diameter and root diameter is set, to access the expected volume expansion results.



Graphic 43 – Over ball diameter ***vs.*** root diameter values and the two different paths followed by the studied parts for normal heat treatment (yellow arrow) and subzero treatment (blue arrow); results JR Sec. Shaft.

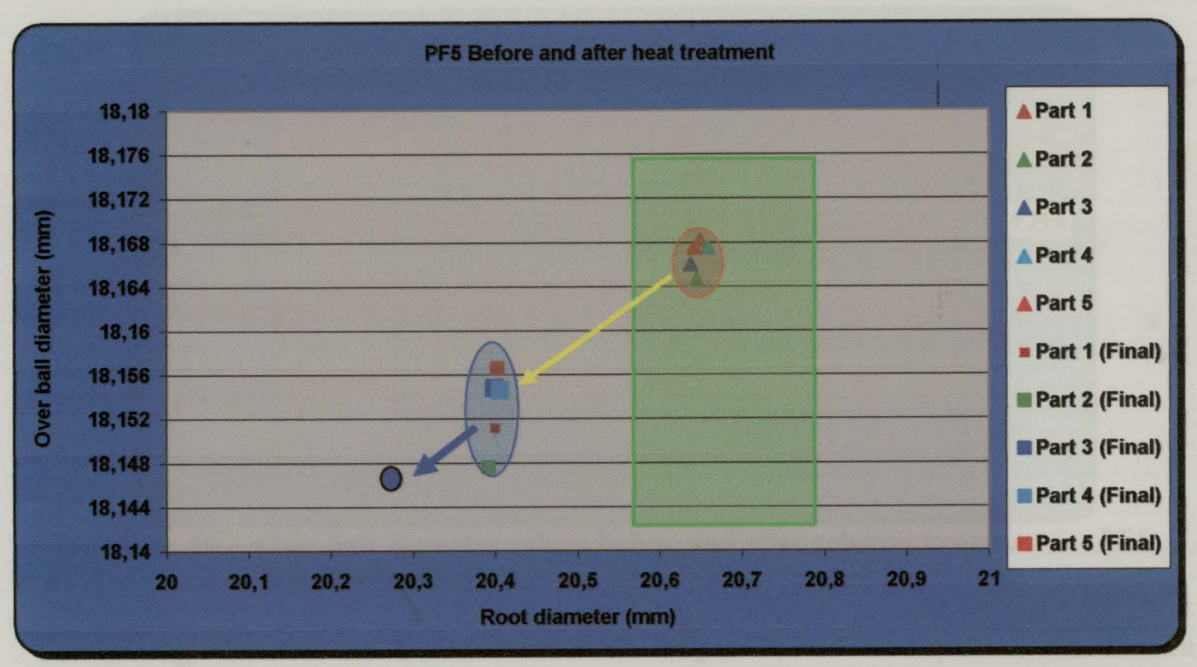
Aiming for the final target area that represents the intervals in which the parts should be located so that the junction effort between JR Shaft and PF5 is within the accepted limits, the path travelled by the parts takes them out of the target area after heat treatment. With subzero cooling a dislocation is expected in the opposite direction regarding root diameter.

After heat treatment (yellow arrow), a rise in over ball diameter and a root diameter decrease is obtained, taking results away from the final objective, whilst subzero treatment imparts result dislocation in the opposite way, rising both root and over ball diameters.

The expansion provoked by the austenite-martensite transformation and the tensile stresses created in the remaining austenite of the case are two disadvantages to be quantified, in order to access the reasonability of the use of such procedure, and mainly to interpret the occurred phase transformations and its repercussions on the part's geometrical and metallurgical properties.

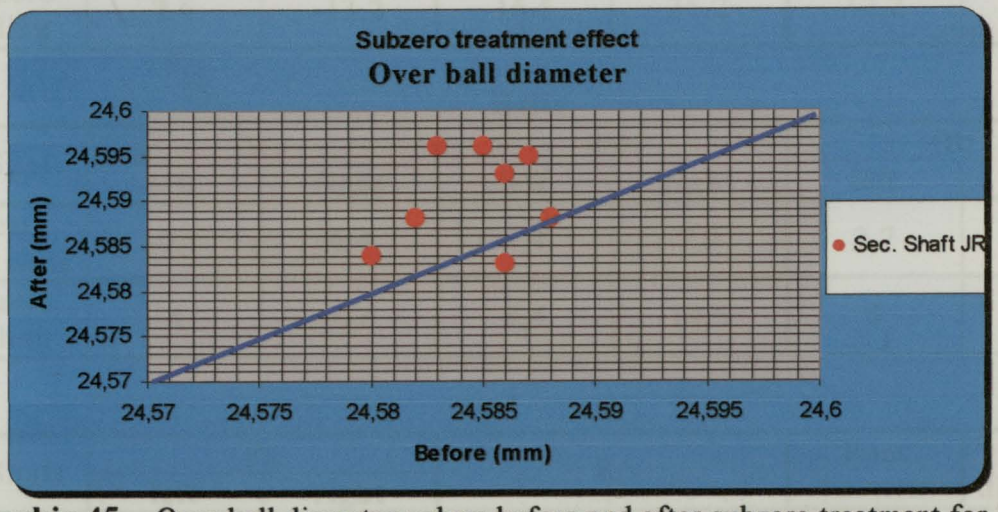
For the PF5 part, the volume expansion imparts an over ball diameter reduction since it is no longer an external gear teeth but an internal one.

The following graphic represents the evolution of the studied parts. The same as represented before for the JR Shaft.



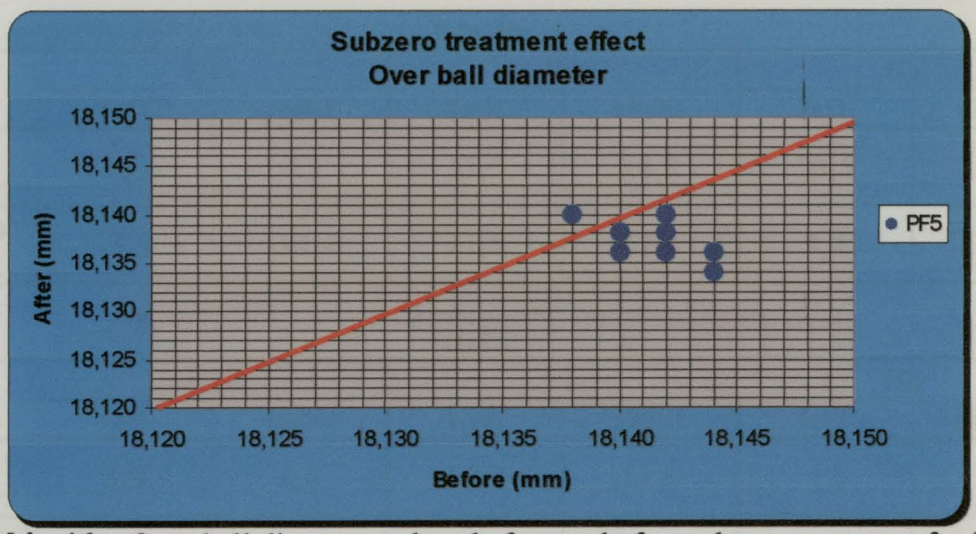
Graphic 44 – Over ball diameter *vs.* root diameter values and the two different paths followed by the studied parts for normal heat treatment (yellow arrow) and the expected path due to subzero treatment (blue arrow); results PF5. ● – expected final result.

In the next graphics, the over ball diameter evolution before and after subzero treatment is represented and the respective volume expansion for each one of the ten possible measures (20 teeth):



Graphic 45 – Over ball diameter values before and after subzero treatment for JR Shaft.

The blue line represents a transformation without volume expansion, which means equal over ball diameter values before and after subzero cooling treatment. The results indicate a slight expansion since over ball diameter values are slightly higher after subzero treatment.



Graphic 46 – Over ball diameter values before and after subzero treatment for PF5. (Red line representing a zero volume expansion transformation).

Concerning the rest of measurements an improvement is expected for reasons previously stated. The results for the JR Shaft:

Profile

JR Shaft	fHa		Fa		ffa	
	left	right	left	right	left	right
Heat Treatment	3,2	-18,1	19,4	35	16,2	27,5
Subzero cooling	7,6	-13,2	16,5	35,2	12,2	32,4

Helix

JR Shaft	fHb		Fb		ffb	
	left	right	left	right	left	right
Heat Treatment	-0,1	4,4	4,4	7,9	2,7	6,1
Subzero cooling	4	-0,6	8,4	14,5	6	12

JR Shaft	Fp		Fr	Root diameter	Tip diameter
	left	right			
Heat Treatment	49,3	58,6	16,9	20,065	21,901
Subzero cooling	47,3	39,1	20,2	20,154	21,878

Board 12- JR Shaft internal gear teeth measuring results (heat treatment/subzero cooling).

Profile

PF5	fHa		Fa		ffa	
	left	right	Left	right	left	right
Heat Treatment	-13,6	-13	13,5	14,9	18,5	19,6
Subzero cooling	-5,3	-14,4	11,6	17,1	9,4	10,7

Helix

PF5	fHb		Fb		ffb	
	left	right	Left	right	left	right
Heat Treatment	3,9	4,8	11,3	13,6	12	12,5
Subzero cooling	8,4	-6,8	12	10,5	9,8	8,2

PF5	Fp		Fr	Root diameter	Tip diameter
	left	right			
Heat Treatment	27,7	28	15,3	22,757	20,642
Subzero cooling	17,7	22,6	14,6	22,772	20,636

Board 13- PF5 internal gear teeth measuring results (heat treatment/subzero cooling).

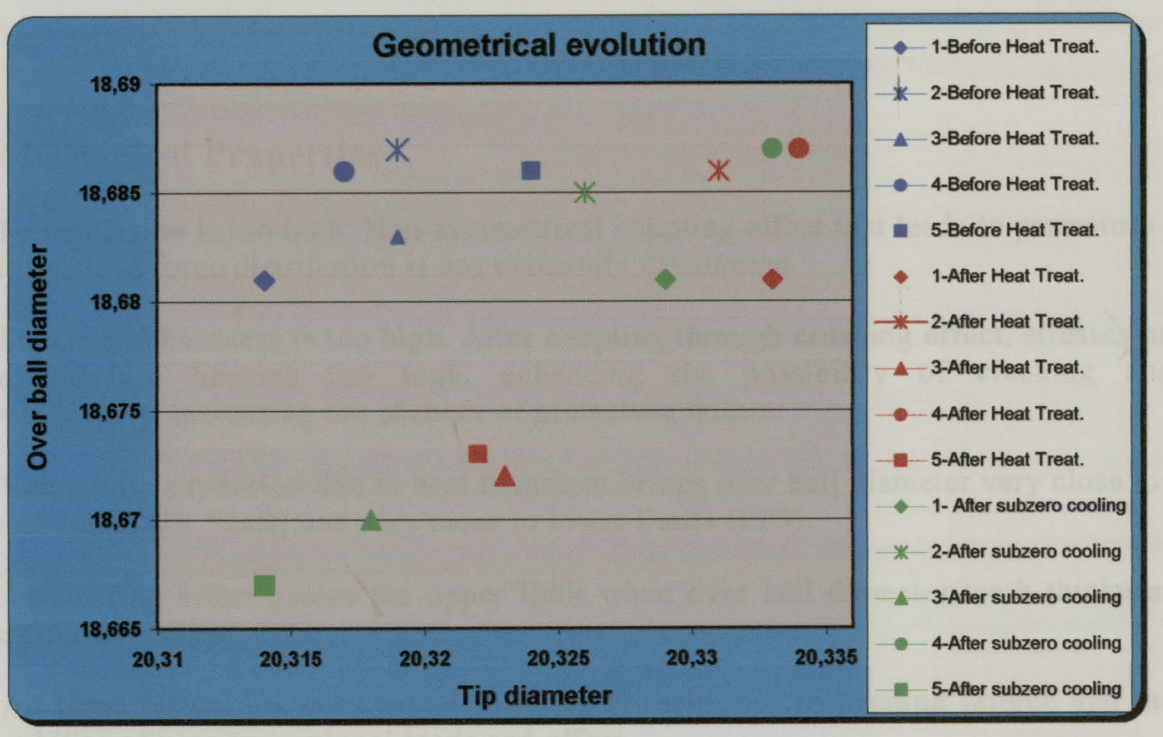
It is visible that a slight improvement was achieved in terms of Fp and Fr measures, this indicates a better tooth division, another important improvement is obtained for values of fHα for right flank and it is visible that in a general manner, all values are fairly good. This confirms the principles that indicate a lower distortion related to the austenite-martensite transformation process, since run-out errors remain fairly the same and pitch deviation is improved.

However, the root diameter grows 0,99 mm which sustains the theory of volume expansion, though a small reduction of tip diameter values is observed.

An interesting result is that root diameter is always increased and tip diameter always decreases, whereas is an internal or external gear teeth.

Another positive experimental finding is that the geometrical evolution is close to the expected, though the root diameter growth takes the part to the right side of the predetermined target area, proving that the subzero cooling does not need such a prolonged treatment period to obtained the desired results.

BIBLIOTECA F.E.



Graphic 47- PF5 geometrical evolution through heat treatment and subzero cooling.

There is a clear shift from a lower to a higher value of tip diameter (volume decrease-internal gear teeth) after heat treatment, and a slight over ball diameter decrease which means a volume expansion, being an internal gear teeth.

After subzero treatment over ball diameter decreases in a general manner, and tip diameter also decreases, meaning an actual volume expansion.

7.4.8 Conclusions

Mechanical Properties

Fp dispersion is too high. Non-symmetrical coupling effort that leads to premature failure since force distribution is not uniformly distributed.

Superficial hardness is too high. After coupling through crushing effect, stresses on the interface become too high, enhancing the possibility of cracking and consequently, increasing the chances of premature failure.

Volumetric expansion due to heat treatment brings over ball diameter very close to upper limits (JR Shaft) and very close to lower limits (PF5).

Assembling effort passes the upper limit when over ball diameter/tooth thickness pass certain values.

All these results are detrimental in terms of resistance to bending fatigue and the capability of bearing torsional loads and effort.

Micro-structure

At the time of quenching operations, micro-structural transformations start at the core developing towards the surface providing a stress distribution that gives compressive stresses at the surface and tensile stresses in core regions. This is favourable in terms of bending fatigue resistance and torsional effort.

Hardness evolution in treated depth is descendent towards the core. Higher carbon quantity at the surface explains it.

Also, the final structure reveals an austenite evolution in the treated depth that goes against a descendent hardness evolution towards the core, but as carbon values also descend towards the core there is more carbon to transform and so austenite quantity is higher near the surface.

Austenite values should not be very high, which is not what seems to happen with JR Shaft and PF5, since micro-photographs show an important amount of 'white areas' in the treated depth of the carbonitrided case. This brings tensile stresses to the case hardened that are detrimental to fatigue resistance and torsional resistance.

Martensite brings more benefits than austenite to the parts' specific application. Compressive stresses obtained through martensitic structures give higher resistance to bending fatigue, torsional loading and higher hardness to the carbonitrided case.

Subzero treatment imparts austenite-martensite transformation, rising hardness values and improving gear teeth division properties though a certain volumetric expansion is also obtained.

After subzero treatment, 'white areas' are diminished. However, this decrease in austenite levels may sometimes reveal an occupation area reduction rather than an actual austenite quantity reduction.

Supposing certain areas are only diminished in size, the straighten austenite zones are now subjected to very high tensile stresses surrounded by the compressive stressed martensitic areas.

Such situation induces an important reduction of bending fatigue resistance and a rise in the probability of premature cracking, and, as a rise in superficial hardness (more martensite) is verified, in this case subzero treatment reveals highly detrimental.

The higher the residual stress level, the lower the distortion will be.

All this can only be assessed with bending and torsional in service simulated fatigue tests.

Final conclusions

Conclusions have been taken in previous sections, still there are some overall conclusions, mainly regarding the obtained structure and how the diverse processes influence the structure.

Distortion imparts important geometrical changes in the desired final product. In small gear box or engine balancing machine pinions several geometrical measures should be taken into account when studying the effects of all machining and heat treatment operations throughout the production process.

The distortion effects produced throughout the heat treatment process are mostly relevant in areas subjected to future fatigue contact, where dimensional tolerances are extremely narrow and any minor geometrical dislocation might represent a big and decisive malfunction in contact zone.

Carbonitriding and quenching have a direct effect on bending and contact fatigue of gears' components.

For example, a delay between carbonitriding and quenching will cause the temperature of the steel to fall before it is quenched, leading to a reduction in the hardening effect. If the tempering is not effective, then the part may remain brittle with undesirable consequences. In these circumstances, brittle gear teeth can break off causing an engine or gearbox failure. If the temperature is not properly maintained while carbon diffuses into the steel, then the case depth will be incorrect and there could be a presence of the high temperature phase called retained austenite.

Obtaining the desired final structure

Constituents	Hardness	Tensile Strength	Fatigue Resistance	Impact Resistance
Ferrite	100 HB	330 N/mm^2	Reliable	Not good
Austenite	150 HB	400 N/mm^2	Very reliable	Very good
Perlite	250 HB	850 N/mm^2	Medium	Medium
Carbonates	Very high	---	---	Very reliable
Martensite	High	Very high	Good	Good
Bainite	High	Medium	Good	Medium

Constituents	Surface finish	Rolling fatigue	Wear contact fatigue	Adhesive use
Ferrite	Not good	Not good	Reliable	Reliable
Austenite	Not good	Not good	Reliable	Reliable
Perlite	Good	Medium	Good	Good
Carbonates	Good	Reliable	Excellent	Excellent
Martensite	Good	Good	Very good	Good
Bainite	Medium	Medium	Medium	Medium

Board 14- Constituents' mechanical properties.

Compressive residual stresses	↗	*Notes*
Crack propagation and brittle fracture	↗	*Compressive stresses induce crack propagation and the structure becomes harder (martensite)*
Quenching temperature	↗	*The rise of quenching temperature enhances the possibility of compressive stresses*
Tempering temperature	↙	*A decrease in tempering temperature rises compressive stresses. In this case more stable martensite means an increase in ductility and decrease in hardness and therefore in brittle fracture*
Martensite	↗	*A rise in martensite quantity induces more compressive stresses*
Retained austenite of subzero cooled specimens	↙	*A reduction of retained austenite raises compressive stresses (more martensite)*

Board 15- Cause-effect board in terms of compressive stresses.

Compressive residual stresses	↗	*Notes*
Crack initiation	↘	*Compressive stresses induce crack propagation and the structure becomes harder (martensite),* ***however****, reduces the risk of crack initiation*
Fatigue life and contact fatigue life	↗	*The rise of compressive stresses also rises fatigue life and,* ***more important****, contact fatigue life*
Grinding	↙	*Grinding imparts tensile stresses.The shorter the time spent on grinding operations the lower the induced tensile stresses will be, and so there is a maintenance of compressive stresses*
Shot Peening	↗	*Shot peening induces compressive stresses by transformed some of the retained austenite*
Volume expansion	↗	*The rise of compressive stresses imparts a volume expansion*

Board 16- Cause-effect board in terms of compressive stresses.

Further Work

Hardness tests and retained austenite assessment before and after tempering are required to access martensite stabilisation and fulfil complete metallurgical behaviour.

Contact fatigue tests in specimens with or without subzero cooling may give comprehension of fatigue resistance and its relation with the obtained microstructures. This way it is possible to understand if the austenite area reduction is related with the actual decrease of retained austenite or with the rise of tensile stresses in the remaining austenite area and compare it with the fatigue obtained results.

If no experiments are possible in terms of changing the heat treatment parameters then it is difficult to relate the obtained results with carbon potential, ammonia flow, treatment temperature, treatment and diffusion times, etc.

Ammonia flow and its interaction with the carbonitrided atmosphere and relation with the obtained results must be undertaken.

Oil life time and its relation with the achieved hardness and distortion levels must be studied.

A statistical study regarding the parts position in the load carry will help to understand the effects on hardness and distortion of oil quenching entering order.



Figure 15- JR Shaft load: the parts located at the bottom (1st level), will warm the oil providing a different oil quenching temperature the ones located above.

References

1. **D.H. Herring**, Comparing Carbonitriding and Nitrocarburizing, *Heat Treat. Prog.* 2002.

2. **Dudley**, **Gear Handbook** – The design, Manufacture, and Application of Gears, McGraw Hill, First Edition.

3. **F.A. Clarkin and M.B. Bever**, The Role of Water Vapor and Ammonia in Case Hardening Atmospheres, *Trans. ASM,* Vol 47, 1955.

4. **G.W. Powell, M.B. Bever, and C.F. Floe**, Carbonitriding of Plain Carbon and Boron Steels, *Trans. ASM,* Vol 46, 1954.

5. **H. Altena and F. Schrank**, Low Pressure Carburised with High Pressure Gas, Quenching in Batch Type Furnaces and Continuous Plants, 2002, Nr. 1665.

6. Henriot Georges, Engrenages Conception Fabrication Mise en Oeuvre, 7e édition, 1999.

7. Klingelnberg Söhne, Manuel d'utilisation, Version 2.0.

9. **Krauss G.**, Bending fatigue of carburised steels. ASM Hanbook, Vol. 19, Fatigue and Fracture. ASM International, 1996, 680-690.

10. **Macherauch E. and Vöhringer O.**, Residual stresses after quenching. Theory and Technology of Quenching. (Eds: B. Liscic, H. M. Tensi, and W. Luty). Springer-Verlag, 1992, 117-181.

11. Metal Handbook, ASM International, 9ª Edition.

12. **Pinto Soares**, 'Aços Características e Tratamentos', 5ª Edição

13. **T. Réti**, Residual stresses in carburised, carbonitrided and case-hardened components. Heat Treatment of Metals, 2003, 83-96.

Agrément des Moyenes et Capabilité, selon la Norme NF E 60-181. Ref: D2273.CF

Institut de L'engrenage et des transmissions, cours special CACIA :
Geometrie de la denture
Engrenement et corrections de denture
Metrologie- Mesure de l'epaisseur des dents
Calcul des dentures
Traitement Thermique (II)

Usines Renault S.A., Appearance of gear teeth including aspects of wear and defects,1992.

Jacques Marc, Yves Desalos, Déformation des dentures traitées par carbonitruration trempe huile chaude, 1993.

APPENDIX 1

Allotropic iron forms

Atomic representation

Ferrite, α iron (body centred cubic) – solubility of carbon: 0.006% at room temperature.

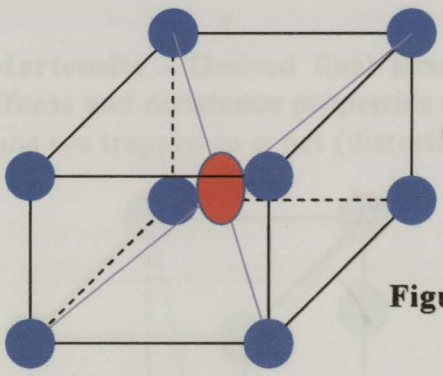


Figure 17- Ferrite.

In ferrite the most evident element present is carbon, which may be presented under the form of diamante, graphite or coal.

From room temperature to 911°C, pure iron presents a cubic centred structure (α iron).

Austenite, γ iron (face centred cubic) – solubility of carbon: depends on temperature and has its maximum value at 1147°C (2.1%).

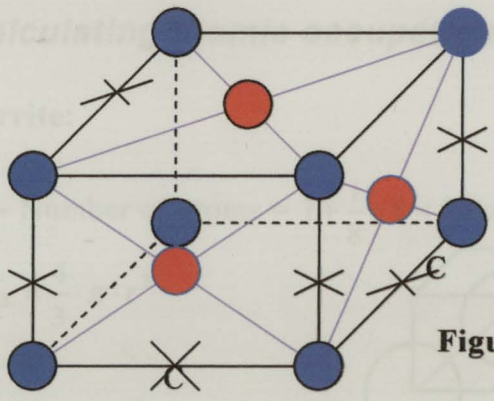


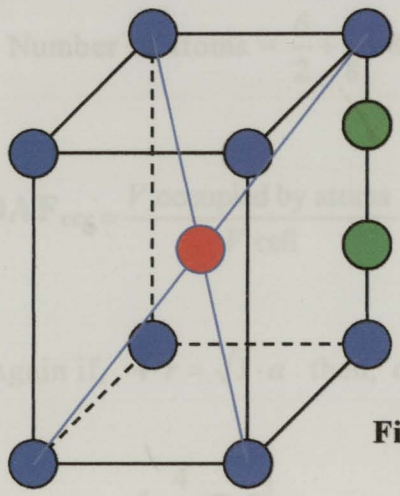
Figure 18- Austenite.

At 911°C iron suffers an allotropic form transformation from α to a cubic face centred stricture (γ iron), which is stable until 1392°C, temperature at which another atomic rearrangement takes place into a new cubic centred structure denominated as δ iron, which carbon's solubility is also quite low.

The carbon's solubility in iron is one of interstitial type, because carbon atoms are much smaller than iron atoms. This solubility varies for different allotropic structure net lengths. So, due to a net length's variation, that is if net length becomes higher, the unstable carbon formed has a tendency for leaving the net.

This is what happens with martensite and its tetragonal centred net. Its mechanical parameters get distant from the ones related to ferrite, as the carbon amount in solution gets higher.

Martensite - Desired final structure in carbonitriding processes, due to its high stiffness and resistance properties and also its highest ability to retain carbon. Carbon atoms are trapped in α net (distortion), leading to a tetragonal net.



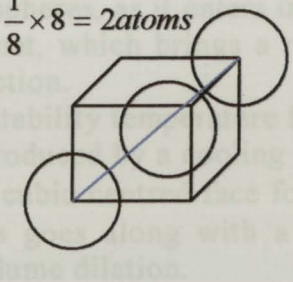
Carbon atoms.

Figure 19- Martensite.

Calculating atomic occupation

Ferrite:

α - Number of atoms = $1+\frac{1}{8}\times 8 = 2 atoms$



$$\mathbf{V_{at.}} = \frac{4}{3}\cdot\pi\cdot r^3$$

$$\mathbf{V} = a^3$$

$$\mathbf{OAF_{ccc}} = \frac{V \text{ occupied by atoms}}{V \text{ cell}} = \frac{2\cdot\frac{4}{3}\cdot\pi\cdot r^3}{a^3}$$

If, $4 \cdot r = \sqrt{3} \cdot a$ then, $a = \frac{4 \cdot r}{\sqrt{3}}$ so;

$$\mathbf{OAF}_{ccc} = \frac{2 \cdot \frac{4}{3} \cdot \pi \cdot r^3}{\left(\frac{4 \cdot r}{\sqrt{3}}\right)^3} = 0.68 \approx 0.7$$

Austenite:

γ - Number of atoms = $\frac{6}{2} + \frac{1}{8} \times 8 = 4 atoms$

$$\mathbf{OAF}_{ccc} = \frac{V \text{ occupied by atoms}}{V \text{ cell}} = \frac{4 \cdot \frac{4}{3} \cdot \pi \cdot r^3}{a^3}$$

Again if, $4 \cdot r = \sqrt{3} \cdot a$ then, $a = \frac{4 \cdot r}{\sqrt{3}}$ so;

$$\mathbf{OAF}_{ccc} = \frac{4 \cdot \frac{4}{3} \cdot \pi \cdot r^3}{\left(\frac{4 \cdot r}{\sqrt{3}}\right)^3} = 1.36$$

It is possible to conclude that when the steel alloy is heated to such temperatures used in carbonitrided atmospheres, as it enters in austenitic dominium, carbon will be trapped in a much denser net, which brings a reduction of specific volume, and so, provoking a volume contraction.

Alternatively, under the stability temperature limit (under 911°C, for pure iron), the allotropic transformation produced by a cooling process, changes the structure atomic form, which passes from a cubic centred face form (γ), to a cubic centred body form (α). This transformation is goes along with a small raise of specific volume and consequently promoting volume dilation.

APPENDIX 2

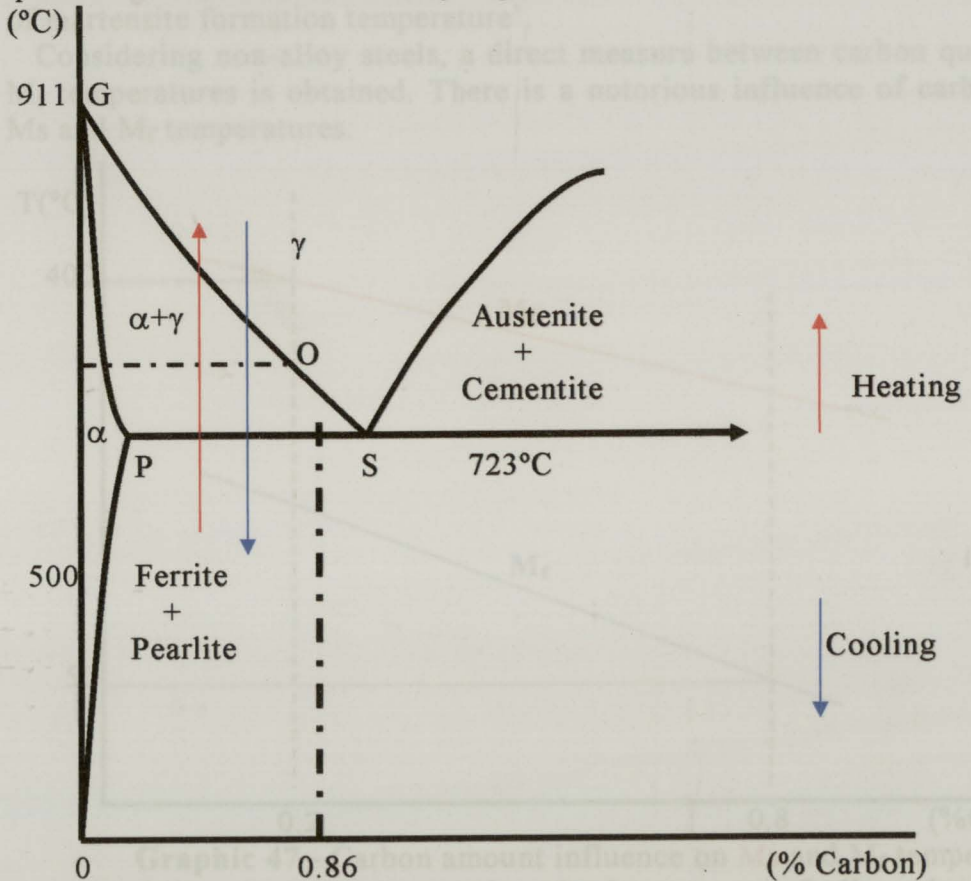
Equilibrium diagrams (Fe-C)

Above 723°C (during heating), ferrite (α) will transform into austenite (γ). This austenite starts to dissolve cementite due to its capability of carbon dissolution.

The process is terminated when 'GOS' line is reached. At this temperature all ferrite is transformed in austenite and carbon is then taken in solution as atoms are distributed through the face-centred cubic form. This could be considered as the α→γ transformation line and its temperature diminishes (<911°C), as carbon presence ascends.

During quenching process carbon is expelled from the solution and it precipitates under the form of carbonates, these carbonates form acicular three-dimensional needles that will join the ones from ferrite to generate pearlite. These 'needles' are created by diffusion (with migration), of carbon in grain joints. As cooling time gets shorter, thinner needles are obtained and less time for diffusion process is available.

As cooling velocity increases, the available time for ferrite to precipitate becomes shorter. If velocity continues to rise, a value is reached where no precipitation occurs. This means that the pearlite in which austenite is transformed has higher quantities of ferrite than usually expected.



Graphic 46 - Austenite transformation during heating and cooling processes.

The maximum carbon amount dissolved by austenite at 723°C is 0.86%. If a superior amount of carbon is present it will precipitate as iron carbonates (Fe_3C).

For temperatures way below 500°C, carbon's diffusion is highly reduced and pearlite is no longer being created. Austenite whose transformation was clogged in the course of a sufficiently rapid cooling velocity converts into an α iron centred net, in which carbon atoms become trapped. The resulting structure (tetragonal) has the shape of thin small needles having high stiffness and resistance due to the high tensions induced by carbon's presence.

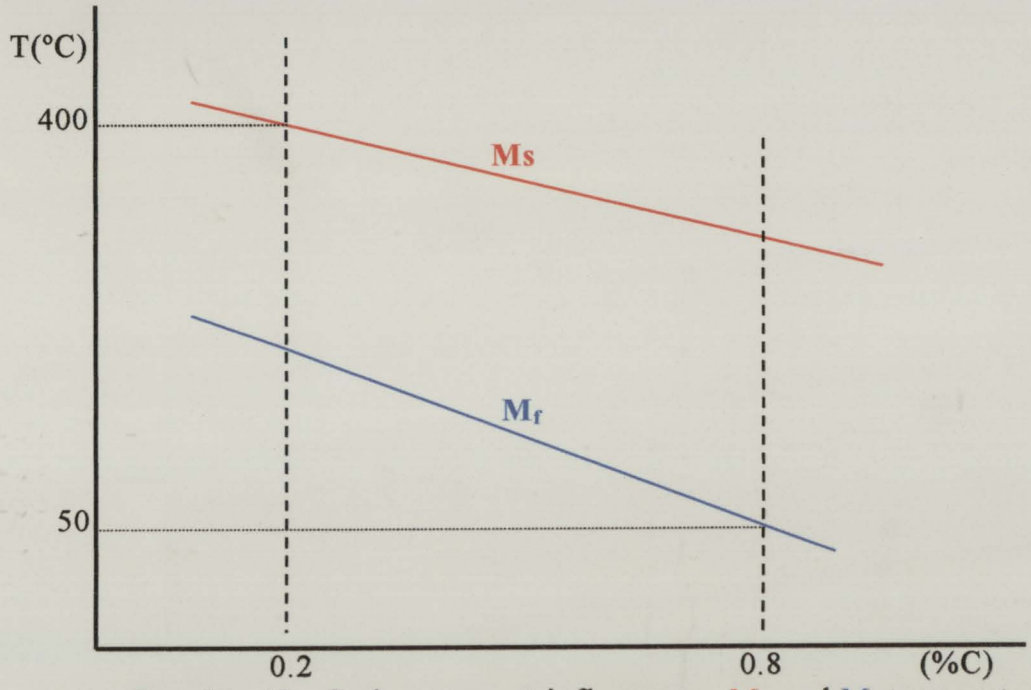
This structure is called martensite.

Two distinctive temperature phases are to be considered during martensite completion process.

The first phase, known as martensite start (Ms), is that temperature, at which steel is required to be cooled so that martensite could be obtained. If steel is cooled at a suitable velocity, martensite is the only structure obtained. Austenite-martensite transformation is exclusively temperature dependent as Ms depends on steel's chemical constitution. If steel's chemical composition holds a considerable amount of alloy elements M_f might be excessively low, this occurrence carries the possibility of steel's retained austenite presence at room temperature since austenite was not completely transformed during all cooling process stages.

The second phase, known as martensite finish (M_f), is the temperature, at which austenite completely converts into martensite. It might also be considered as the 'end of martensite formation temperature'.

Considering non-alloy steels, a direct measure between carbon quantity and Ms or M_f temperatures is obtained. There is a notorious influence of carbon magnitude in Ms and M_f temperatures:



Graphic 47 - Carbon amount influence on Ms and M_f temperatures.

A conclusion is taken concerning the importance of alloy elements and carbon quantity control in avoiding retained austenite during martensite formation process.

Martensitic transformations are produced without carbon diffusion through a shear mecanism over γ net.

Using slower cooling velocities, carbon atoms will precipitate from α net, since the net has an insufficiency to dissolve all the existing carbon, however if sufficiently rapid cooling velocities are used, carbon atoms will be trapped in the α net, provoking a net distortion, and making martensite a tetragonal net (fig. 5), holding a height/width ratio that is higher for higher carbon values.

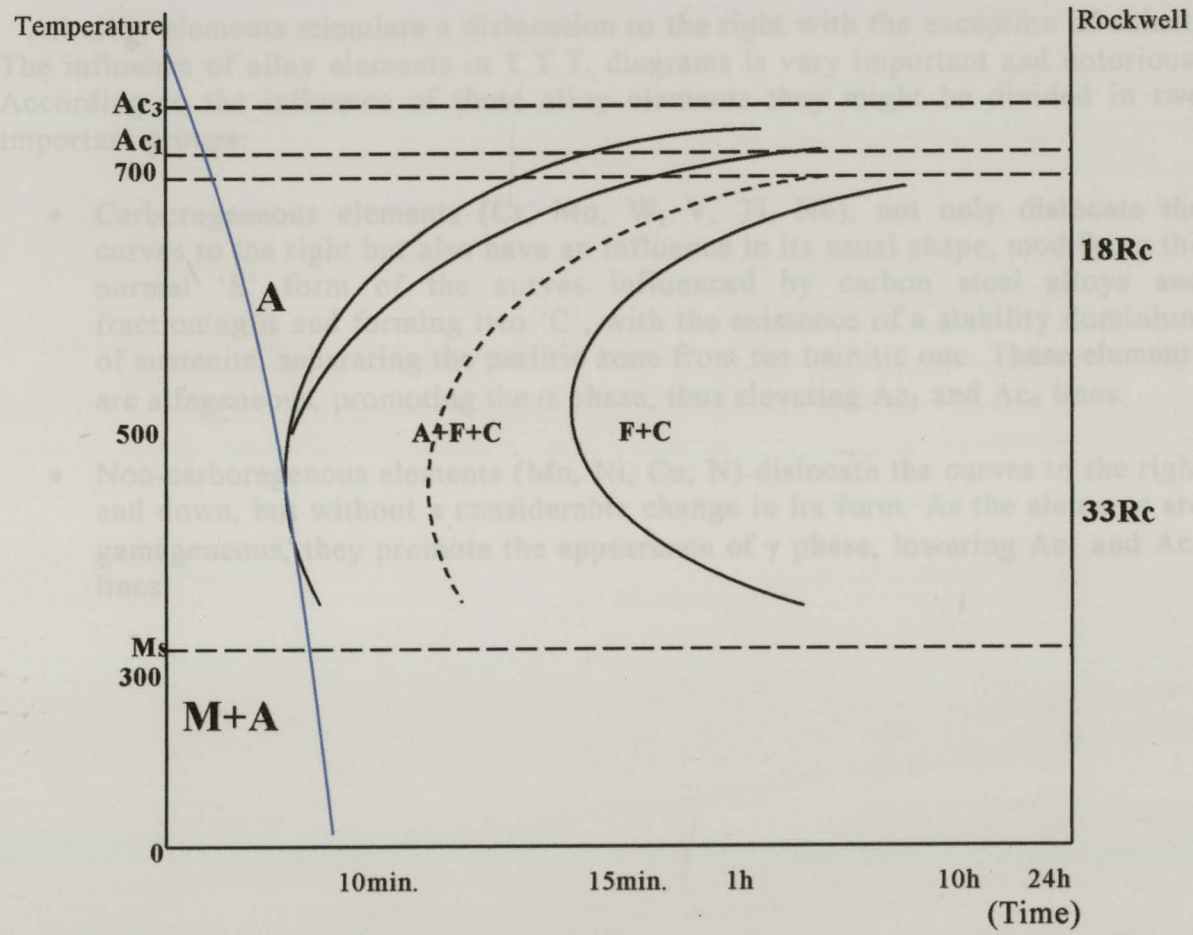
The minimum velocity that allows this complete martensitic transformation is known as critical steel tempera velocity. It is important to know that martensitic structures are hard but have low toughness too. This is another important reason why a nice compromise between hardness, toughness and distortion is normally unfeasible to achieve through thermo-chemical treatments such as carburising, nitriding and carbonitriding.

T.T.T. Diagrams (Transformation –Time – Temperature)

The T.T.T. curves might be defined as austenite transformation curves, subjected to predetermined heating conditions. Variations of the austenizing conditions obligate T.T.T. curves to certain dislocations along the diagram axis, mostly along the diagram's xx axis.

These curves provide, among other information, the indication of the forming steel structure as the steel is subjected to a certain cooling process, departing from the austenizing temperature, or tempera temperature. The curves also indicate, for a given temperature, the necessary time to accomplish the beginning and end of the austenite transformation. The necessary time to achieve the austenite transformation start at a given temperature is sometimes used to provide the maximum time that the steel may be kept in the 'cooling atmosphere' (gas, oil, water), at that temperature, without any phase or constituent transformation.

Consequently, the diagram indicates the temperature at which the martensite starts its formation, being martensite start, independent from the cooling velocity.



Graphic 48 - Transformation – Time – Temperature curves. **A** – austenite; **F** – ferrite; **C** – cementite; **M** – martensite.

——— The blue line represented in the previous graphic shows the critical steel tempera velocity. (As explained in the previous chapter, is the minimum velocity that allows a complete martensitic transformation).

The curved line positioned to the right corresponds to the end of the isothermal transformation, with the middle line corresponding to a 50% transformation.

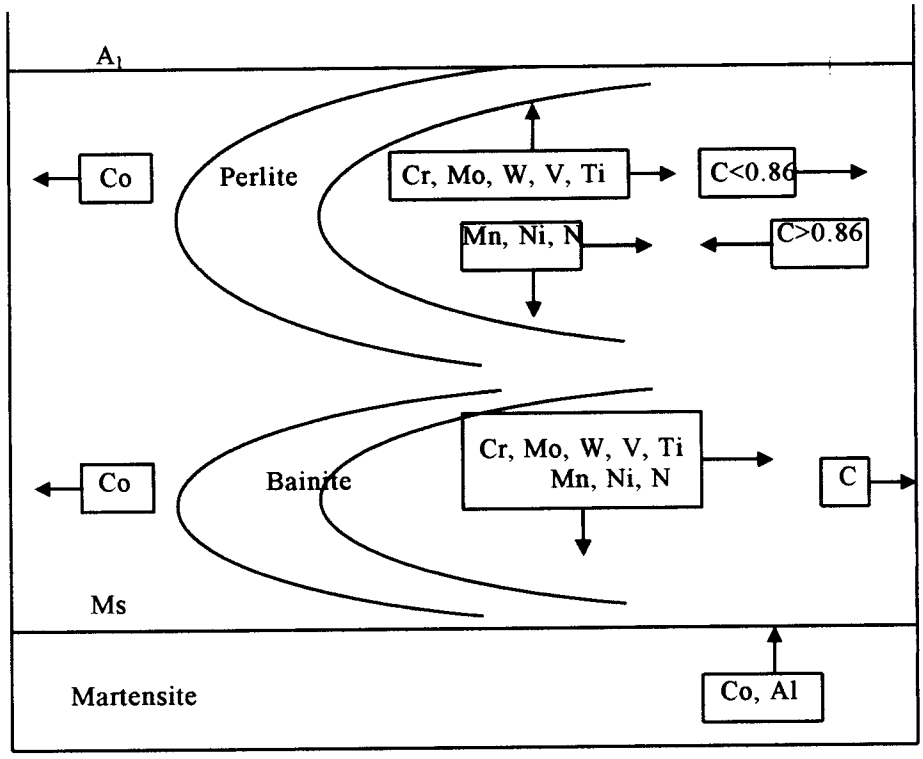
Several aspects have a direct influence on the positioning of such curves; the most important one is chemical composition. Concerning carbon steel, the quantities of carbon have a direct influence on the positioning of the curves. Under the eutectoid point, a raise in carbon values will move the curves to right and below as above the eutectoid point the opposite happens.

Alloy Elements

All alloy elements stimulate a dislocation to the right with the exception of cobalt. The influence of alloy elements in T.T.T. diagrams is very important and notorious. According to the influence of these alloy elements they might be divided in two important groups:

- Carboregeneous elements (Cr, Mo, W, V, Ti, Nb), not only dislocate the curves to the right but also have an influence in its usual shape, modifying the normal 'S' form of the curves influenced by carbon steel alloys and fractioning it and forming two 'C', with the existence of a stability dominium of austenite, separating the perlitic zone from the bainitic one. These elements are alfageneous, promoting the α phase, thus elevating Ac_1 and Ac_3 lines.

- Non-carboregenous elements (Mn, Ni, Cu, N) dislocate the curves to the right and down, but without a considerable change in its form. As the elements are gamageneous, they promote the appearance of γ phase, lowering Ac_1 and Ac_3 lines.



Graphic 49 – Influence of alloy elements in the form and position of T.T.T. curves.

As it is exposed in the previous graphic, only Cobalt and Aluminum elevate the martensite start temperature line, as all other elements retard the initiation of martensite transformation.

Note that nitrogen is a gamageneous and non-carboregeneous element moving curves to right, hence improving hardenability. However nitrogen lowers Ms and M_f lines delaying martensitic transformation. Its presence promotes therefore, retained austenite at room temperature.

APPENDIX 3

Microstructure analysis

Microstructures of castings look different from those of wrought products, even if they have the same chemical composition and are given the same heat treatment. In general, it is easiest to identify heat-treated structures after transformation and before tempering. For example, if a mixed microstructure of bainite and martensite is formed during quenching, these constituents will become more difficult to identify reliably as the tempering temperature used for the product increases toward the lower critical temperature. The difficulty of phase distinction is so high that certain ferrous metallographers tend to use special techniques almost exclusively for etching.

For instance, alpha iron, strictly speaking, refers only to the bcc form of pure iron, which is stable below 912°C (1674F) while ferrite is a solid solution of one or more elements in bcc iron. Often these terms are used synonymously, which is incorrect. Ferrite may precipitate from austenite in acicular form under certain cooling conditions. Acicular means the shape is like a needle, three dimensionally speaking.

However, this is not the actual shape of acicular ferrite in three dimensions. Figure 1 shows the appearance of ferrite grains in carbon steel used for laminations. There are also ferritic stainless steels, which contain high chromium contents and very little carbon.

Ferrite is a very soft, ductile phase, although it looses its toughness below some critical temperature.

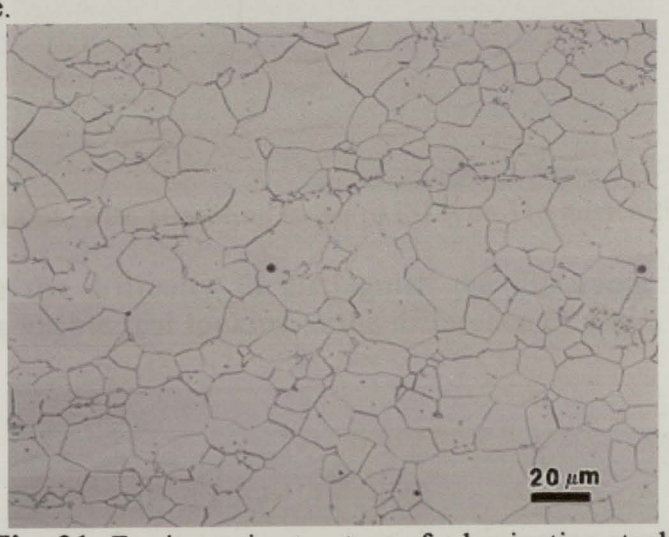


Fig. 21- Ferrite grain structure of a lamination steel.

Gamma iron, as with alpha iron, pertains to only the face-centred cubic (fcc) form of pure iron that is stable between 912°C and 1394°C (1674 and 2541F) while austenite is a solid solution of one or more elements in fcc iron. Again, these terms are often used interchangeably, which is incorrect. For heat-treatable steels, austenite is the parent phase for all transformation products that make ferrous alloys so versatile and useful commercially. Austenite is not stable at room temperature in ordinary steels. In chrome-nickel (Cr-Ni) steels, know as stainless steels, there is a family of very important grades where austenite is stable at room temperature.

Some of the steels treated in this work are chrome-nickel steels, though they might have other alloy elements. These steels, which are used for carbonitriding, and then for the assembling and coupling of several structural gear box sections, have different carbon percentages, geometry and different heat treatment cycles. Given the difference of chemical compositions and the distinguish production cycles, the difficulty of obtaining similar

Figure 2 shows an example of the microstructure of AISI type316 austenitic stainless steel. Austenite is a soft, ductile phase that can be work hardened to high strength levels, particularly in the fully austenitic manganese steels.

In high-carbon, high-alloy steels, such as tool steels, use of an excessively high austenitizing temperature will depress the temperatures where martensite begins and completes its transformation. These martensite start and end temperatures are depressed to such an extent that the austenite is not fully converted to martensite during quenching and the remaining austenite, called retained austenite, is present (but not necessarily stable) at room temperature.

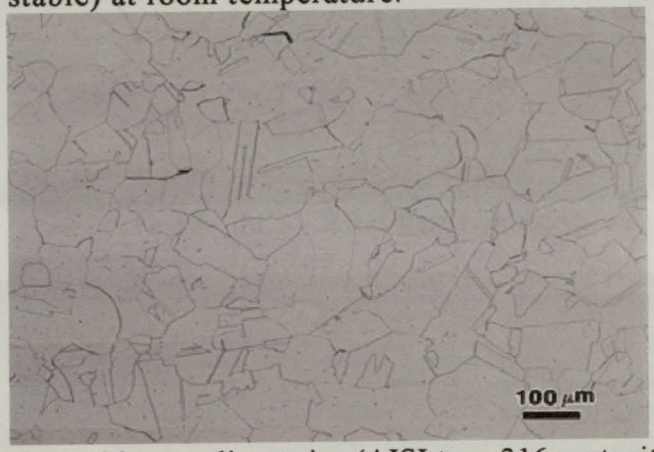


Fig. 22- Austenite grains, with annealing twins (AISI type 316 austenitic stainless steel).

One can observe the difficulty to distinguish the difference from the previous picture, though it is visible that looking at the difference of scale, conclusions can be withdraw.

The next pictures are from a PF5 part where microstructure analysis was made after heat treatment and after subzero treatment.

Zoom factor: X200 and X500.

The two last pictures reveal the indentations from hardness measures.

Blue areas due to excess of cutting force by an excessive pressure applied to the carbon disk.

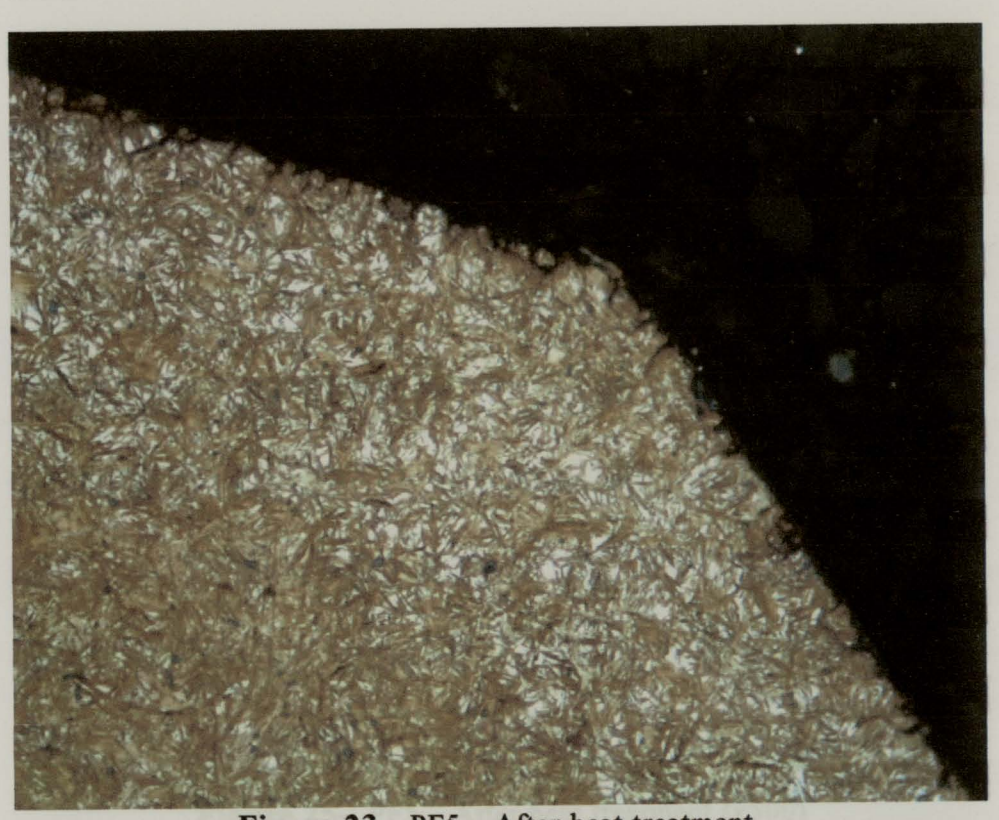


Figure 23- PF5 – After heat treatment.

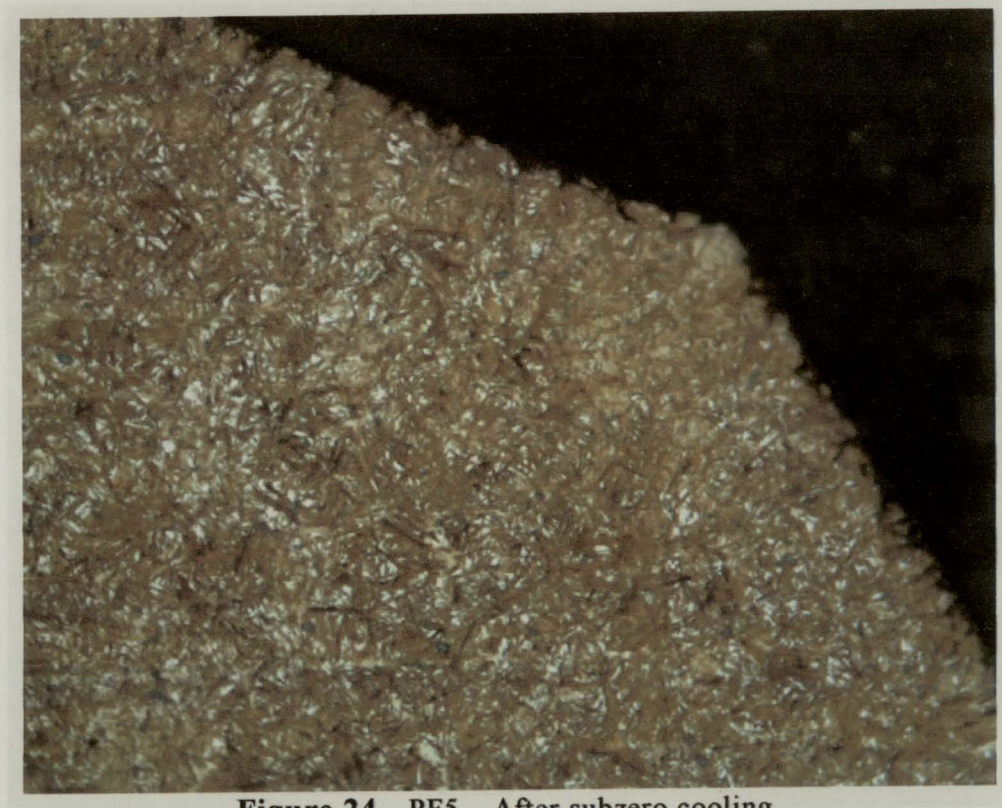


Figure 24- PF5 – After subzero cooling.

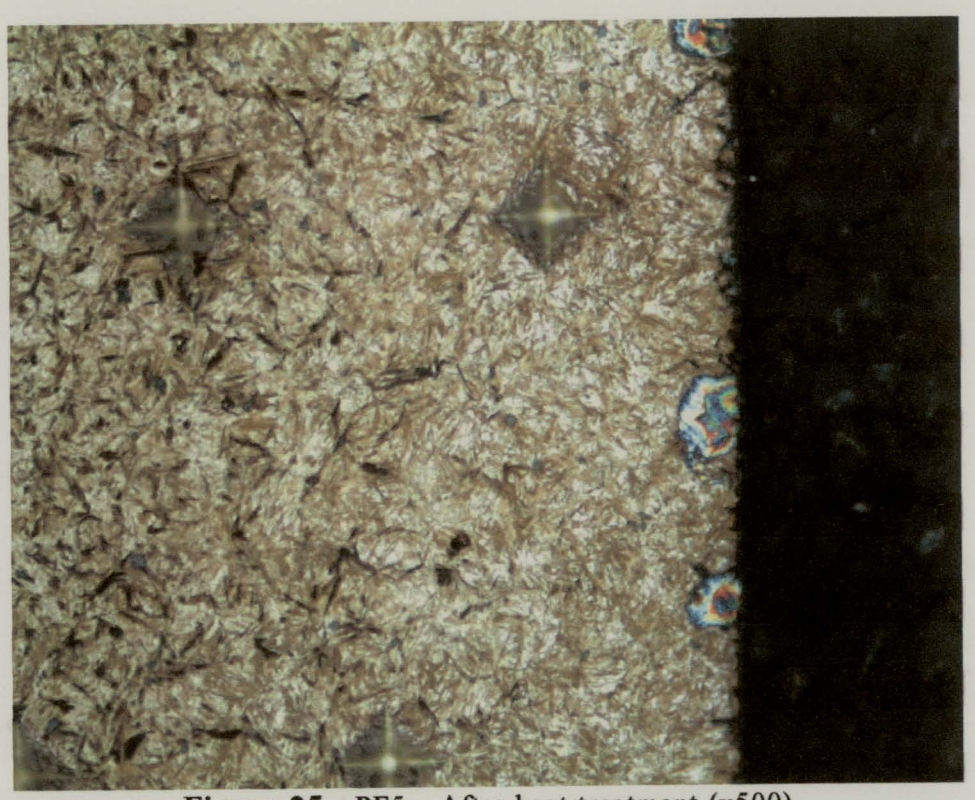


Figure 25- PF5 – After heat treatment.(x500)



Figure 26- PF5 – After subzero cooling.(x500)

APPENDIX 4

X-ray diffraction

When x-rays contact with a crystal, electromagnetic waves penetrate the crystalline structure.

$$Ey(x,t)=Ey0\sin(kx-\omega t)$$

E_{y0} : Wave vector

$k=2\pi/\lambda$: Wave vector

$\omega= 2\pi f$: Angular frequency

$(kx-\omega t)=\Phi$: Phase

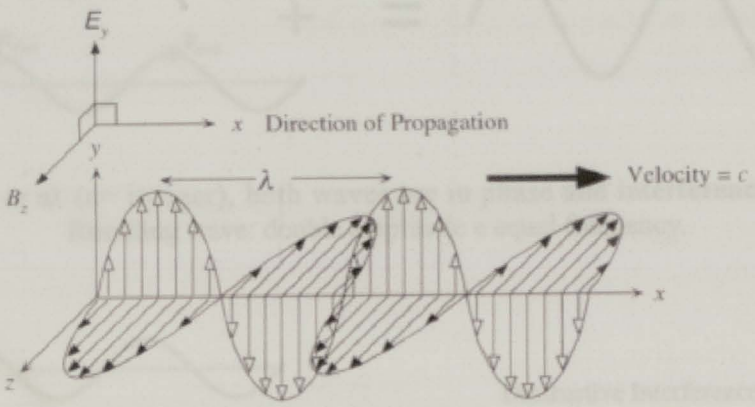


Figure 27- Sinusoidal wave travelling in x axis direction. Phase velocity: $c= \omega/k= f/\lambda$.

X-Rays: Rays where λ is approximately 1nm.

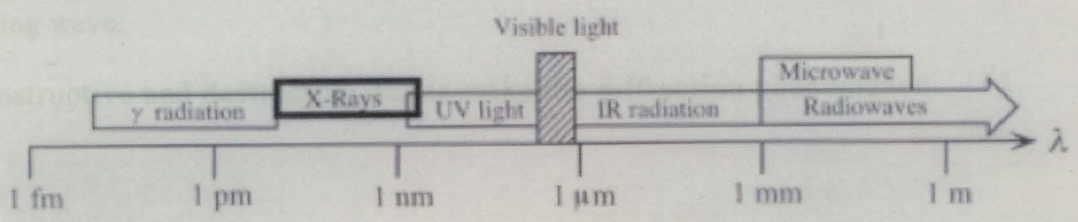


Figure 28- Wave spectral (visible to human eye where λ is between 390 and 780 nm).

Every wave has interference phenomenon. When two waves of equal frequency and amplitude are superposed, the resulting wave depends of the phase difference between both.

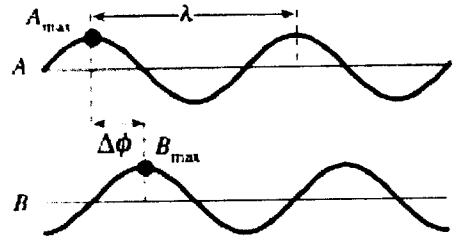


Figure 29- ΔΦ: Phase interval between A máx. And B máx..

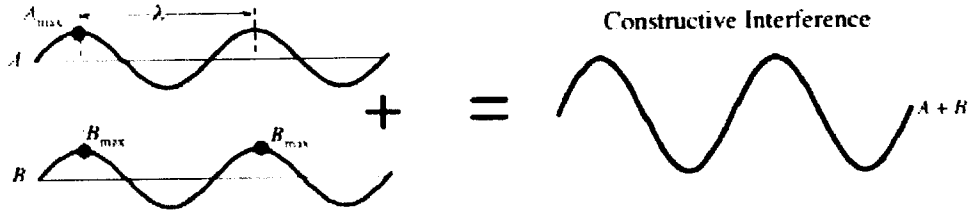


Figure 30- ΔΦ=0 or nλ (n= integer), both waves are in phase and interference is constructive. Resulting wave: double amplitude e equal frequency.

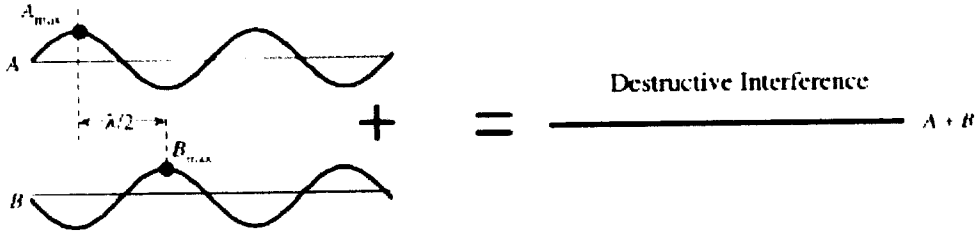


Figure 31- ΔΦ=λ λn/2 (n= integer), waves out of phase: destructive interference. No resulting wave.

Constructive and destructive waves make the diffraction phenomenon.

Bragg's Diffraction

A diffracted beam is obtained through the interaction of different wave plans at an angle of 2θ of the incident beam. Each atomic plan reflects a part of the waves.

A part of this incident beam is not diffracted. The part diffracted by the crystalline structure only exists in well defined directions: angles 2θ of the incident beam.

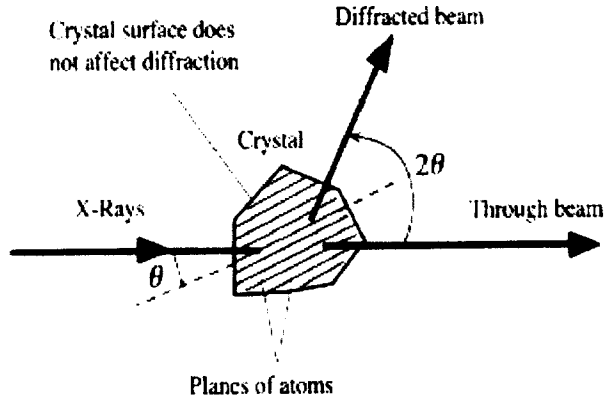


Figure 32- Bragg's diffraction.

The diffraction angle, 2θ, depends on the x-rays wave length and the plane separation, d:

$$2d\sin\theta = n\lambda \; ; \; n = 1,2,3,\ldots \; : \text{Bragg's Law}$$

Considering two waves A and B in a beam of x-rays reflected by two consecutive atomic planes. Initially the two waves are in phase, being A reflected through the first plane and B through the second. Wave B travels a bigger distance than the wave A. This distance is equivalent to 2dsinθ before it reaches wave A. Constructive interference happens when the difference between A and B nλ= integer. If not, the interference becomes destructive and both waves cancel one another.

APPENDIX 5

External gear teeth

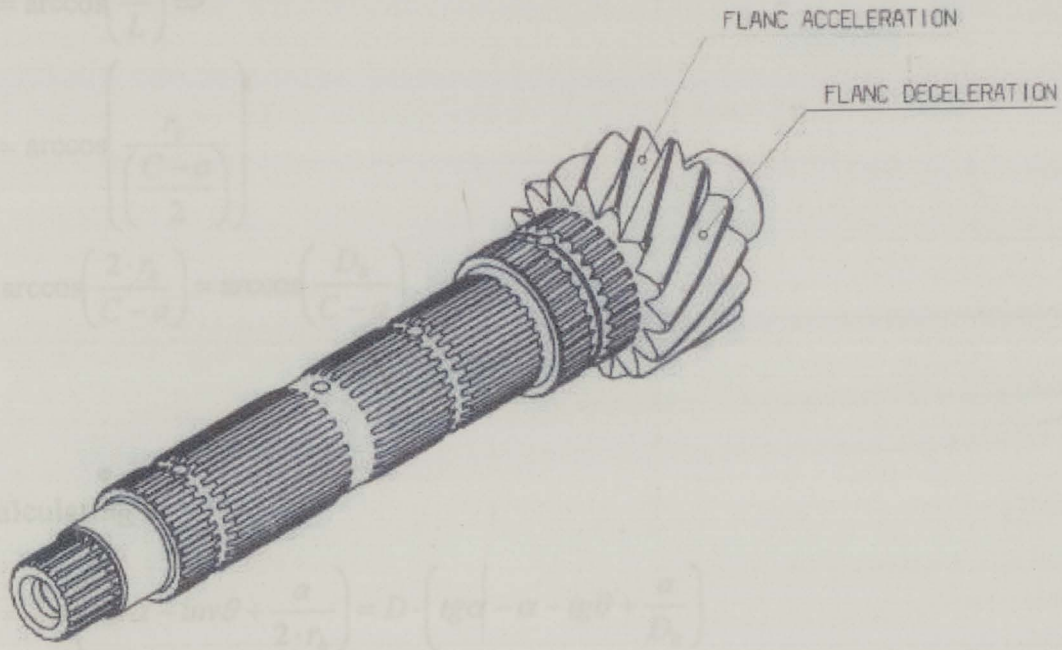


Figure 33- JR Shaft.

$$D = 2 \cdot L + a$$

$$L = \frac{D - a}{2}$$

From figure 5 :

$$L \cdot \cos\theta = r \cdot \cos\alpha_0 = r_b$$

$$\theta = \arccos\left(\frac{r_b}{L}\right)$$

Substituting variable D, (D→C);

$$\theta = \arccos\left(\frac{r_b}{L}\right) \Rightarrow$$

$$\theta = \arccos\left(\frac{r_b}{\left(\frac{C-a}{2}\right)}\right)$$

$$= \arccos\left(\frac{2 \cdot r_b}{C-a}\right) = \arccos\left(\frac{D_b}{C-a}\right)$$

Calculating *e*:

$$e = 2 \cdot r\left(inv\alpha - inv\theta + \frac{a}{2 \cdot r_b}\right) = D \cdot \left(tg\alpha - \alpha - tg\theta + \frac{a}{D_b}\right)$$

$$= D\left(tg\alpha - \alpha - tg\left(\arccos\frac{D_b}{C-a}\right) + \arccos\frac{D_b}{C-a} + \frac{a}{D_b}\right)$$

And tooth thickness:

$$S_b = r_b\left(\frac{s}{r} + 2 \cdot inv\alpha\right)$$

$$S = (\pi \cdot m - e) = \pi \cdot m - D \cdot (tg\alpha - \alpha - tg\theta + \theta + \frac{a}{D_b}) \Rightarrow$$

$$S_b = r_b \cdot \left(\frac{\pi \cdot m - D \cdot \left(tg\alpha - \alpha - tg\theta + \theta + \frac{a}{D_b} \right)}{r} + 2tg\alpha - 2\alpha \right)$$

$$= r_b \left(\frac{\pi \cdot m - D \cdot tg\alpha + D \cdot \alpha + D \cdot tg\theta - D \cdot \theta - \frac{a \cdot D}{D_b} + D \cdot tg\alpha - D \cdot \alpha}{r} \right)$$

$$= \frac{r_b}{r} \left(\pi \cdot m + D \cdot tg\theta - D \cdot \theta - \frac{a \cdot D}{D_b} \right)$$

$$= 2 \cdot r_b \left(\frac{\pi \cdot m}{D} + tg\theta - \theta - \frac{a}{D_b} \right)$$

$$= D_b \left(\frac{\pi \cdot m}{D} + tg\theta - \theta \right) - a$$

HELICAL GEAR

$a \rightarrow a'$ $E14 \rightarrow E24$

$m \rightarrow m'$ $E6 \rightarrow E21$

$\alpha \rightarrow \alpha'$ $E7 \rightarrow E22$

$$a' = \frac{a}{\cos\beta_b}$$

$$m' = \frac{m}{\cos\beta}$$

$$tg\beta_b = tg\beta \cdot \cos\alpha' \qquad tg\alpha' = \frac{tg\alpha}{\cos\beta}$$

$$S_b = r_b\left(\frac{\pi \cdot m' - e}{r} + 2 \cdot inv\alpha'\right)$$

$$S_b = D_b\left(\frac{\pi \cdot m}{D} + tg\theta' - \theta'\right) - a'$$

$$= D_b \cdot \left[\frac{\pi \cdot m'}{D} + tg\left(\arccos\frac{D_b}{C - a'}\right) - \arccos\left(\frac{D_b}{C - a'}\right)\right] - a'$$

Internal gear teeth

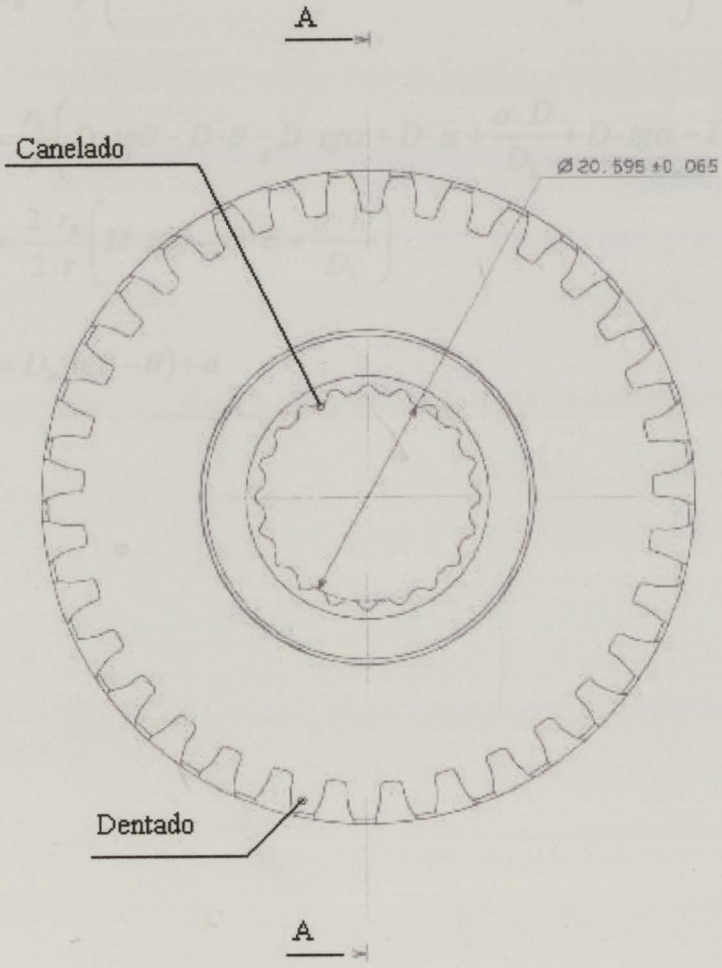


Figure 34- PF5.

$$L = \frac{C - a}{2}$$

$$\theta = \arccos\left(\frac{2 \cdot r_B}{C - a}\right) = \arccos\left(\frac{D_b}{C - a}\right)$$

$$e = D \cdot \left(inv\theta - inv\alpha + \frac{a}{D_b}\right)$$

$$S_b = r_b\left(\frac{s}{r} + 2\cdot inv\alpha\right) = D\cdot(tg\theta - \theta - tg\alpha + \alpha + \frac{a}{D_b}) \Rightarrow$$

$$S_b = r_b \cdot \left(\frac{D\cdot tg\theta - D\cdot\theta - D\cdot tg\alpha + D\cdot\alpha}{r} + 2tg\alpha - 2\alpha\right)$$

$$= \frac{r_b}{r}\left(D\cdot tg\theta - D\cdot\theta - D\cdot tg\alpha + D\cdot\alpha + \frac{a\cdot D}{D_b} + D\cdot tg\alpha - D\cdot\alpha\right)$$

$$= \frac{2\cdot r_b}{2\cdot r}\left(D\cdot tg\theta - D\cdot\theta + \frac{a\cdot D}{D_b}\right)$$

$$= D_b\left(tg\theta - \theta\right) + a$$

APPENDIX 6

Shot Peening

Shot peening might not decompose retained austenite. It is more likely to either damage the surface of the steel, or induces further stresses into the steel surface, which can lead to the potential for movement in the part at a later stage.

Shot peening imparts is a deformation induced transformation of retained austenite into martensite, that increases the case compressive residual stresses, and so, improving bending fatigue strength. Surface finishing is of higher quality. The 'color' difference from a part subjected to shot peening and another not subjected to it, is visible in the next picture.

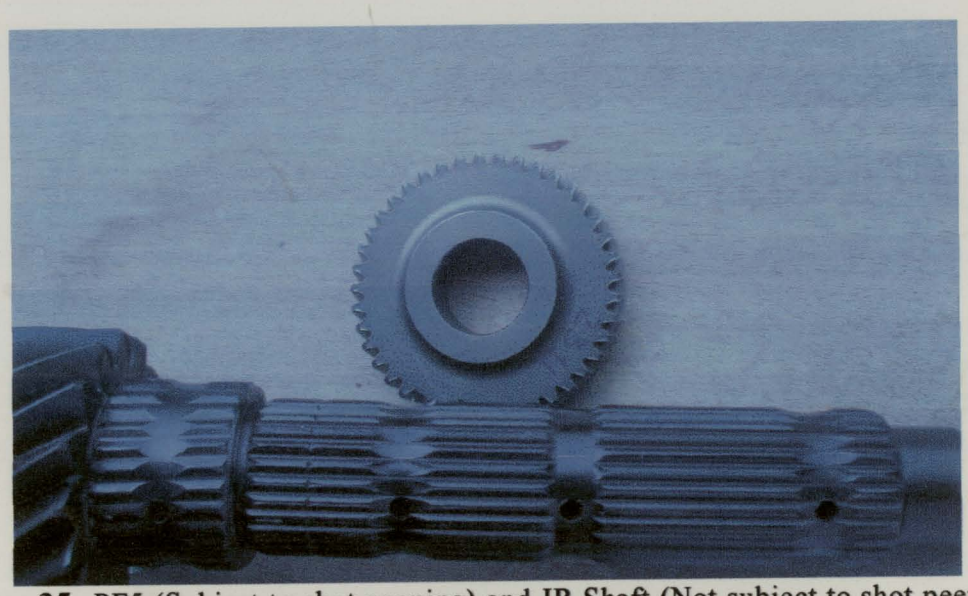


Figure 35- PF5 (Subject to shot peening) and JR Shaft (Not subject to shot peening).



Figure 36- PF5 superficial aspect before entering the shot peening machine.

APPENDIX 7

Preparing hardness measuring- methodology

1- Positioning the part in the cutting machine with the right angle, in terms of the cutting carbon disk position and, the oil pump pipe towards the cutting area.

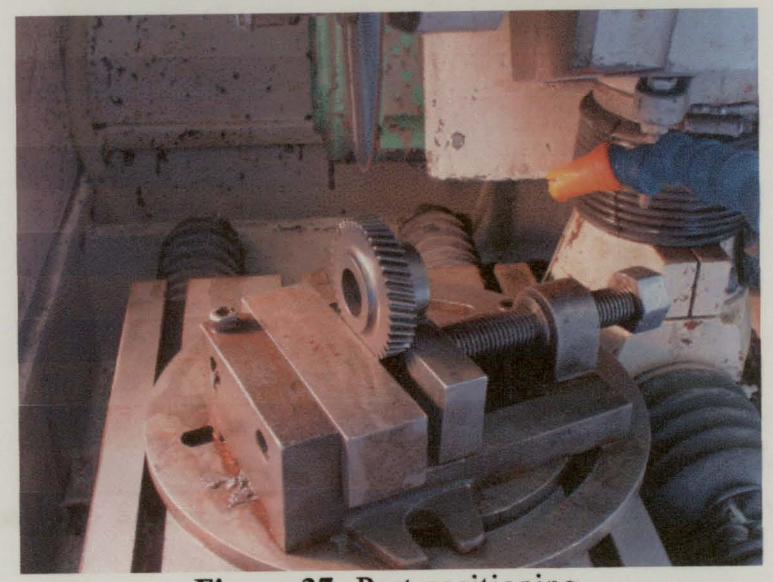


Figure 37- Part positioning.

2- By turning the spear wheel that gives a translation movement to the device supporting the part and at the same time lowering the carbon disk, which cuts the part with an additional rotating movement.

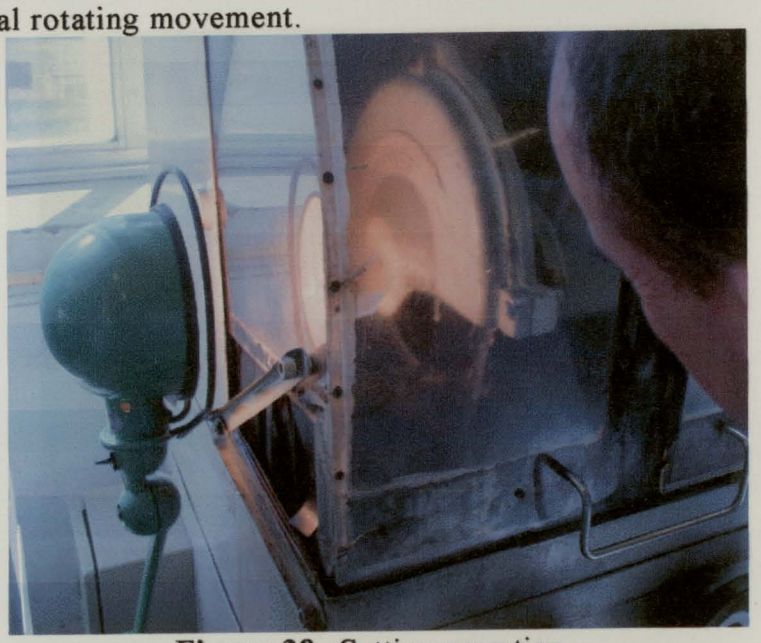


Figure 38- Cutting operation.

BIBLIOTECA F.E.

3- After extracting the teeth from the pinion, using a molding pressure machine the sample is prepared.



Figure 39- Sample preparation (teeth are positioned upside down).

4- The sample is obtained with attention to the teeth order so that these can be properly recognised when the measuring surface comes out in the upper part of the sample.

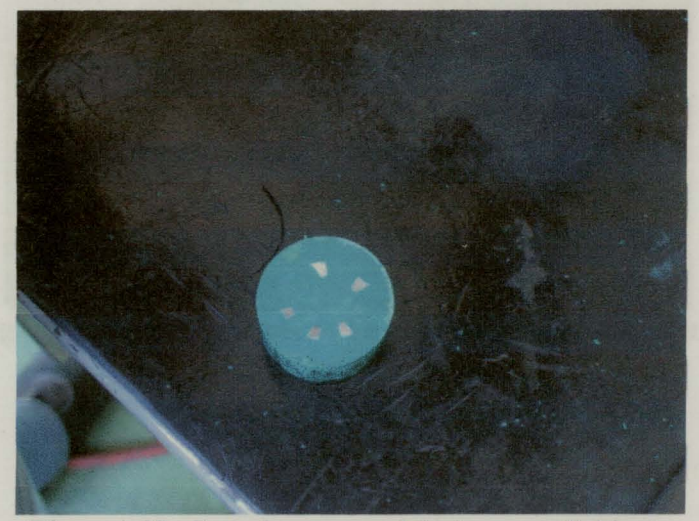


Figure 40- Sample prepared (prior to polishing).

5- The sample is properly polished in different stages.



Figure 41- Polishing the sample.

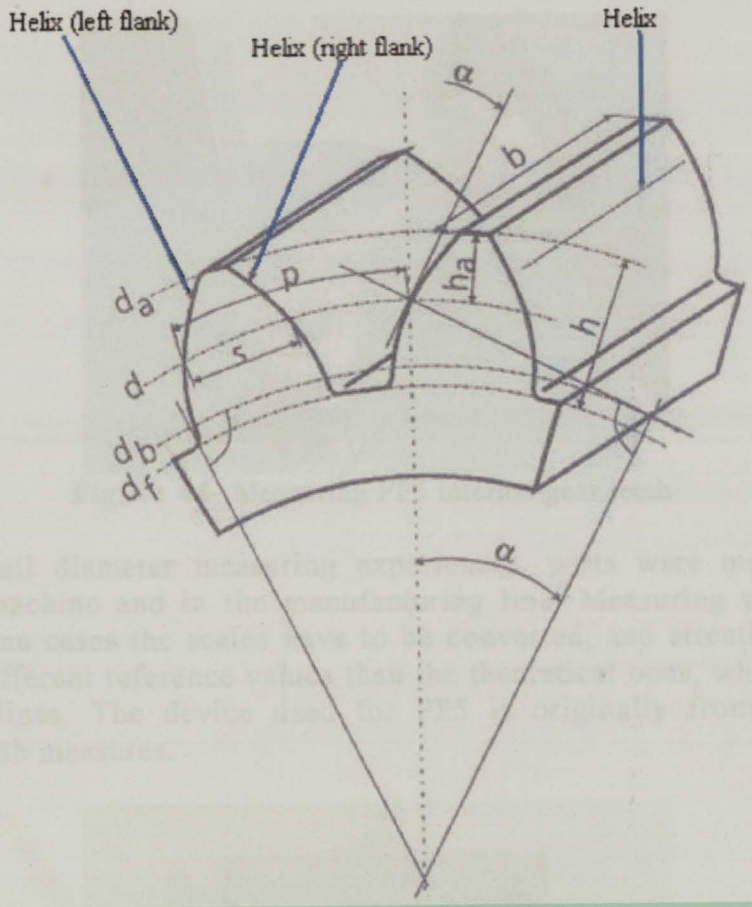
6- And it is finally ready to be attacked with an alcohol solution and then preferentially immediately measured to avoid any possible risk of oxidation.



Figure 42- Sample ready to be attacked and to measure hardness.

APPENDIX 8

Gear teeth geometrical properties



α= Pressure angle (alpha)
b= Tooth width

da= Head diameter
d= Reference primitive diameter
db= Base diameter
df= Root diameter

p= Reference primitive cylinder division
s= Reference primitive cylinder thickness

h= Tooth height
ha= Projected height

Figure 43- Basic geometry gear teeth properties.

Measuring the profile, helix and gear teeth division properties was made with **Klingelnberg** machine. The device used to the internal gear teeth measuring has a measuring sphere of 0,1 mm. It is a very difficult and precise work!

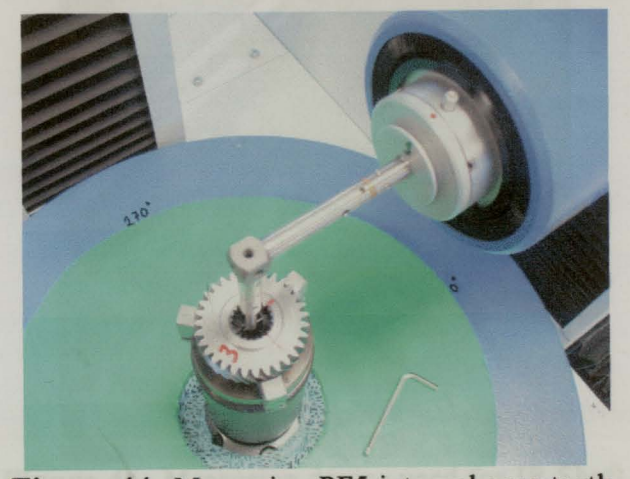


Figure 44- Measuring PF5 internal gear teeth.

In all over ball diameter measuring experiences, parts were measured both in **Klingelnberg** machine and in the manufacturing line. Measuring procedures were different. In some cases the scales have to be converted, and attention is needed to measure with different reference values than the theoretical ones, when measuring in manufacturing lines. The device used for PF5 is originally from another part's internal gear teeth measures.

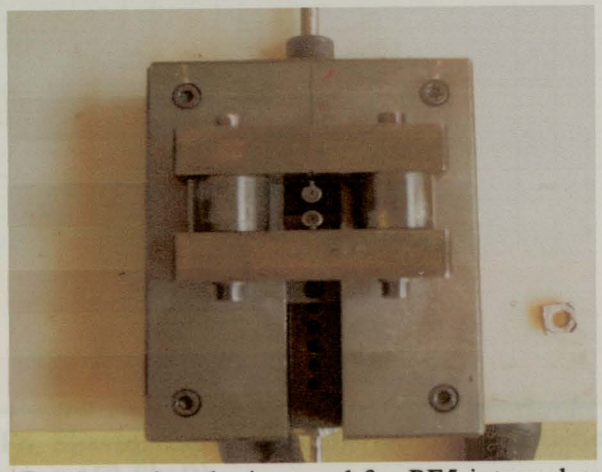


Figure 45- Measuring device used for PF5 internal gear teeth.

The same happens for JR Sec. Shaft. The manufacturing process is not totally under control and some adjustments have been made to suppress this lack of geometrical accuracy. Scales are adjusted, leading to additional difficulties.

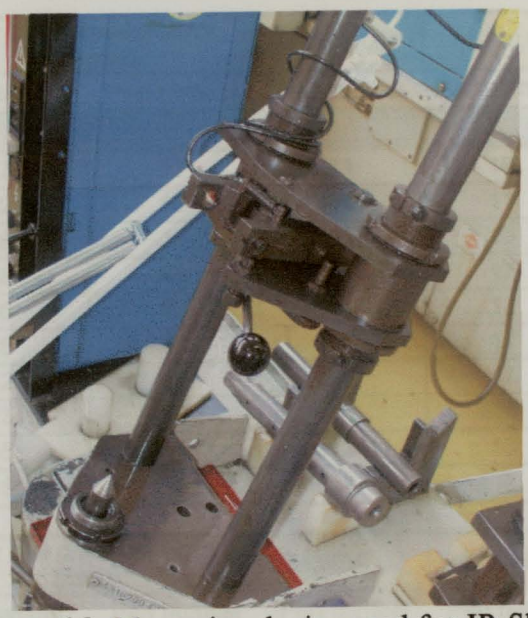
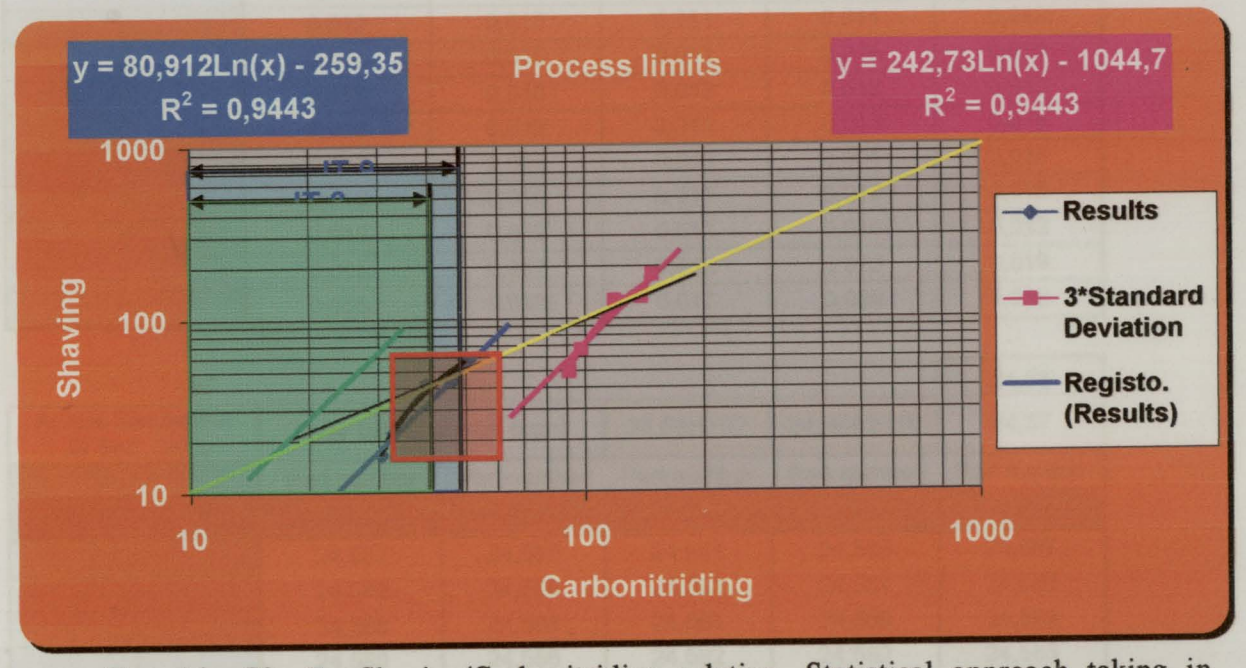


Figure 46- Measuring device used for JR Shaft.



Graphic 50- Fp Shaving/Carbonitriding relation. Statistical approach taking in consideration two IT values, (JR Shaft).

The next pages are an example of measuring problems when reference values are changed.

	Valor tabelado/ Original value
	Valor da linha de maquinagem/ Manuf. Line reference value

Árvore Secundária JR Sec. Shaft	Over ball diameter error (microns)		24,58±0,02	24,57+0,010	
20 Teeth	Part number	Part number	Part number	Part number	Part number
	1	2	3	4	5
1	17	17	11	19	17
2	12	15	11	11	18
3	18	18	11	15	13
4	18	16	12	12	15
5	16	12	11	13	15
6	15	10	11	11	15
7	12	16	11	17	18
8	13	12	11	14	12
9	15	17	12	13	19
10	15	13	17	9	18

Árvore Secundária JR Sec. Shaft	Over ball diameter error (mm)		24,58±0,02	24,57+0,010	
20 Teeth	Part number	Part number	Part number	Part number	Part number
	1	2	3	4	5
1	0,017	0,017	0,011	0,019	0,017
2	0,012	0,015	0,011	0,011	0,018
3	0,018	0,018	0,011	0,015	0,013
4	0,018	0,016	0,012	0,012	0,015
5	0,016	0,012	0,011	0,013	0,015
6	0,015	0,010	0,011	0,011	0,015
7	0,012	0,016	0,011	0,017	0,018
8	0,013	0,012	0,011	0,014	0,012
9	0,015	0,017	0,012	0,013	0,019
10	0,015	0,013	0,017	0,009	0,018

					24,58
Árvore Secundária JR Sec. Shaft	Over ball diameter (mm)		24,58±0,02	24,57+0,010	24,57
20 Teeth	Part number	Part number	Part number	Part number	Part number
	1	2	3	4	5
1	24,587	24,587	24,581	24,589	24,587
2	24,582	24,585	24,581	24,581	24,588
3	24,588	24,588	24,581	24,585	24,583
4	24,588	24,586	24,582	24,582	24,585
5	24,586	24,582	24,581	24,583	24,585
6	24,585	24,580	24,581	24,581	24,585
7	24,582	24,586	24,581	24,587	24,588
8	24,583	24,582	24,581	24,584	24,582
9	24,585	24,587	24,582	24,583	24,589
10	24,585	24,583	24,587	24,579	24,588
Average	24,585	24,585	24,582	24,583	24,586
Variance	20,097	20,099	20,091	20,09	20,093

0,068	0,034	18,215	18,165
18,176	18,142	0,043	-0,007

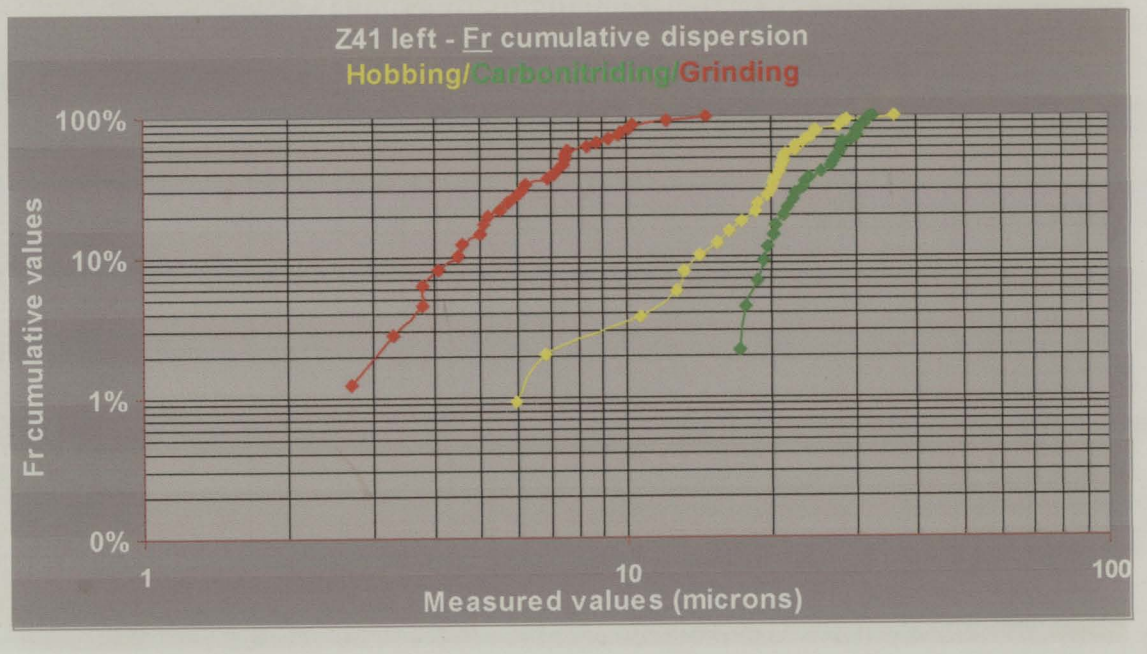
Pinhão 5ª Fixo PF5	Over ball diameter error (microns)		18,108 +0,068 and +0,034		18,172+0,043 and -0,007
20 Teeth	Part number	Part number	Part number	Part number	Part number
	1	2	3	4	5
1	-4	-10	-10	-4	0
2	-4	-4	-8	-2	2
3	-2	-6	-2	-6	-2
4	-4	-6	0	-2	-2
5	-4	-10	-6	-4	-4
6	-4	-6	-2	-6	-10
7	-4	-6	-8	-6	-4
8	-10	-6	-10	-8	-12
9	2	-14	-6	2	-6
10	-4	-6	-8	-8	-6

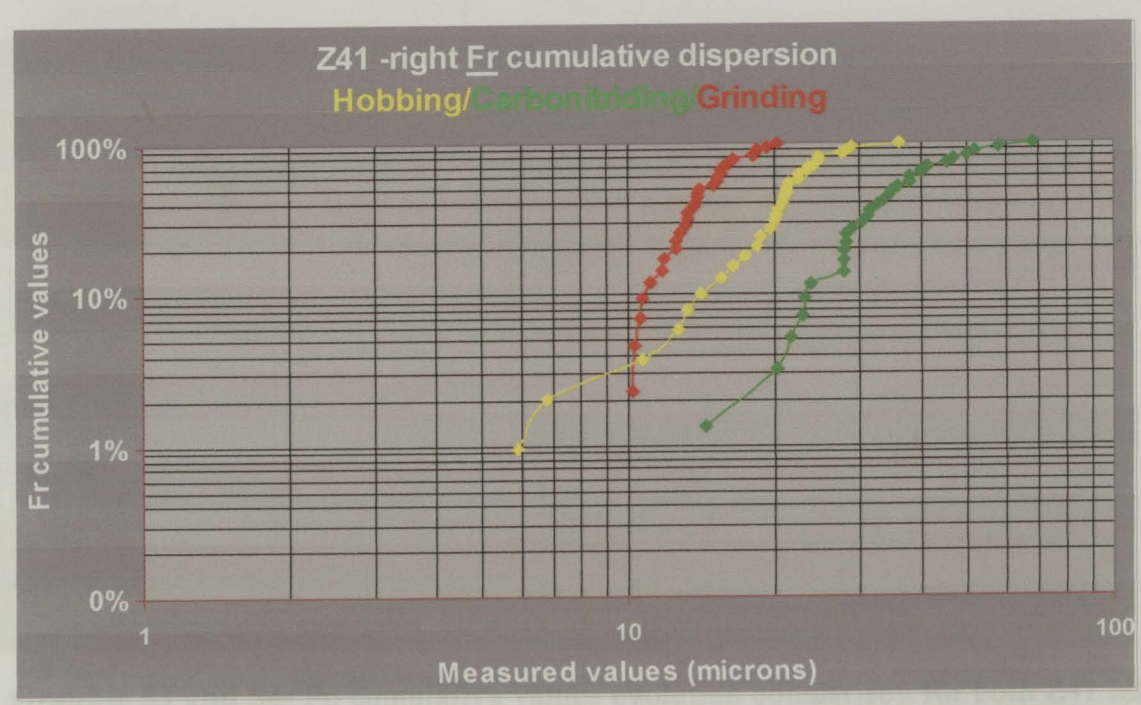
Pinhão 5ª Fixo PF5	Over ball diameter error (mm)		18,108 +0,068 e +0,034		18,172+0,043 e -0,007
20 Teeth	Part number	Part number	Part number	Part number	Part number
	1	2	3	4	5
1	-0,004	-0,01	-0,01	-0,004	0
2	-0,004	-0,004	-0,008	-0,002	0,002
3	-0,002	-0,006	-0,002	-0,006	-0,002
4	-0,004	-0,006	0	-0,002	-0,002
5	-0,004	-0,01	-0,006	-0,004	-0,004
6	-0,004	-0,006	-0,002	-0,006	-0,01
7	-0,004	-0,006	-0,008	-0,006	-0,004
8	-0,01	-0,006	-0,01	-0,008	-0,012
9	0,002	-0,014	-0,006	0,002	-0,006
10	-0,004	-0,006	-0,008	-0,008	-0,006

Pinhão 5ª Fixo PF5	Over ball diameter (mm)		18,108 +0,068 e +0,034		18,172 +0,043 e -0,007	
20 Teeth	Part number	Part number	Part number	Part number	Part number	18,142
	1	2	3	4	5	18,176
1	18,168	18,162	18,162	18,168	18,172	
2	18,168	18,168	18,164	18,170	18,174	
3	18,170	18,166	18,170	18,166	18,170	
4	18,168	18,166	18,172	18,170	18,170	
5	18,168	18,162	18,166	18,168	18,168	
6	18,168	18,166	18,170	18,166	18,162	
7	18,168	18,166	18,164	18,166	18,168	
8	18,162	18,166	18,162	18,164	18,160	
9	18,174	18,158	18,166	18,174	18,166	
10	18,168	18,166	18,164	18,164	18,166	

APPENDIX 9

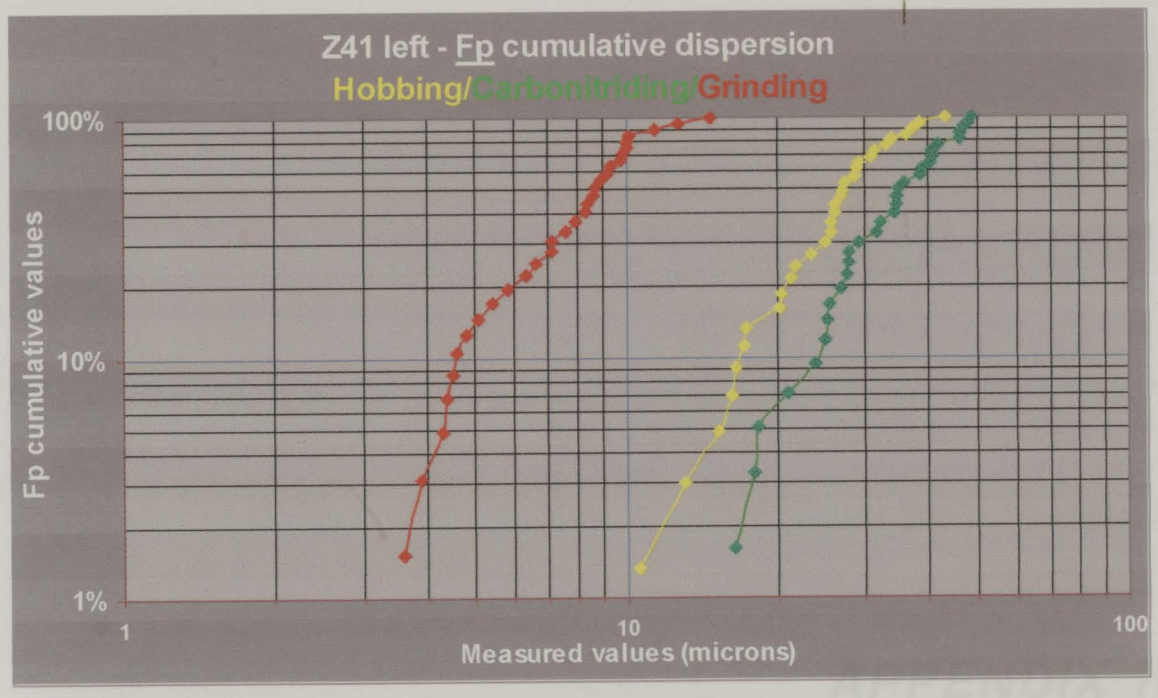
Deformation evolution for Z41

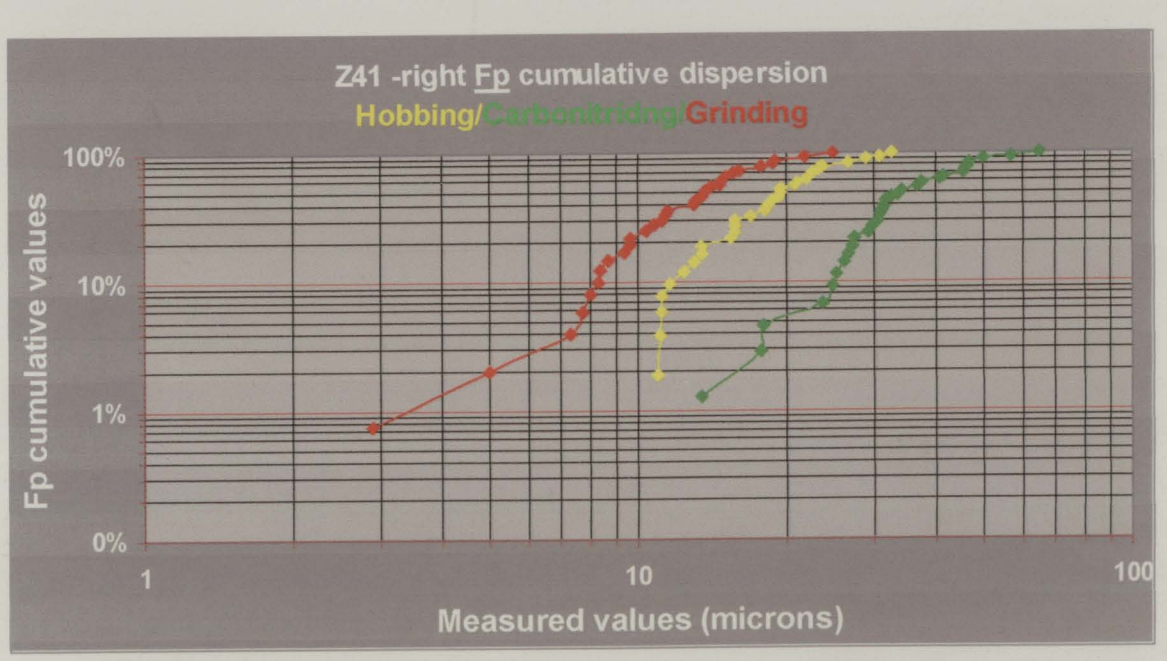




Graphics 51 and 52- Fr cumulative values evolution comparison for both Z41 left and right parts, throughout manufacture process (logarithmic scale).

BIBLIOTECA F.E. PORTO

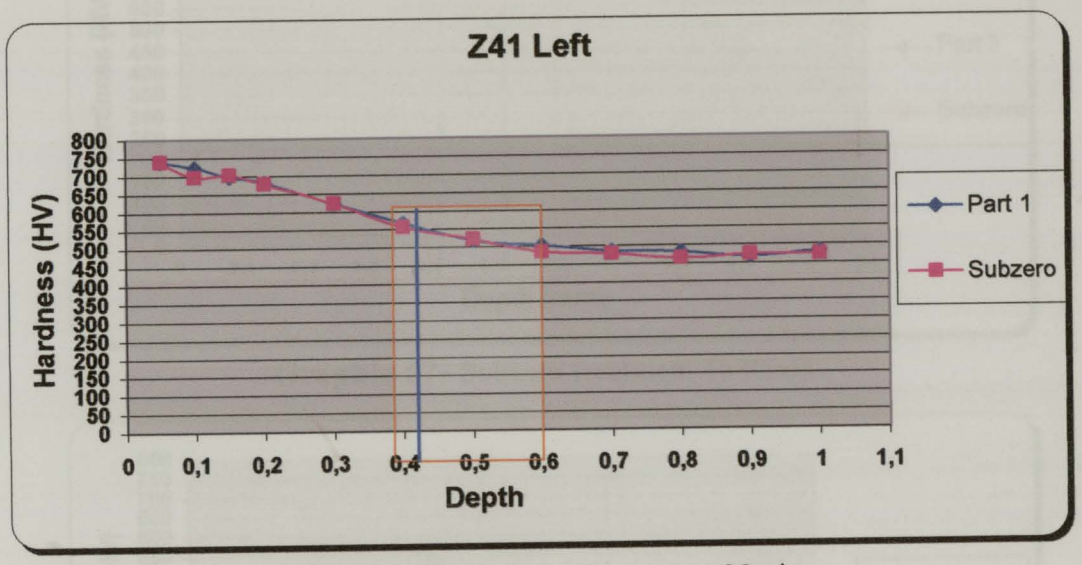




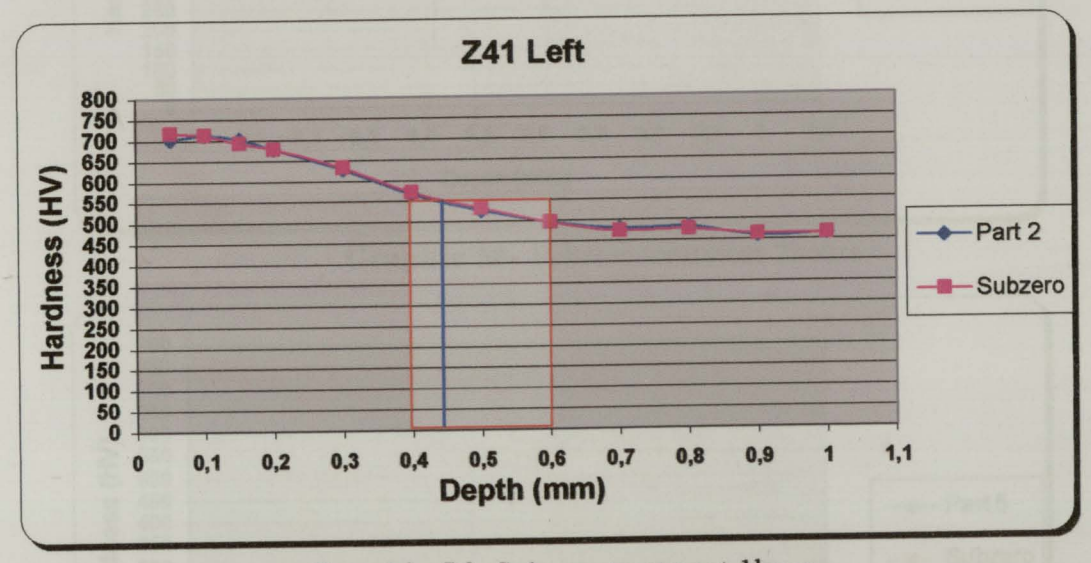
Graphic 53 and 54- Fp cumulative values evolution comparison for both Z41 left and right parts, throughout manufacture process (logarithmic scale).

APPENDIX 10

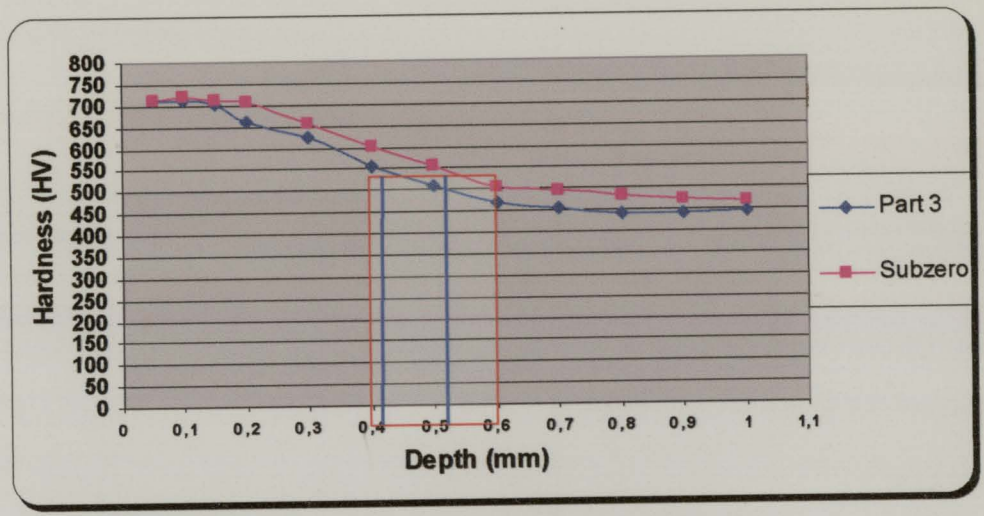
Z41 left pinions heat treatment and subzero cooling hardness comparison results



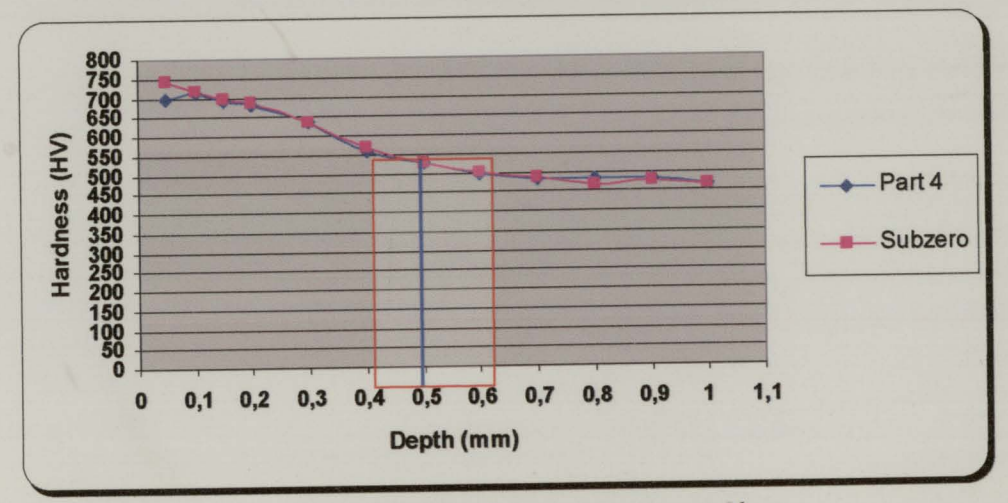
Graphic 55- Subzero treatment 30min..



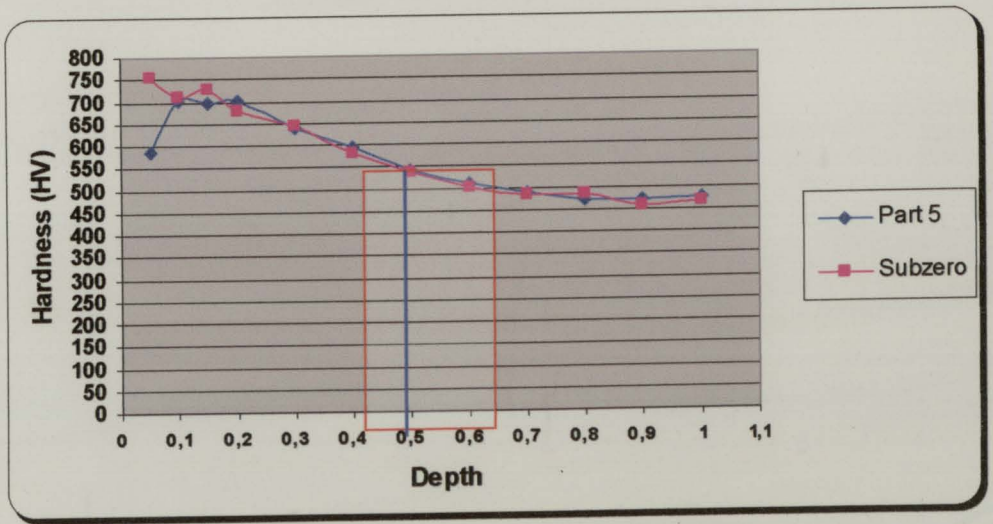
Graphic 56- Subzero treatment 1hour.



Graphic 57- Subzero treatment 1h30min..



Graphic 58- Subzero treatment 2hours.



Graphic 59- Subzero treatment 2h30min..

FACULDADE DE ENGENHARIA
UNIVERSIDADE DO PORTO
BIBLIOTECA
0000087327